GENERATION OF ANTI-TUMORIGENIC MET RECEPTOR VARIANTS BY SPLICING INTERFERENCE

by

TRUSHAR RATHOD

A dissertation submitted to the

School of Graduate Studies

Rutgers, The State University of New Jersey

In partial fulfillment of the requirements

For the degree of

Doctor of Philosophy

Graduate Program in Cellular and Molecular Pharmacology

Written under the direction of

Professor Luca Cartegni

And approved by

_____

_____

_____

_____

New Brunswick, New Jersey

May, 2019

ABSTRACT OF THE DISSERTATION

GENERATION OF ANTI-TUMORIGENIC MET RECEPTOR VARIANTS BY SPLICING INTERFERENCE

By TRUSHAR RATHOD

Dissertation Director:

Professor Luca Cartegni

Aberrant activation of MET, a receptor tyrosine kinase (RTK), leads to tumor growth, invasion and metastasis and is implicated in multiple types of cancers. Hence, various strategies have been employed to target MET for cancer therapy including recombinant form of MET ectodomain to sequester ligand and suppress MET activity. Here, we describe multiple C-terminal truncated MET decoys receptors (sdMET) with therapeutic potential. We show that these sdMET isoforms are translated from stable mRNA variants which are generated via Intronic polyadenylation (IPA) of MET's pre-mRNA in a U1-snRNP (U1) dependent manner. Moreover, we demonstrate increase in sdMET IPA isoforms of choice at expense of full-length MET with our antisense-based strategy by blocking U1 binding to specific 5' splice site and activating downstream intronic poly (A) site. Our strategy is an improvement of current methods due to its two-pronged approach: suppress MET activity in targeted cells by converting oncogenic MET into

soluble decoy to have dominant negative effect on surround microenvironment in paracrine manner.

Acknowledgements

In my progress towards my graduate studies, I was encouraged and motivated to work on projects for which I received persistent help and guidance from individuals whom I worked with and learned from. Over the past six years, I was privileged to received support for graduate work-related tension from friends and family. I thank them all for everything

Foremost, I would like to express my gratitude to my thesis advisor Dr. Luca Cartegni. He has been a great mentor over the course of my graduate studies. I could not have imagined having a better advisor and mentor. I always wanted to learn about RNA biology and therapeutics and I was fortunate enough to be trained by an expert in the field.

In addition to my advisor, I would like to thank my thesis committee members: Dr. Nanjoo Suh, Dr. Renping zhou, and Dr. Maurizio Scaltriti for their encouragement, insightful comments, and valuable time. I especially thank Dr. Suh for always having her door open and her calendar available.

I would also like to thank current and former members of Dr. Luca Cartegni's lab: Dr. Prasad Subramaniam, Dr. Jeong-Eun Park, and Dr. Lee Spraggon. I especially thank Dr. Subramaniam for his support through tough times and guidance during my thesis writing process.

I would also like to thank the faculty of Laboratory for Cancer Research for their advice and guidance: Dr. Suzie Chen, Dr. Philip Furmanski, Dr. Fang Liu, and Dr. Wei-Xing Zong.

More importantly, I am extremely grateful to fellow graduate students in my department for their support: future Drs. Niang Lin shan, Raj Shah, and Kevinn Eddy. I especially thank you all for laughter we shared on topics beyond science.

A bigger thanks goes to my friends outside of cancer research, my housemates Carlos Cocovi Higueras, Mohammad Ramenazali, and Erica He for all the good times and support during my early years of graduate studies.

Finally, would like to thank my family members: my father, mother, aunts, uncles, grandmother, sister, and cousins. However, no one is a bigger supporter than my mother even with all the hardship I caused. she always encouraged my academic goals. Words cannot express how grateful I am for her support. I have always wanted to make her proud and I hope I have done it with this achievement. My PhD is dedicated to her.

Table of Contents

Chapter II

Therapeutic use of anti-sense compounds

Chapter III

Generation of Anti-tumorigenic MET Receptor Variant by Splicing Interference

Appendix

Alternative Splicing Generates p53 isoform with Possible Metastatic Function

List of Figures

List of Tables

Chapter I

MET Receptor

1. General introduction to MET receptor

Initially identified in 1984, *MET* proto-oncogene located on chromosome 7q21-31 encodes a cell surface receptor tyrosine kinase (RTK) which is involved in multiple biological processes [1, 2]. MET is a 155 kDa transmembrane receptor and expressed in various organs, such as liver, lung, pancreas, stomach, and kidney [3, 4]. MET promotes tissue remodeling for morphogenesis during embryonic development and organ regeneration in adulthood [5, 6]. External stimuli allow MET receptor to controls organ homeostasis under normal physiological conditions by receiving and integrating environmental signals for growth, survival and migration [6-11]. The underlying mechanism involves activating complex network of multiple signaling pathways which can regulate transcription and translation, protein stability and localization [11, 12].

However, aberrant activation of MET receptor is implicated in tumorigenesis and metastasis [6, 13, 14]. When dysregulated, MET promotes cancer cell proliferation, anti-apoptosis, and migration [12, 15-17]; hence, MET signaling allows tumor to sustain growth and undertake aggressive phenotype [7, 18]. Furthermore, MET receptor is frequently activated in cancers undergoing targeted therapy to others RTKs to drive mechanism of resistance [19-23]. Therefore, MET is an attractive candidate for cancer therapeutics.

2. MET receptor structure and regulation at cell surface

Broadly, the topology of MET is organized in extracellular, transmembrane, and intracellular domains (figure 1.1) [24]. Extracellular domain is responsible for interacting

with ligand, hepatocyte growth factor (HGF), whereas the intracellular domain exerts MET's physiological functions [6, 11]. Once activated, MET initiates downstream signaling pathways necessary for numerous biological processes such as RAS-MAPK, PI3K-AKT, and STAT3 pathways [5, 6, 25].

2.1. MET receptor domains

MET receptor is initially synthesized as a single polypeptide precursor protein [6, 26]. in the Golgi compartment, pro-MET undergoes proteolytic processing into α- and β-chain [11, 15]. the α/β chains are joined by a disulphide bond forming a heterodimer

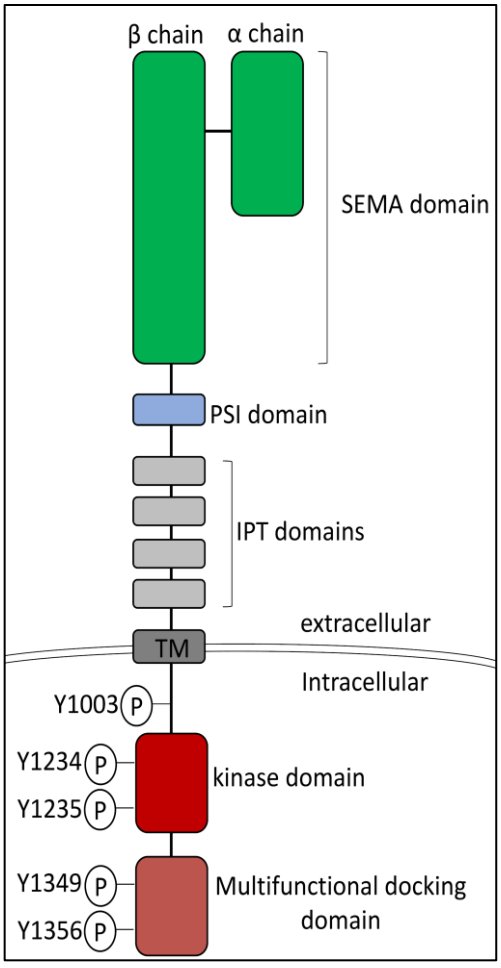

Figure 1.1: **Domain structure of MET.** The extracellular portion is composed three domains: 1, N-terminal semaphorin (sema) domain spans the entire α-chain and part of β-chain. 2, plexin-semaphorin-integrin (PSI) domain. 3, four immunoglobulin-plexin-transcription (IPT) domains. The Intracellular portion is composed of three domains: 1, juxta-membrane negative regulatory domain containing Y1003 residue. 2, kinase domain with Y1234 and Y1235 residues. 3, multifunctional docking domain with Y1349 and Y1356 residues.

single-pass cell surface receptor (figure 1.1). The extracellular part of MET receptor is divided into three domains [24, 27]. The N-terminal semaphorin (sema) domain encompasses the entire α-chain and part of the β-chain [24]. Sema domain forms seven blade β-propeller structure allowing ligand-receptor interaction and shares structural homology to cell surface proteins in semaphorin and Plexin families [13, 28-30]. Following sema domain is the plexin-semaphorin-integrin (PSI) domain which includes four disulphide bonds. In between the PSI domain and transmembrane (TM) domain are four immunoglobulin-plexin-transcription (IPT) domains [31]. The IPT domains provide 'stalk' like structural support for the sema domain to interact with MET receptor ligand, hepatocyte growth factor (HGF) [32]. Furthermore, recent studies have identified a second ligand binding site in IPT3 and IPT4 adding a layer of complexity to HGF and MET interactions [31].

Three domains define the intracellular part of MET receptor. Immediately following the TM domain is juxta-membrane negative regulatory (JNR) domain containing of Y1003 residue [33]; following phosphorylation of Y1003, MET is ubiquitinylate by E3 ubiquitin-protein ligase thereby promoting internalization and lysosomal-mediated receptor degradation [26, 33, 34]. After the JNR domain is the tyrosine kinase (TK) domain which positively modulates MET activity upon trans-phosphorylation of Y1234 and Y1235 [6, 15]. Lastly, C-terminal multifunctional docking domain have Y1349 and Y1356 residues which are critical to recruiting adaptor proteins to initiate signaling pathways.

2.2. Ubiquitin-mediated regulation of MET

Main determinant of controlling MET expression at cell surface is endosomal-mediated degradation of MET in the lysosomal compartment (figure 1.2) [35-39]. After phosphorylation of Y1003 residue in the JNR domain of MET, E3 ubiquitin-protein ligase, casitas b-lineage lymphoma (CBL), are recruited to monoubiquitylation of MET at multiple

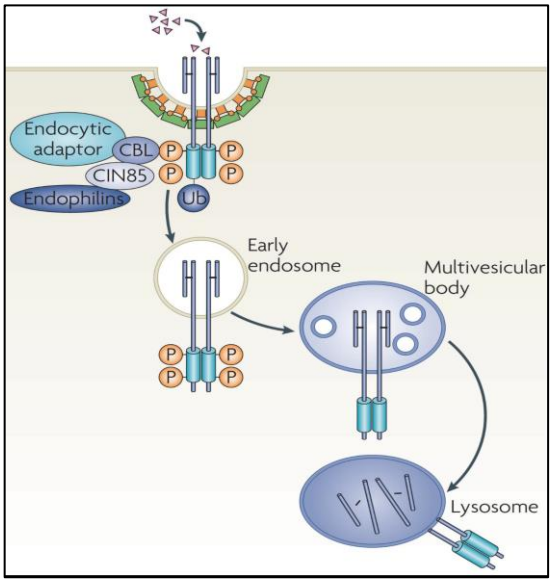

Figure 1.2: **Endosomal mediated internalization and lysosomal degradation of MET receptor**. MET containing endosome form multivesicular bodies that fuse with lysosome for receptor degradation. Reprint with permission from [5].

sites [39]. Ubiquitylated MET is recognized by endocytic adaptors with ubiquitin-binding domains. Furthermore, CBL attracts endophilin proteins which promote negative curvature and invagination of cell membrane during early steps of endocytosis [40]. Collectively, CBL is responsible for tagging MET, physical formation of clathrin-coated early endosome and its subsequent sorting to the endosomal network; within this network, MET containing endosome accumulates to form multivesicular bodies which eventually merges with lysosomes for MET degradation [5].

What determines MET towards degradation rather than sustained signaling from endosomal network is unknown. For EGFR, degradation predominates in conditions of abundant ligand, whereas signals from endosomes is favored during low levels of EGF in the microenvironment [41]. A comparable situation might apply to MET though such scenario lacks experimental evidence.

2.3. Regulation of MET with Proteolytic cleavage

Receptor proteolysis is an alternative route to regulate MET expression at cell surface [42]. This mechanism involves two successive proteolytic cleavage of MET (figure

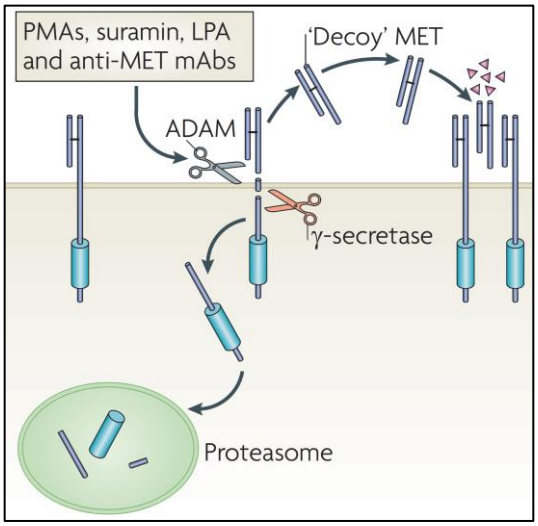

Figure 1.3: **Sequential proteolysis of MET receptor at the cell surface**. The first cleavage liberates ectodomain by extracellular metalloprotease, ADAM. ADAM activity is stimulated by phorbol esters (PMA), suramin, lysophosphatidic acid (LPA) or MET monoclonal antibodies. The released ectodomain can behave as a decoy receptor to block full-length MET activation. The second cleavage is by γ-secretase to release intracellular fragment which is degraded by proteasomes. Reprint with permission from [5].

1.3). An extracellular protease, a disintegrin and metalloprotease (ADAM), performs the first cleavage to generate MET ectodomain and membrane anchored cytoplasmic tail [42-44]. The second proteolytic reaction is done by membrane associated γ-secretase to release the intracellular domain which is unstable and swiftly degraded by cytoplasmic proteasomes [45, 46]. Various agents can promote ADAM metalloprotease activity, such as lysophosphatidic acid, suramin, phorbol esters or monoclonal antibodies targeting MET [47-52]. Notably, shedding of MET ectodomain has a dual function: first, shedding decreases level of full-length (FL) receptor at cell surface; second, inhibition of FL-MET activity by generate a decoy moiety to sequester HGF, prevent dimerization and transactivation of FL receptor [5, 12, 51, 53]. Therefore, agents which reduce FL-MET and induce MET ectodomain can be utilized to target MET for cancer therapy.

Proteolysis of MET is distinct from endosomal mediated degradation. Proteolytic cleavage does not require ligand induced kinase activity and is independent of receptor ubiquitinylation [5]. This mechanism prevents chronic MET activation and weaken signal input under basal conditions [5].

3. MET ligand, hepatocyte growth factor (HGF)

HGF, also known as scatter factor (SF), was independently identified by two groups in the late 1980s [54, 55]. the first group named the ligand, HGF, due to its ability induce hepatocyte proliferation, while the latter group identified it as a SF because it promoted ‘scattering’ of epithelial cells (figure 1.4).

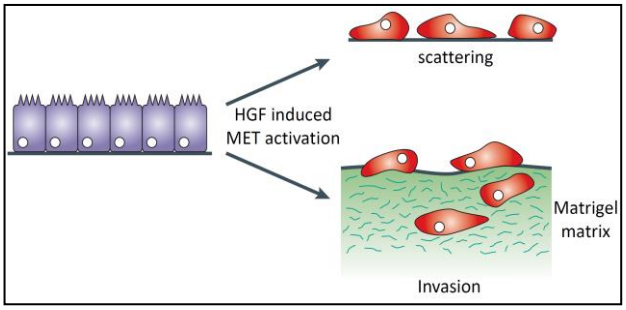

Figure 1.4: **MET induced scattering and invasion.** Reprint with permission from [11].

Initially, HGF is synthesized and secreted as a single-chain polypeptide precursor [11]. In the extracellular space, proteases converted the pro-HGF into α- and β-chain which are remain together by disulphide bridge to form an active heterodimer (figure 1.5A) [56, 57]. The α-chain contains N-terminal hairpin loop (HL) domain followed by four Kringle domains, while the β-chain consists of serine protease homology (SPH) domain. SPH domain is required for HGF-MET interaction, receptor activation and subsequent ligand mediated dimerization (figure 1.5B).

In addition to full-length HGF, two C-terminal truncated isoforms of HGF are produced by alternative splicing variants NK1 and NK2 [58, 59]. NK1 variant encodes HL,

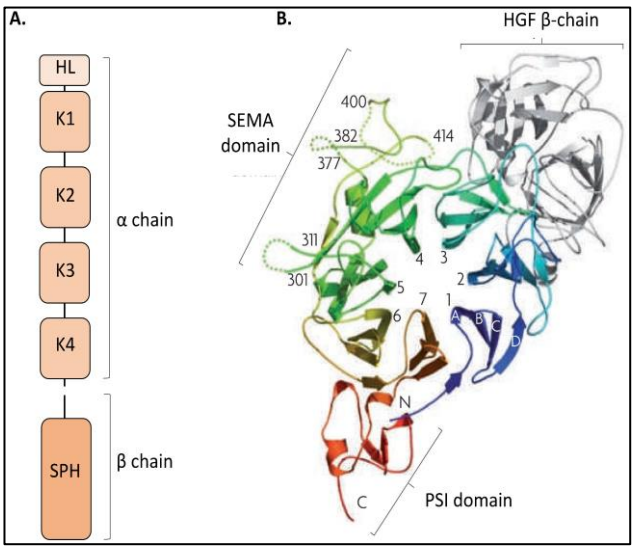

Figure 1.5: **A**. HGF is composed of six domains: N-terminal hairpin loop (HL) domain. Four Kringle domains (K1-K4. Serine protease homology (SPH) domain. **B.** Crystal structure of between sema domain and HGF β chain. reprint with permission from [5].

and K1 domain while NK2 variant encodes HL, K1, and K2 domain. In vivo studies have demonstrated NK1 can serve as a partial agonist, whereas the role of NK2 in MET activation is unclear [59].

4. MET activation and downstream pathways

After HGF binds MET, two HGF-MET complex dimerizes in a ligand-dependent manner, induces a conformational change and activates the intracellular kinase domain (KD) (figure 1.6). One receptor trans-phosphorylates its dimer partner's KD (Y1234/Y1235) and vice versa [6]. The following step is phosphorylation of Y1349/Y1356 in the multifunctional docking domain and recruitment of various docking protein to this site, such as GAB1, phospholipase C (PLC), GRB2, and SRC [60]. After their localization to the cell surface, these docking proteins are phosphorylation and serve as scaffold to attract protein involved in signaling cascade. For example, phosphorylated GAB1 bound to MET recruits PI3K and SHP2, while phosphorylated GRB2 recruits SOS, guanine nucleotide exchange factor [61-66]. Eventually, these complex interactions lead to activation of downstream signaling, mainly RAS-MAPK, PI3K-AKT and STAT3 pathways [5, 6, 11, 12].

4.1. Signaling pathways regulated by MET receptor

MET regulated signaling are arranged in pathways that transmit biological information from outside to inside of cell cytoplasm. Once HGF is release into

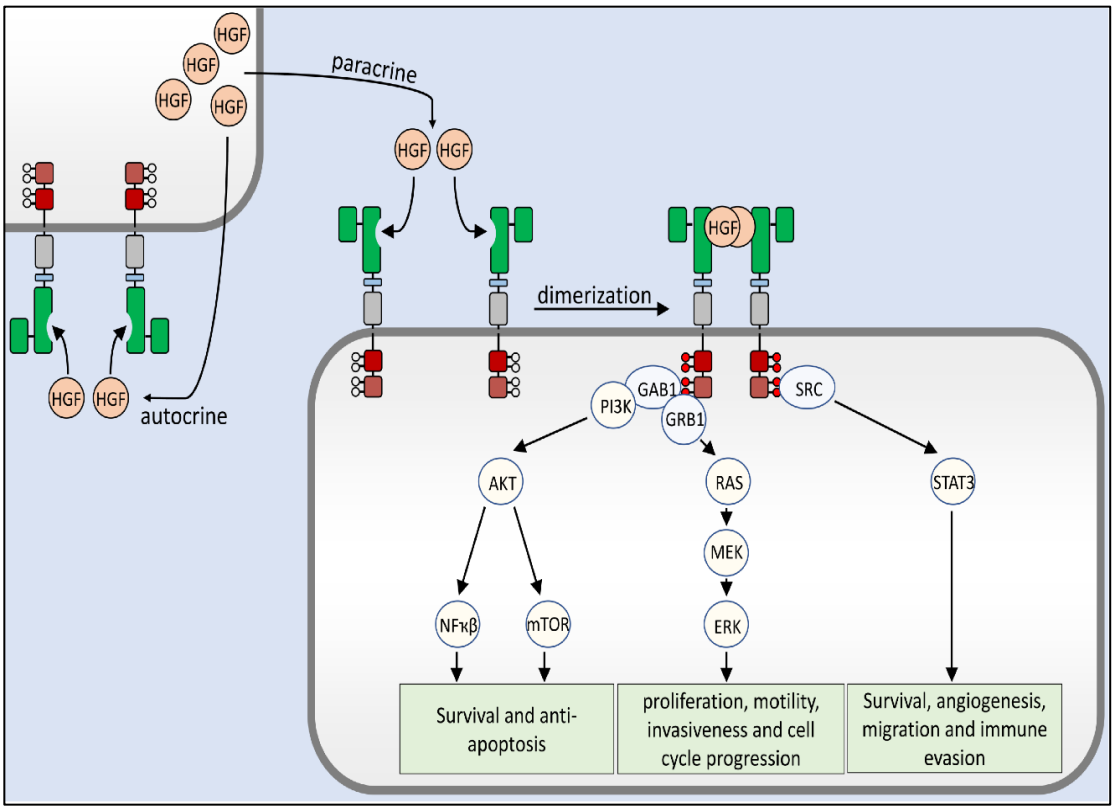

Figure 1.6: **Major signaling pathways regulated by MET receptor**. MET can be activated by HGF in autocrine and paracrine manner leading to ligand-mediated dimerization of HGF/MET dimer. Adaptor proteins are recruited to cell surface to attract effector molecules and trigger several biologically relevant signaling cascades, such as PI3-AKT, RAS-MAPK, and STAT3 pathways.

microenvironment, it acts in an autocrine or paracrine manner (figure 1.6) [67-70]. For instance, fibroblast release HGF to activate MET on neighboring epithelial cells during tissue repair [70]. The signaling apparatus, such as docking and transducer molecules are unique to MET. However, the downstream response to activated MET depends on conventional signaling pathways that are shared among different RTKs and are reviewed in the following three sections.

4.1. RAS-MAPK pathway

Mitogen-activated protein kinase **(**MAPK) proteins, also known as extracellular signal-regulated kinases (ERKs), are part of a subfamily with a distinctive phosphor-relay system involving multiple kinases [71, 72]. The ERKs are primarily activated by tyrosine kinase-mediated stimulation of RAS, a small GTPase [72]. For example, MET bound GRB/SOS complex can phosphorylate and activate RAS [7]. Through its effector loop domain, activated RAS binds serine threonine kinase, RAF [73-75]. This association inducing conformational change in RAF and allows RAF to phosphorylate intermediate kinases in MAPK system, MEK1 and MEK2 [75-77]. Finally, MEK1 and MEK2 phosphorylate ERK1 and ERK2, the final effectors of the pathways [77]. Activated ERK1 and ERK2 are translocated to the nucleus where they phosphorylate and stabilize multiple transcription factors to modulate multiple genes involved in cell-cycle regulation, cell motility, invasion and proliferation [78, 79].

In addition to ERKs, MET can activate signaling kinases in the p38 MAPK and JNK subfamilies [80, 81]. Through RAS, MET can stimulate RAC, another small GTPase [82]. RAC activation leads to phosphorylation of MEK3, MEK4, MEK6, and MEK7. As a consequence, activated MEK4 and MEK7 proceeds to phosphorylate JNKs [80], whereas activated MEK3 and MEK 6 leads to phosphorylation of multiple p38 isoform [81]. JNKs and p38s stimulated in MET-dependent manner regulated cellular differentiation and transformation.

4.2. PI3K-AKT pathway

MET-dependent activation of phosphoinositide 3-kinases (PI3K)-AKT pathway occurs via two mechanisms [5, 83, 84]. For instance, MET can directly phosphorylate PI3K or indirectly through adaptor protein, GAB1 [62, 84]. In both scenarios, activated PI3K results in phosphatidylinositol-3,4,5-triphosphate (PIP3) formation at the cell surface. PIP3 recruits and activate serine threonine kinase, AKT to initiates signaling pathways required for cell survival and growth [85]. AKT is able to suppress apoptosis by increasing expression of (B-cell lymphoma) BCL-2 and the degradation of p53 via activation of ubiquitin-protein ligase MDM2 [85]. Moreover, AKT can stimulate protein synthesis by activation of activate mammalian target of rapamycin (mTOR) [85].

4.3. STAT pathway

As in PI3K-AKT activation, MET can initiate Signal transducer and activator of transcription 3 (STAT3) pathway directly or indirectly through adaptor protein, SRC [5].

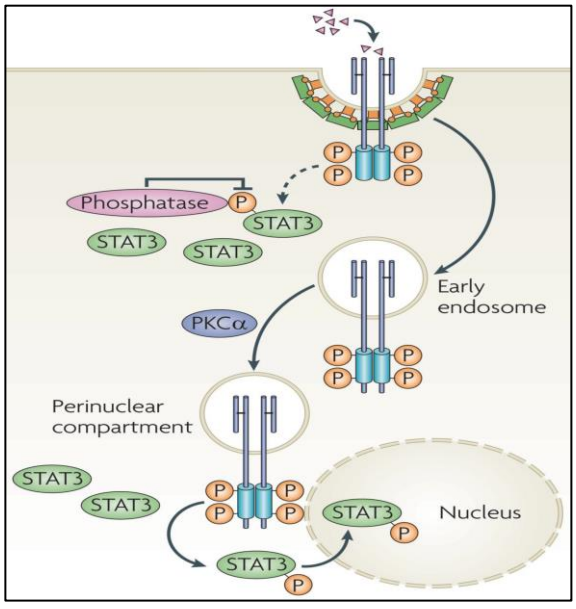

Figure 1.7: **Activation of STAT3 pathway by MET from endosomal compartment**. MET containing endosome are trafficked to the perinuclear compartment to activate the STAT3 pathway. Reprint with permission from [5].

Furthermore, as an alternative route, recent evidence has described PKCα-mediated activation of STAT3 pathway by MET from endosome (figure 1.7) [86, 87]. After internalization, MET containing endosome are trafficked along network of microtubule to accumulate in the perinuclear compartment [88]. From this juxtanuclear space, MET phosphorylate STAT3 [88]. In any case, phosphorylation and activation of STAT3 leads to homodimerization. Ultimately, the STAT3 homodimers is translocated to the nucleus where they function as transcription factors to control expression of multiple genes involved in proliferation, differentiation, angiogenesis, survival and migration [89].

5. MET and other cell surface receptors

In recent years, cooperative signaling have been described between MET and other cell surface receptor, such as CD44 isoforms, integrins, and other RTKs [13]. The signaling pathways initiated by MET is potent and specific because of complex interaction between MET and co-receptors at the cell surface (figure 1.8). MET interacting partners can strengthen and/or expand MET mediated signals from microenvironment and translate them into definite and meaningful biological outcomes.

5.1. CD44 isoforms and MET

CD44 isoforms due to alternative splicing have been shown to functionally interact with MET and regulate actin cytoskeleton in epithelial and endothelial cells (figure 1.8A) [90, 91]. CD44s are cell adhesion molecules localized at the cell surface and provides physical cell-to-cell linkage through intracellular actin cytoskeleton and extracellular matrix [92, 93]. CD44v1 through CD44v10 isoform differ from one another due to

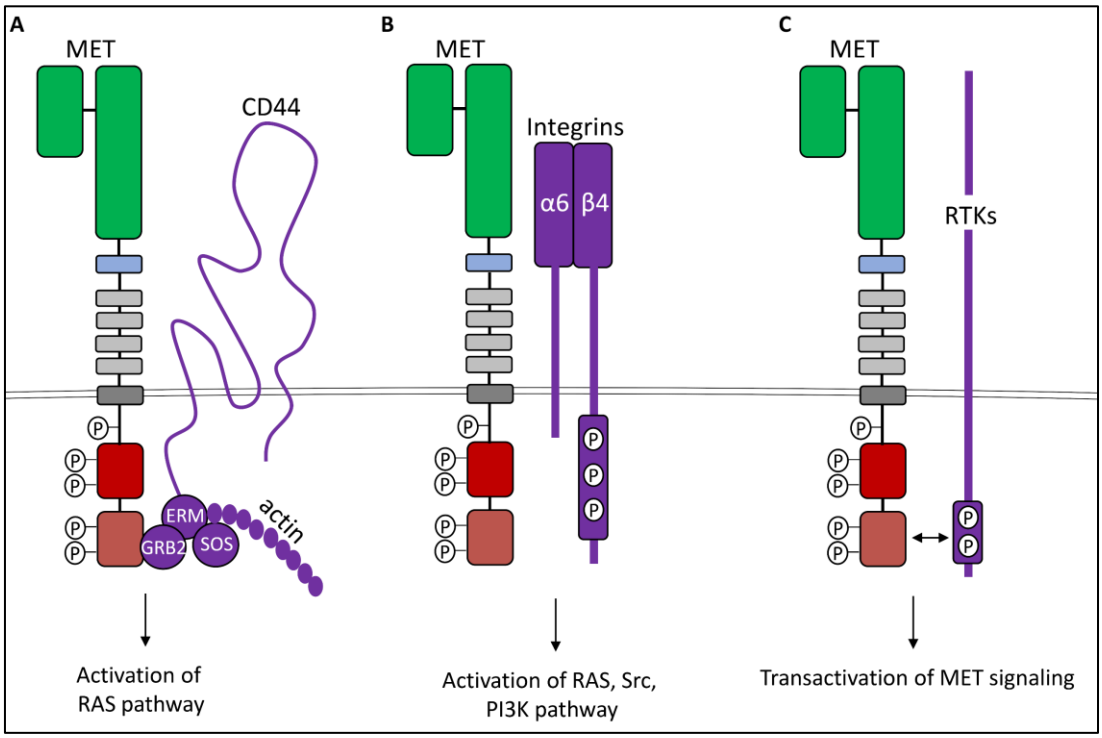

Figure 1.8: **Cooperative interaction between MET and cell surface receptors**. **A**. MET receptor can associate CD44 hyaluronan receptor splice variant V6 and activate RAS-MAPK pathways **B**. α4β6 integrin can interact with MET to stimulate of PI3K, RAS and SRC pathway. **C**. Functional crosstalk between MET and other RTKs (EGFR, RON, PDGFR, AXL) can occur in normal physiological context or in multiple type of tumors.

insertion of variable regions in their extracellular domain [90]. The CD44v6 isoform contributes in MET signaling via multiple mechanism [91, 94, 95]. For example, extracellular domain of CD44v6 is essential for ternary complex formation between MET/HGF/CD44v6 and for successful activation of MET. Furthermore, CD44v6-mediated MET activation initiates assembly of complex association of MET's intracellular domain, GRB2, and ERM proteins to recruit SOS and efficiently activate the RAS-MAPK pathway

[96]. Moreover, C44v10 isoform promotes MET trafficking into caveolin-enriched microdomains along with TIAM1, dynamin and cortactin, an actin cytoskeletal regulator [97]. Thus, CD44 association assists in precise localization of MET within cellular compartments to amplify signal output and regulate actin cytoskeletal.

5.2. Integrins and MET

MET signaling can be strengthened with selective interaction with α4β6 integrins (figure 1.8B) [6]. Activated MET can interact with α4β6 integrin through its GAB1 adaptor protein [98-100]. Thereafter, activated MET can proceed to phosphorylation cytoplasmic domain of β4 subunit and initiated recruitment of effector molecules, SHC, PI3K, and SHP2 [100]. Through this mechanism, cytoplasmic domains of MET and α4β6 integrin serve as additional docking stage for recruitment of downstream proteins that synergize with those already bound to MET. This mode of action strengthens and sustains activation of downstream pathways through amplification of MET signaling

5.3. MET and other RTKs

Numerous studies have described crosstalk between MET and other RTKs, such as EGFR, RON, PDGFR, FGFR, and AXL, in great detail due to its likely implications in normal physiology and resistance to cancer therapy (figure 1.8C) [101].

In particular, physical interaction between MET and epidermal growth factor receptor (EGFR) was recently reported [102-104]. Furthermore, even in the absence of HGF, stimulation with EGFR ligands EGF can induce MET phosphorylation in cells with expression of both receptors [105]. Moreover, synergistic activation of downstream

pathways is demonstrated when ligands for both receptors are utilized, indicating a functional crosstalk between both receptors [106]. Furthermore, MET interaction can also crosstalk with the other EGFR family members, such as ERBB3 [23]. Similar to MET-EGFR crosstalk, transactivation of ERBB3 and MET was demonstrated with HGF or ERBB3 ligand, neuregulin [107].

Additionally, MET can interact with the closely related RON receptor [108]. With the absence of HGF, this association can induce transphosphorylation of the MET receptor. It was recently found that subset of tumors addicted to MET signaling feature transactivation of RON by MET [109]. Lastly, MET association with platelet-derived growth factor receptor (PDGFR) and AXL was demonstrated in lung and bladder cancer [110].

The number of cell surface receptors that play a part in MET signaling is constantly growing. The MET receptor relies on numerous co-receptors and adaptors proteins to exert its biological responses. Although much work has been done to describe these interactions, our understanding of the complex network of MET-mediate signaling remains incomplete.

6. MET in developmental and regenerative biology

Most RTKs pathways amplify complex protein–protein interactions and participate in numerous signaling feedback loops to ensure signal intake and increase functional capability. As for MET, downstream protein fulfill signaling requirements in a tissue specific manner which contributes towards embryonic development and organ regeneration (figure 1.9) [5]. Furthermore, depending on spatiotemporal and biological

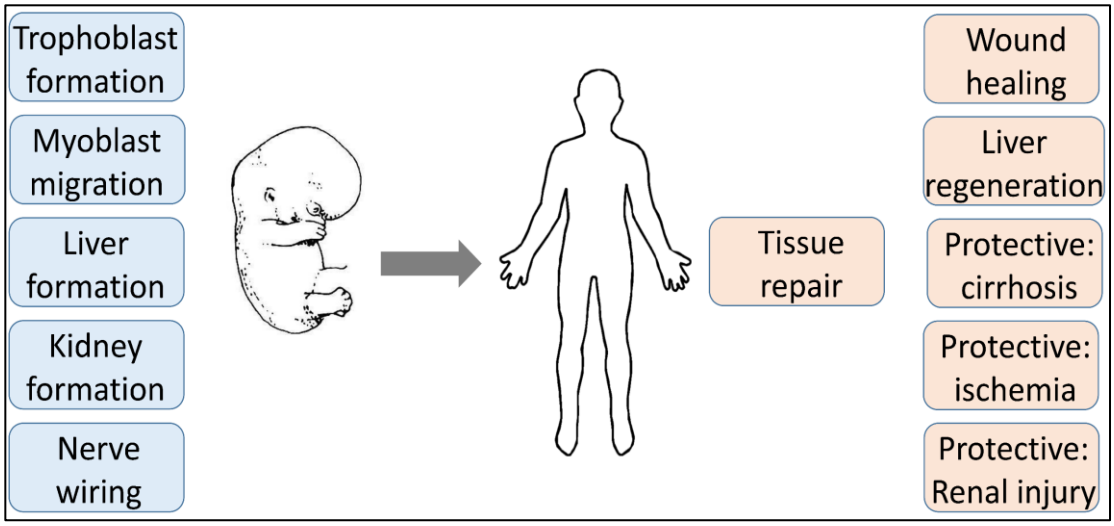

Figure 1.9: Selected contribution of MET receptor in development and tissue repair.

context, some downstream molecules dominate over others to relay signals (summarized in table 1.1). The following two sections outline several examples of biological functions of MET with genetic and pharmacological studies.

Table 1.1: *In vivo* response to MET signals.

Factors	Position in pathway	Molecular activity	Biological activity
GAB1	Direct or indirect interaction with MET	Adaptor	limb development and liver regeneration
GRB2	Direct or indirect interaction with MET	Adaptor	Limb development and liver regeneration
SRC	Direct interaction	Tyrosine kinase	Proliferation of placenta and myoblast
PI3K	Direct or indirect interaction with MET	Lipid kinase	Neuron outgrowth and branching
STAT3	Direct or indirect interaction with MET	Transcription factor	Tubulogenesis and angiogenesis
AKT	Downstream transducer	Ser/Thr kinase	Liver regeneration
ERK1/2	Downstream transducer	Ser/Thr kinase	Liver regeneration

6.1. MET and embryonic development

MET relays required signals for proliferation and survival of hepatocytes and placental trophoblasts during embryonic development [111, 112]. In *MET* knockout (KO) mice, there is substantial reduction in liver size and defect in formation of placental labyrinth [111]. The consequence of abnormal placenta is insufficient nutrient exchange between fetal and maternal blood leading to death *in utero* [111]. Also, MET activity is

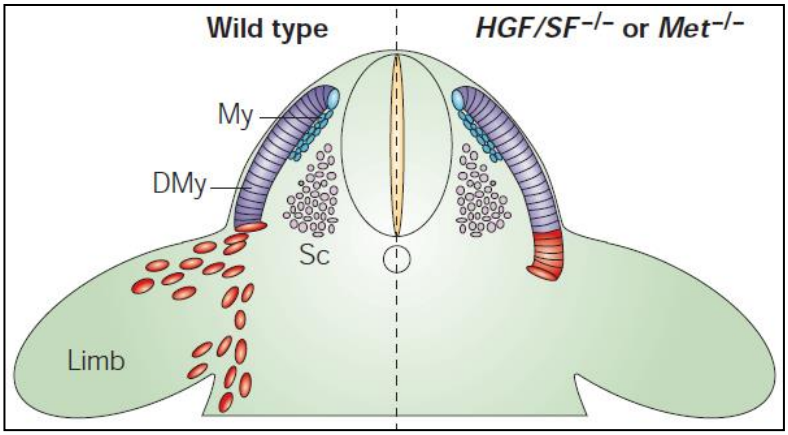

Figure 1.10: MET in development. Myogenic precursors (red) detach from dermomyotome (DMy) and migrate in a MET-mediated manner to development limb buds. Reprint with permission from [11].

crucial for motility and proliferation of myoblast which undergo long range migration (figure 1.10) [113-116]. These muscle progenitor cells undergo epithelial-mesenchymal transition (EMT) to detach from epithelial layer of ectoderm. Once in their mesenchymal state, they migrate, differentiate, and populate selective regions which eventually develop into limbs, tongue and lung diaphragm [11, 117, 118]. Indeed, specific muscle types are absence *MET* KO mice [114, 115, 118]. Finally, perturbation in MET signaling

impairs proper wiring of neuronal network leading to abnormal axon outgrowth and reduced survival of sensory and motor neurons.

Genetic knock-in mouse models have been utilized to determine developmental significance of different downstream signaling regulated by MET. For instance, recent study describes rescue of specific phenotypes with mutant form of multifunctional docking domain which selectively binds adapter proteins PI3K, SRC or GRB2 [119]. When MET exclusively binds GRB2, mice are viable and normal demonstrating that GRB2 is adequate in recruiting all necessary components downstream of MET [119]. However, embryonic lethality was observed when MET only associated with SRC or PI3K. although incompatible with survival, tissue specific SRC activation restore myoblast and placental trophoblast proliferation, while selective activation of PI3K is enough to promote branching and outgrowth of motor neurons [119]. Together, these studies demonstrate that MET regulated processes during development are accomplished in a spatiotemporal and tissue specific manner by different downstream proteins.

Defects observed in MET knockout embryos are identical to GAB1-null mice indicating that GAB1 is critical to MET dependent signaling pathways [120]. The mode of GAB1 and MET association can have biological implication in a tissue-specific manner *in vivo* [120]. Both direct and indirect GAB1 binding to MET is necessary for MET-mediated placenta and liver development [120]. However, either direct or through GRB2, but not both, is essential for developing limb muscles. Similar to its interaction with MET, GAB1 association with individual downstream factors modulates specific processes during different stages in embryo formation [121]. For instance, PI3K and GAB1 interaction is

critical for eyelid formation, while this associate is dispensable for MET-mediated organogenesis [119-121]. Furthermore, MET signals are primarily relayed via GAB1-SHP2 interaction [119, 120]. Mutations in GAB1 which prevent SHP2 interaction are undistinguishable from MET-null mice; these mice have defects in placenta formation and suppress myoblast cells migration similar to MET KO mice [120, 121]. To conclude, prerequisite of specific pathway in MET signaling is time- and tissue-dependent during development.

6.2. MET and organ regeneration

The mechanism of MET-mediated signaling during organ regeneration and tissue repair is extensively studied *in vitro* and *in vivo*.

For *in vitro*, culture conditions mimicking three-dimensional environment is utilized in morphogenetic assays [122]. For example, normal proliferating epithelial cells form spheroids when embedded in collagen matrix [122]. In addition, these spheroids have polarized cells surrounding a hollow lumen [122, 123]. Spheroids elongation to form hollow tubules is mediated by MET signaling in sequence dependent manner [124]. Initially, polarized epithelial cells undergo EMT to transform into invading mesenchymal cells that project spindle-shaped extensions in their surrounding matrix [122, 124, 125]. Thereafter, these cells form single file chains which lengthen and resist apoptosis [123, 125]. Finally, cells revert back to epithelial state to restore polarity and form elongated tubule. The above process is repeated to add length to the growing lumen. This biological mechanism of tubulogenesis has been precisely described at the molecular level and is

dependent of MET-mediated signaling; broadly, tubule formation requires activated MET to initiate RAS-MAPK, STAT3 and NF-κb pathways [123]. Initially, early stages of EMT is dependent of MET-GAB1-mediated activation of ERKs to proliferate transformed cells; in addition, ERKs can increase expression of SNAIL family of transcription factors to initiate migration and suppress apoptosis along with NF-κb [123]. Finally, the late phase of tubulogenesis requires STAT3 pathway for expression of matrix metalloproteases (MMPs) and proteases required for MMP activation [126, 127]. MMPs are indispensable for extension and formation of hollow mature tubules [126-128].

For *in vivo*, Cre-loxP system is employed to generate conditional *MET* KO and decipher its function in liver regeneration [120, 129-131]. MET activation is essential for liver regeneration due to chronic or acute injury [132]. Subsequent to liver damage, there is a substantial increase in HGF expression from stromal fibroblast of injured tissue [132]. This HGF can activate MET on hepatocytes in autocrine or paracrine manner to deliver mitogenic and survival signals for organ repair [132]. Accordingly, conditional *MET* KO in liver prevents organ regeneration after hepatic injury or resection [130]; at the molecular level, there is lack of mitogenic signals due to reduced ERK1/2 activation and its downstream transcriptional target: cyclins, and enhances activity of cyclin-dependent kinase (CDK) inhibitor p21 [120]; this suppresses hepatocyte proliferation and impaired liver injury repair. Similar phenotype of diminished liver regeneration was demonstrated in conditional deletion of GAB1 or SHP2 in mice, adding significance to GAB1-SHP2 interaction in MET-mediated responses [120, 133].

MET activity provides similar protective functions in kidneys [134]. In renal epithelial cells, proliferation and survival signals can be induced by activation HGF-MET axis [134]; for instance, MET-mediated RAS-MAPK pathway can transmit mitogenic signal, while PI3K-AKT can increase transcription of BCL-2 and BCL-X to promote cell survival [134, 135]. This important renal protective function played by MET enhances kidney regeneration prevents tubular necrosis.

Persistent damage to liver and kidneys can cause fibrosis [134]. Over production of fiber deposits in extracellular matrix from renal myofibroblast is mediated by sustained TGFβ signaling [135]. MET can act as a forceful anti-fibrotic agent in multiple ways: MET can transcriptionally suppress TGFβ and phosphorylate ERKs to inhibit SMADs, transcription factors for TGFβ signaling pathway [136].

Lastly, HGF/MET axis is also utilized by epithelial cells in wound healing [137]. Hyperproliferative epithelium at the wound edge is formed by keratinocytes [137, 138]. To provide fresh layer of epithelium, these cells enter multiple cell division cycles to cover and repopulate the injured dermis [138]. Keratinocytes from conditional *MET* KO mice are impaired in their ability to produce hyperproliferative epithelium to repair injured area [139, 140]. In an *in vitro* scratch wound assay, MET promotes proper keratinocyte positioning. This re-orientation allows focal adhesion molecules, actin fibers, and microtubules to be directed towards wound edges as a requirement for subsequent locomotion [137]. Once in correct orientation, MET initiates proliferation and migration of epithelial cells to cover the empty space [140]. The key MET-regulated signaling factors in wound healing are GAB1, ERKs, AKT, and p21-activated kinases (PAKs) which all

together modulates protrusion formation and actin polymerization to promote migration [140, 141].

7. MET and cancer

In cancer, regulation of MET signaling observed during development and regeneration is aberrantly altered. Number of mechanisms can cause this deviation, such as gene amplification, activating point mutations, transcriptional deregulation, impaired degradation, crosstalk with other RTKs or synergies with downstream signaling factors [7, 12]. Ultimately, these variations can lead to tumorigenesis, metastasis, or resistance to cancer therapy.

7.1. Genetic alterations of MET in cancer

Genetic changes in MET are observed in many types of tumors [142]. These variations occur at primary site to act as oncogenic drivers or secondary events to promote metastases and evade exposure to treatment. Gene amplification is the most common alteration found in MET-dependent tumors [142]. Numerous studies have reported *MET* amplification in primary tumors and in metastatic sites [7]. Increase in *MET* copy number substantially increases expression and leads to ligand-independent MET activation [7, 9, 19, 23, 101]. *MET* amplification have been identified for several cancers, such as non-small cell lung cancer, gastric cancers, and pancreatic adenocarcinomas.

Furthermore, point mutations is an alternative mechanism for constitutive MET activation (figure 1.11) [142]. Mutations can occur in the kinase or juxta-membrane domains. Kinase domain mutants induce overactive MET signaling independent of HGF.

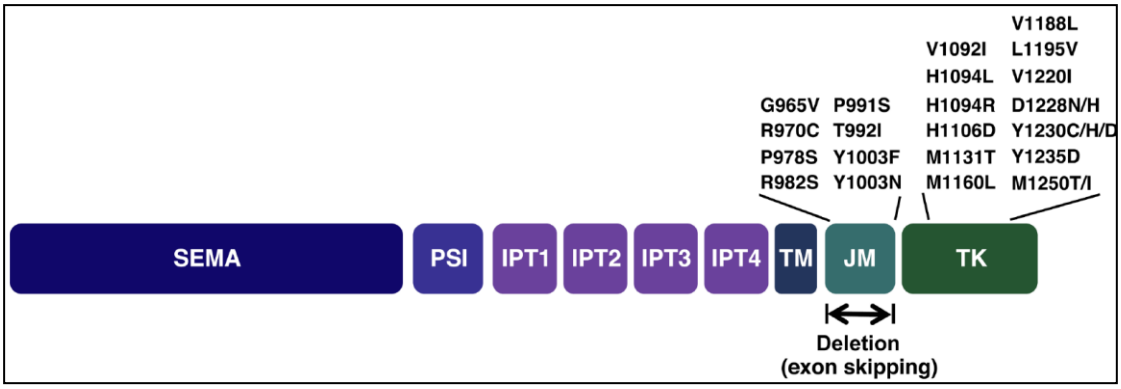

Figure 1.11: MET mutation in intracellular domain. Missense mutation in the tyrosine kinase domain (TK) results in constitutive activation. Missense mutation or deletion of juxta-membrane domain (JM) due to splice site mutation can promote receptor recycling to cell surface. Modified and reprint with permission from [142].

On the other hand, missense or splice site mutation can alter juxta-membrane domain; this results in aberrant increase in signaling due receptor recycling to cell surface rather than endosomal-mediated degradation [143-145]. Indeed, isoforms carrying activating mutations can cause basal-like breast carcinomas when expressed in mice mammary glands [146-149]. In addition, clonal selection of MET activating mutations occurs during metastasis of head and neck cancer [150, 151]; for instance, frequency of activating mutations increases from 2% in the primary site to 50% in the metastases in patients with head and neck cancers [152-154].

The following three sections highlight MET contribution in selected types of cancers which were studies for this thesis.

7.2 MET and lung cancer

Lung cancer is the leading cause of cancer related death worldwide. An average of 1.6 million lung cancer-related deaths are reported each year [155]. Common cause is tobacco smoking which represent 80% of cases [155]. the remaining 20% are never smokers who were affected from inherited genetic susceptibility, second hand smoking, or environmental carcinogens [155]. Nearly 80% to 85% of lung cancer are histologically categorized as non-small cell lung cancer (NSCLC) and the rest as small cell lung cancer (SCLC) [155]. Understanding lung cancer biology is critical for developing effective therapies. As in other malignancies, lung cancer is collection of clonal sub-populations of cells [155]. Each population has distinct genetic features which can possibly promote metastases, resistance to treatment and relapse (figure 1.12). Hence, its crucial to identify

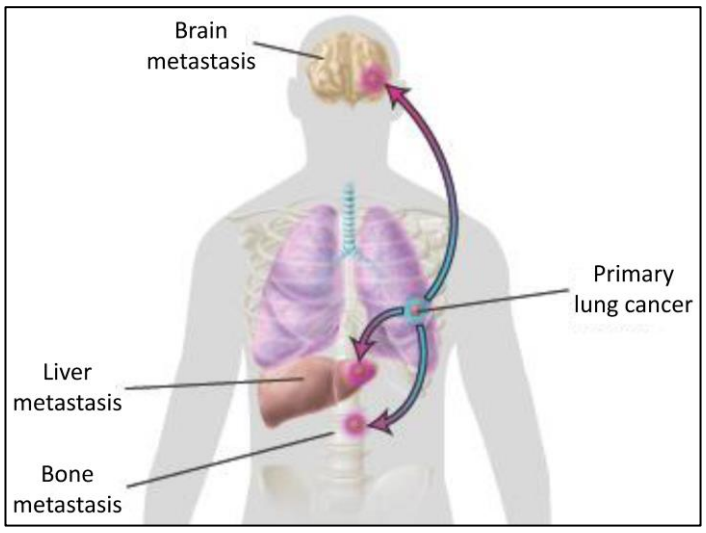

Figure 1.12: Primary lung cancer metastasis to brain liver, and bone. Reprint with permission from [172]

targetable clonal genetic variations within tumors to design successful therapeutic approaches.

Multiple genetic events can lead to constitutive MET activity in NSCLC or SCLC, such as activating mutation or gene amplification [156-158]. Dziadziuszko et al demonstrated increase *MET* copy number in lung adenocarcinoma tumor bank using fluorescence in situ hybridization [159]. Furthermore, this group reported MET expression correlated with higher immunohistochemical staining for MET phosphorylation (pMET) at Y1234/1235 when compared to adjacent normal tissues. Notably, preferential staining of pMET was detected in cell near invading front of the tumor [159].

Another mechanism of aberrant MET activity in lung cancer are mutations in the cytoplasmic portion of the receptor [157]: primarily in the juxta-membrane domains. For example, one study with SCLC samples identified two mutations in juxta-membrane domain: R988C and T1010I which prevent Y1003 phosphorylation [160]. As mentioned previously, these class of mutation enable MET recycling to cell surface and prevent ubiquitin-mediated lysosomal degradation [5]. Similar mutations were also characterized in NSCLC. For instance, R988C, T1010I, and S1058P were identified in a study of more than 100 lung adenocarcinoma tumor tissues [161]. In addition, this group also detected an alternative splice variant; this isoform lack 47 amino acids in the juxta-membrane domain due to exon 14 splice site mutation which results in exon skipping [157, 161].

Finally, another link between lung cancer and MET are the lung stem cells. These cells are localized at bronchioalveolar duct junctions, able to self-renewal and repopulate

injured regions. Because they express HGF and MET, it is proposed that aberrant MET activation promote lung tumorigenesis or aid tumors to resist therapy [162-165].

7.3 MET and gastric cancer

The most common form of stomach malignancies is gastric adenocarcinomas (GAC) [166, 167]. After lung, breast, colorectal and prostate cancers, GACs is the fifth most diagnosed cancer and causes roughly 700,000 deaths/year worldwide [166]. As other cancers, GACs is a heterogeneous disease which can be categorized based of molecular, histological or anatomical profile [166, 167]. Early stage I and II GACs are successfully treated with surgical resection and chemotherapy [166]. On the other hand, patients with late stage III and IV GACs have median survival of 8-10 months and approximately 15% survival rate even with high doses of chemo-and-radiotherapy [167]; the reason for poor response in advanced GACs is due to its ability to metastasize to proximal and distal sites with high efficiency [166]. Indeed, most common organs for GAC metastasis are liver, peritoneum, lymph nodes, bone and lung (figure 1.13).

H. pylori is a well-known risk factor for GACs [168]. *H. pylori* causes gastritis due to inflammatory response resulting in destruction of cells lining the cavity of gastric lumen [168]. Thereafter, gastric stem cells differentiate and proliferate to restore the damaged tissues [168]; at this point, aberrant proliferation can lead to GACs due to mutations in tumor suppressor or cell cycle-related genes, such as *TP53*, *PTEN, CDK2 or retinoblastoma (RB)* [167].

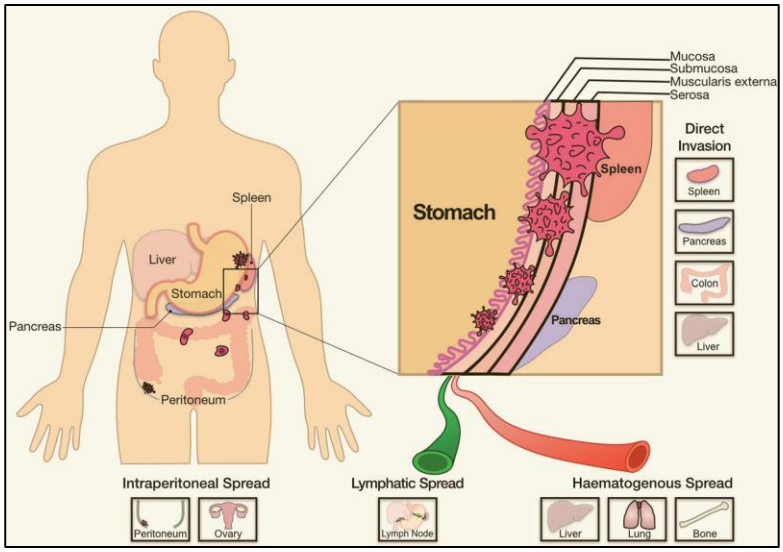

Figure 1.13: Metastatic sites of Gastric cancer. reprint with permission from [166]

In addition, aberrant MET activation is reported in ≈20% of differentiated GACs and scirrhous gastric cancer [169]. Main source of overactive MET in GACs is gene amplification and activating mutation [146, 170, 171]. Indeed, increase in MET expression is commonly identified in precancerous lesions in the stomach [172]. For example, recent studies reported correlation of MET expression in GACs to disease progression and metastasis to lymph nodes, liver and lung [173, 174]. Furthermore, the same group also detected increase in MET mRNA is peripheral blood, possibly from metastatic cells traveling to distal organs suggesting MET promotes GAC metastasis [173]. Notably, recent analysis of 120 tumors with immunohistochemistry reported phosphorylated MET (pMET) in approximately 60% in these samples [175]. Moreover, pMET immunostaining was associated with metastasis to lymph nodes, disease stage and poor prognosis [176].

Albeit less frequent, activating point mutations, slice variants such as the exon 14 skipping isoform and R988C, T1010I, S1058P mutations have been identified in GAC [176,

177]. All of these alterations promote aberrant signaling by rescuing MET from degradation and their precise mechanism were described above in sections 4.1 and 6.2.

7.4 MET and pancreatic cancer

Pancreas consists of enzyme-secreting acinar cells, bicarbonate-secreting ductal cells, hormone-secreting endocrine islets and fairly inactive stellate cells [178]. Common form of cancers of pancreas are ductal adenocarcinomas (PDAC) which arise from epithelial layer of pancreatic duct, whereas less common forms are neuroendocrine tumors and acinar carcinomas. PDAC (figure 1.14) presents a health risk with over 100,000 cases reported worldwide in 2016 [178]. The overall 5-year survival rate of patients with late stage PDAC is <10%. Several reasons contribute to poor prognosis [178]; PDAC is commonly diagnosed at late stages due to nonspecific symptoms and difficulties imaging

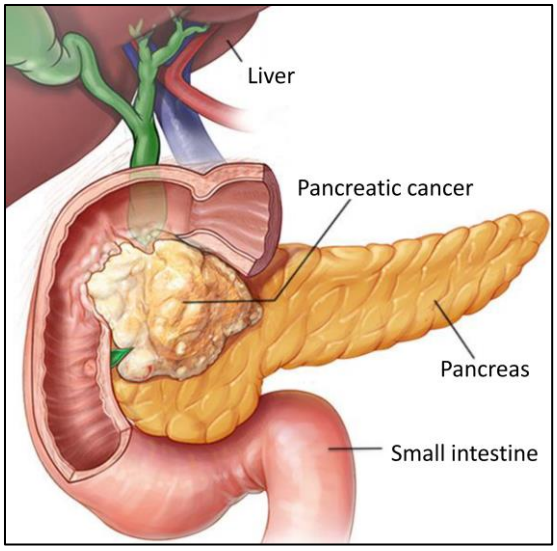

Figure 1.14: Aggressive pancreatic cancer and surrounding organs. reprint with permission from [178]

tumors at early-stage. For these reasons, PDAC is an aggressive form of all cancers with early metastases to surround organs that prevent surgical resection [178]. Conventional treatment regimen for PDAC patients is nucleotide analog, gemcitabine in combination

paclitaxel; however, resistance develops within weeks due to intrinsic genetic factors or acquired mechanisms [178, 179]. For the latter, de novo activation of signaling pathway, such as MET, modulate crosstalk between tumor and microenvironment [179].

PDAC harbors numerous oncogenic genetic alterations and have complex tumor microenvironments promoting tumor growth and metastasis [178]. Indeed, multiple reports have described role of cancer-associated fibroblasts (CAFs) and pancreatic stellate cells (PSCs) in PDAC metastasis [180-185]. Within tumor, CAFs and PSCs deposit excessive fibrous material into microenvironment forming stiff desmoplastic extracellular matrix (ECM) [186, 187]. This form of ECM prevents tumor angiogenesis thereby preventing uptake of nutrient and therapeutic agents [187-189]; notably, absence of blood vessels promotes hypoxic conditions, early metastasis and drug resistance [190, 191]. Finally, dense ECM serve as a reservoir for growth factors which orchestrate aggressive nature of PDAC.

Recent approaches to develop effective drugs for PDAC involves detecting tumor specific biomarker [178]. Biomarkers can aid in identifying subgroups within PDAC patients for personalized medicine with a focus on targeting microenvironment in addition to primary tumor [189]. Once such recently identified biomarker and therapeutic target is MET receptor for PDAC [179].

Multiple studies have targeted MET in PDAC because of its contribution in PDAC progression [179, 192-194]. High expression of HGF in tumor stroma is related to poor survival rate for PDAC patients [192]. While loss of or mutations in *KRAS*, *TP53* and *p16*

are considered initiators of pancreatic cancers, aberrant MET activation is associated with PDAC's aggressive phenotype: tumor growth and metastases [193, 195]. In comparison to normal adjacent tissues, MET expression is significantly higher in PDAC lesions [196, 197]; recently, this expression pattern was correlated to DYRK1A kinase, a regulator of MET turn-over [198]. Furthermore, MET expression directly effect PDAC tumor grade which supports metastatic function of MET [196].

Moreover, studies have demonstrated that PSCs and CAFs can migrate together with PDAC cells to proximal or distal metastasis [180, 182]. This evidence proposes a heterogeneous PDAC in the primary and metastatic sites where HGF-MET auto/paracrine loops in the microenvironment can contribute towards tumor dissemination [188, 197]. Lastly, MET signaling in stromal mesenchymal cells promotes HGF secretion from CAFs resulting in a positive feedback loop [179, 199].

Irregular MET signaling in PDAC contributes to drug resistance via several mechanisms [188, 191, 196]. MET expression is detected in pancreatic cancer stem cells (P-CSC) and HGF-MET loop contribute towards mesenchymal system in the stroma [200, 201]. Recent preclinical studies inhibiting MET activation suppressed cell survival, migration and invasion in naïve or gemcitabine resistant P-CSC [201, 202]; furthermore, markers for EMT, which were detect in drug resistant P-CSC, were reduced with MET inhibition [202]. Lastly, MET inhibition with monoclonal antibodies in PDAC mouse model restored sensitivity to cancer therapy [179].

7.5 MET and tumor angiogenesis

Angiogenesis refers to formation of blood vessels from present vasculature. Irregular sprouting of new vessels contributes to several diseases, such as cancer, arthritis, glaucoma, macular degeneration [203]. Angiogenesis is promoted by numerous growth factors and their receptors. In solid malignancies, a critical factor for angiogenesis is signaling pathway of vascular endothelial growth factor (VEGF) and its receptor VEGFR [204]. Indeed, inhibiting VEGFR signaling with antibodies against VEGF or VEGFR suppressed angiogenesis in tumor mouse models [205, 206]; in addition, same outcome was demonstrated with the use of small molecule tyrosine kinase inhibitor (TKI) for VEGFR [206]. Hence, FDA has approved Inhibitors of VEGF or VEGFR for use in treatment of cancer patients. Bevacizumab, an antibody against VEGF, was the first drug approved to inhibit tumor angiogenesis in 2004 [207]. Thereafter, non-selective TKI, sorafenib and sunitinib, which can inhibit VEGFR were approved in 2005 and 2006 respectively [208]. Unfortunately, VEGFR inhibitor cannot remove all blood vessels and eventually progression of angiogenesis is restored [209]. Therefore, identification of additional target to suppress angiogenesis is critical to develop effective therapies.

One such promising target is HGF-MET signaling pathway [210]. Multiple studies have established that MET activation promotes endothelial cell proliferation and angiogenesis in vitro and in vivo [211, 212]; furthermore, MET activation leads to increase in VEGF expression and vessel formation through SRC, which is a adaptor protein for both

VEGFR and MET [213]. Synergistic effect of MET and VEGFR pathway in endothelial cells and angiogenesis was demonstrated by multiple groups [211-214]. The reason for this synergy is not due to physical interaction or transphosphorylation, but rather activation of common signaling cascades such as RAS-MAPK, PI3K-AKT, and STAT3 [214]. Indeed, use of MET TKIs in tumor mouse models significantly reduced number of blood vessels in addition to tumor growth [215, 216]. In line with these finding, recent reports have shown modulation of MET expression in hypoxic conditions. Hypoxia occurs during low nutrient state and promotes expression of hypoxia-inducible factor 1α (HIF1α), a transcription factor [217, 218]. Several reports have identified MET as transcriptional target of HIF1α in various types of solid tumors [218-220]. Hence, VEGFR inhibitor can reduce tumor vasculature but increase expression on MET in HIF1α dependent manner to restore blood vessel formation. Moreover, since MET can promote metastasis in multiple cancers, VEGFR inhibitors can promote spreading of tumor cells. For these reasons, it is argued to combine anti-angiogenic and MET inhibitors to reduce tumor burden. Recent preclinical studies have tested this concept in mouse xenograft models [215]; these experiments show promising effect with combinatorial inhibition of MET and VEGFR; the combine inhibitors not only suppress blood vessel formation and tumor mass, but also reduced number of metastatic lesions.

7.6 MET and Metastasis

Metastasis is a foremost hurdle in treatment of cancer and remains the most common cause of deaths in cancer patients. Metastatic cells migrate beyond their borders, invade juxtapose tissues, and colonize proximal or distal organs (figure 1.15).

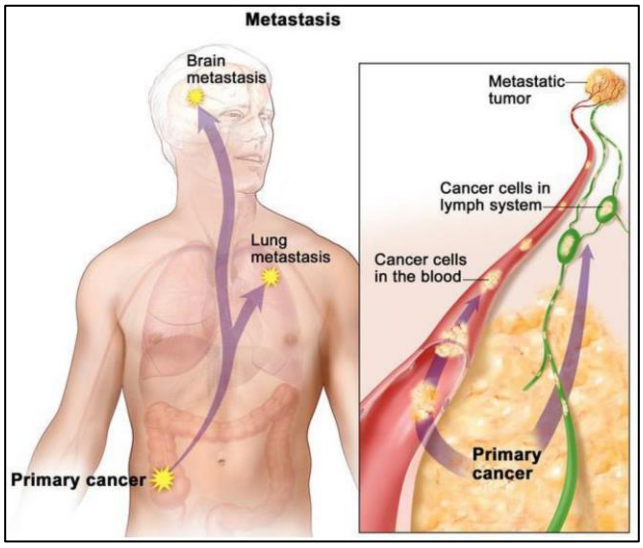

Figure 1.15: Brain and lung metastasis via blood and lymph vessels. [cancer.gov]

Metastatic cells use blood or lymphatic vessels to populate environment favorable to proliferation and angiogenesis. Metastatic dissemination is orchestrated via complex mechanism [221]: (1) cancer cells enter EMT; (2) dissociate from primary tumor; (3) invade adjacent tissue; (4) intravasate blood and lymph vessels; (5) migrate through vessels; (6) extravasate from vessels; (7) proliferate, survive immune response and induce angiogenesis to form a metastatic colony. Each of these steps are collection of multiple processes and can occur on a timescale of minutes to hours [221]. Moreover, it can take years to form detectable metastatic lesion.

Proteins which promote invasion of adjacent tissues and propagate supportive microenvironment are considered metastatic initiating gene. Loss of cell-to-cell adhesion molecule, E-cadherin, is a prerequisite to enter EMT which can be induced by key cell surface receptors including notch, hedgehog and certain RTK, especially MET [5, 11, 221].

MET's contribution to metastasis has been extensively investigated since its initial discovery in 1984 [1, 2]. MET can activate RAS-MAPK and STAT3 pathway to promote

angiogenesis, migration and invasion [11, 162]. Multiple studies have utilized MET-dependent cancer cells xenografts to characterize its metastatic potential [11]; collectively, these studies show that MET is responsible for metastases to multiple sites depending on type of cells used for xenograft [162, 165, 174]. Furthermore, several reports have showed MET amplification from metastatic lesions from mouse models for lung, brain, and pancreatic cancers. Indeed, the association of MET and metastatic progression is well-known for patients suffering from lung, gastric, pancreatic, and renal cancers [7, 67]. Hence, MET is an attractive target to prevent metastases. As a proof of concept, Kucerova et al reported reduced frequency of metastasis with MET TKI in an *in vivo* lung colonization assay with hyper-metastatic human melanoma cells [222]. Moreover, Basilico et al recently demonstrated reduction in lung metastases with MET inhibition utilizing orthotopic pancreatic mouse model [223].

7.7 MET and cancer stem cell

EMT transform cancer cells to mesenchymal state. This transition is correlated to high frequency of cancer stem cells (CSC) [224]. Depending on the type of cancer, CSC represent variable portion of tumor cell population. Just as adult stem cells, CSC have the ability to self-renew and differentiate to multiple cell types [224]. However, only CSC, not normal stem cells, can efficiently reconstitute whole tumor after transplantation [224]. Therefore, the presence of CSC in tumor have implications for cancer therapy.

Developmental signaling pathway, such as MET, play an integral role in maintenance and self-renewal of normal stem cells and CSC [225, 226]. Functional

characterization of HGF-MET signaling in mesenchymal and hematopoietic stem cells was recently demonstrated [226, 227]. For example, Urbanek et al demonstrated MET activation induces motility and migration of cardiac stem cells after myocardial infarction [228]. In addition, Yamada et al showed presence of MET activity in skeletal muscle and how it can activate satellite cells, muscle progenitors [229]. Furthermore, HGF-MET autocrine/paracrine loop is enriched in hepatic stem cells during liver regeneration after injury and is important to stem cells of adult and developing pancreas [201, 230].

In cancer, studies have demonstrated important role of MET in self renewal of colon CSC [231]. These CSC rely on stromal fibroblast for HGF; this HGF engages MET on colon CSC to promote WNT-β-catenin signaling and maintain stemness [232-234]. Similar to previous example, cooperative signaling between MET and WNT-β-catenin pathways are implicated in CSC from multiple forms of tumor [235, 236]. For instance, overactivation of MET and WNT was reported for multiple myeloma and suppression of either pathway prevented myeloma cell proliferation [237, 238]. In addition, WNT signaling activated by autocrine or paracrine HGF-MET loop promoted human breast cancer metastasis to the bones [239-241]. Lastly, stromal HGF-mediated MET activation in NSCLC patients increase tumor burden and lower prognosis [242-244]. With many examples, it stands to reason that more examples of cooperative signaling may exist between MET and other pathway, such as notch or hedgehog, in maintaining CSC.

7.8 MET crosstalk with receptor of EGFR family in cancer

In cancers, MET and receptor in EGFR family are often co-expressed [102, 245]. EGFR-dependent MET activation was demonstrated with EGFR ligand, EGF or TGFα [245]. On the other hand, EGFR phosphorylation is reported with HGF stimulation in gastric, NSCLC and breast cancer cell lines which express of both receptors [102]. Use of both HGF and EGF to stimulate cells enhances activation of several downstream pathways – PI3K-AKT, and RAS-MAPK [102]. Furthermore, physical interaction between MET and EGFR was recently confirmed with co-immunoprecipitation experiments in human squamous cell carcinoma and lung cancer cells [246]. These studies support transactivation and initiation of downstream pathway through a heterodimeric MET-EGFR complex.

Indirect cooperative interaction can also occur between MET and EGFR [101, 247, 248]. For example, MET activated SRC can activate EGFR and its downstream signaling pathways [248-250]. Furthermore, HGF-MET pathway can increase transcription of heparin binding EGF like growth factor (HB-EGF), an EGFR ligand, to induce activation of EGFR in glioma cells [251]. Conversely, activated EGFR regulates shedding of MET ectodomain leaving behind an oncogenic membrane bound cytoplasmic portion [252]. indeed, MET lacking extracellular domain was able to transform NIH 3T3 cells to be more proliferative and invasive [253]. Likewise, EGFR TKI gefitinib can prevent HGF-dependent proliferation, cell scatter, and invasion in multiple mammary carcinoma cell supporting the concept of MET EGFR crosstalk [254, 255].

MET phosphorylation can also be induced in a ligand-independent manner by EGFRvIII isoform in gliomas [256-259]. Indeed, MET activation in glioblastomas correlates with expression levels of EGFRvIII isoform [258, 259]. Xenograft of cells expressing both

MET and EGFRvIII require inhibition of both receptors to suppress tumor growth [258, 259]. Similarly, effective growth inhibition of NSCLC cells and their xenografts requires inhibitors targeting MET and EGFR, highlighting EGFR-MET collaboration in disease progression [260, 261].

In addition, multiple studies have reported functional interaction between MET and other EGFR family members – HER2 [262]. increase MET expression in HER2-amplified breast cancer was reported suggesting cooperative signaling between these two receptors [263, 264]. For example, MET inhibition in MET-amplified gastric cancer cells abrogates basal levels of HER2 phosphorylation [265, 266]. MET and HER2 cooperative signaling enhances invasion and EMT of epithelial cells in *in vitro* three-dimensional cell culture assay [267]. Combinatorial inhibition of HER2 and MET with transtuzumab and MET TKI, SU11274, in breast cancer cells enhanced suppression of AKT and ERK pathway and inhibit proliferation compared to single treatments [268].

7.9. MET as mechanism of resistance in cancer

The main hurdle to long term utility of and response to target therapy is mechanism of resistance. Due to its ability to crosstalk with other receptors as outlined above, MET activation as a bypass pathway has emerged as a common resistance mechanism for numerous types of malignancies (figure 1.16). Accumulation of several studies have explained the unique role of MET as bypass pathway to sustain survival, proliferation, promote EMT, and evade treatment [269]. Resistance emerges to inhibitors for RTKs, such as EGFR, HER2, PDGFR, or IGF1R, because of MET activation has been reported in multiple

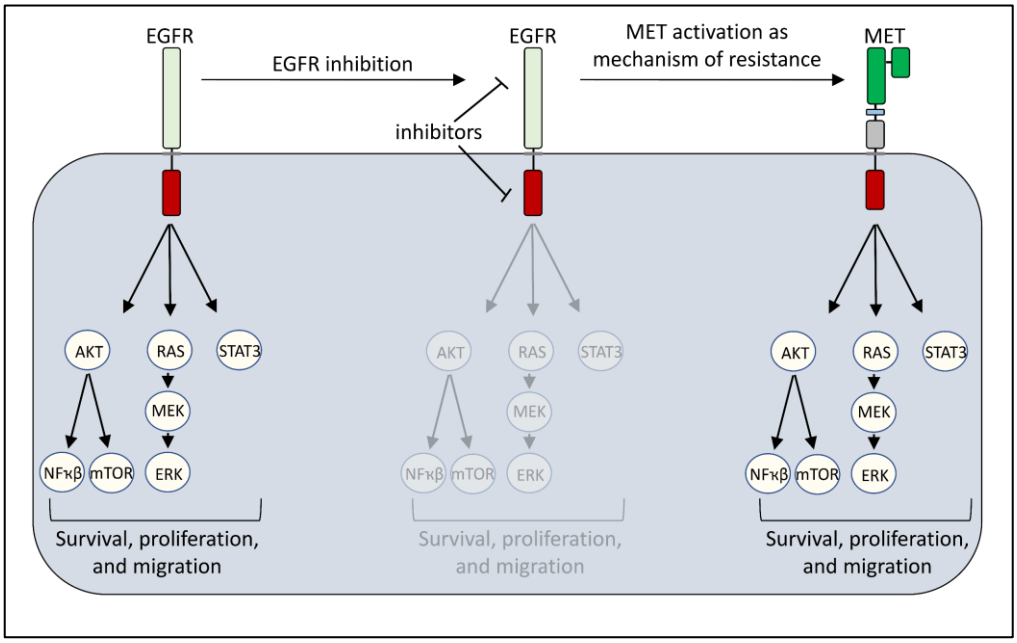

Figure 1.16. Mechanism of resistance to EGFR inhibitors with MET activation. Constitutive activity due to MET amplification or mutation in intracellular domain are contributing factors to resistance mechanism.

cancers [269]. For example, MET amplification can activate PI3K–AKT and RAS-MAPK signaling in lung, gastric or brain cancers with EGFR mutants that are resistant to EGFR TKI [270-273]. *MET* amplification is frequently detected in patients with lung cancer who develop resistance to the EGFR TKI gefitinib. Indeed, MET was activated in resistant clones derived from *in vitro* selection against gefitinib in NSCLC cells [157]; this MET-mediated resistance activated ERBB3 signaling to PI3-AKT pathway for survival and proliferation in presence EGFR-TKI [23]. Also, MET inhibition in erlotinib-resistant NSCLC cells results in cell death in vitro and reduction of tumor growth *in vivo* [274]. In these studies, Gefitinib and erlotinib resistance was due to MET amplification; MET amplification resulted in MET overexpression, HGF-independent MET phosphorylation, and activation of downstream

signaling [19, 23, 274, 275]. Moreover, an alternative mechanism is reported to bypass EGFR inhibition with MET receptor; in EGFR-TKI resistant breast cancer cells, MET-SRC complex mediated EGFR phosphorylation [276]. These phosphorylated EGFR favored binding of adaptor proteins to initiate PI3K-AKT pathway in the presence of EGFR TKI providing a multiple resistance mechanism facilitated by MET [276].

MET and EGFR may play a redundant role in cancer. For example, a switch to MET dependency was observed with EGFR inhibition, whereas cells reverted back to EGFR addiction with MET inhibition [101, 257, 277]; this concept was confirmed in gastric cancer and glioma cells [257, 266]. Indeed, concomitant treatment of gefitinib-resistant gastric cancer cell xenografts with gefitinib and MET inhibitor is necessary to inhibit cell growth and blood vessel formation [278]. Likewise, dual inhibition of EGFR and MET is vital to inhibiting AKT, ERK, and STAT3 pathways to produce complete regression of lung cancer cell xenografts [266]. Furthermore, MET protein expression is elevated in response to HER2 inhibitor, transtuzumab, in breast cancer cells with HER2 overexpression suggesting MET may compensate in context of HER2 inhibition [264].

Hence, all these evidence supports attractive option in combination of MET inhibitor with drugs targeting receptors in EGFR family to improve tumor response.

8. Current approaches for MET inhibition in cancer

Better understanding of HGF-MET structural interactions and molecular mechanism leading to downstream signaling has permitted development MET targeting drug for cancer therapeutics. MET targeting compounds are categorized into four broad

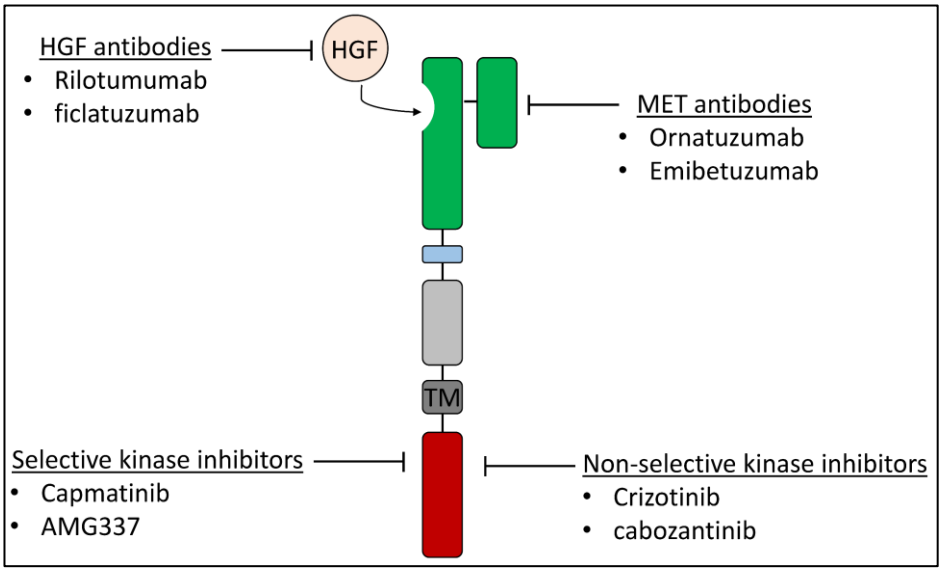

Figure 1.17. Current approaches to target MET receptor.

class of inhibitors (figure 1.17). Two classes are biologic compounds: HGF neutralizing antibodies and antibodies against MET ectodomain to prevent ligand binding and receptor dimerization; the remaining two classes are non-selective or selective small molecule tyrosine kinase inhibitor (TKI). Multiple MET biologics and TKI have entered clinical trial with variable success (table 1.2). Large fraction has failed due to toxicity or lack of efficacy [279]. Furthermore, after some period of favorable response, resistance emerged from either reliance of bypass RTK or mutation which rendered the inhibitor ineffective.

8.1 HGF antibodies

HGF neutralizing antibodies was initially developed by Vande Woude and colleagues to inhibit growth in glioblastoma (GBM) cancer cell [280]. More importantly, with a collection of HGF antibodies, previously described HGF-MET autocrine signaling in

GBM was suppressed resulting in impaired GBM cell xenografts. Subsequent studies have described individual HGF monoclonal antibody to block HGF-MET binding [281]. Multiple HGF antibodies, rilotumumab and ficlatuzumab, were evaluated in clinical trials to evaluate their safety and efficacy in advanced or metastatic gastric, lung, and head and neck cancer [282, 283]. However, rilotumumab trial was discontinued due to lack of efficacy because more deaths observed with HGF antibody compared to control arm. As for ficlatuzumab, clinical trials also yielded unfavorable results with no significant improvement in progression free survival [279].

8.2 MET antibodies

Many of the initially designed MET antibodies were bivalent and resulted in receptor crosslinking and activation of downstream pathways [27]. For this reason, monovalent onartuzumab antibody was developed by Genentech [284]. onartuzumab binds SEMA domain, prevented HGF-mediated MET signaling, and reduced tumor size in GBM cell xenograft mouse model [284]; furthermore, tumor growth was abolished in

Table 1.2. Summary of selected clinical trial with MET

Drug	Mechanism	Phase	Tumor types	Comments
Rilotumumab	HGF antibody	III	Gliomas, colorectal, gastric, and esophageal cancers	Failed due to lack of efficacy
Ficlatuzumab	HGF antibody	II	Recurrent metastatic NSCLC	Failed due to lack of efficacy
Onartuzumab	MET antibody	III	NSCLC and hepatocellular cancers	Failed due to lack of efficacy
Emibetuzumab	MET antibody	II	NSCLC and gastric cancers	
Crizotinib	Non-selective TKI	II	NSCLC, urothelial, gastric cancers	Approved for +ALK NSCLC; resistance detected in patients
Cabozantinib	Non-selective TKI	II, III	NSCLC, colorectal, and head and neck cancers	Approved as angiogenic inhibitor
Capmatinib	Selective TKI	I, II	NSCLC and head and neck cancers	
AMG337	Selective TKI	II	Gastric and esophageal cancers	Failed due to lack of efficacy

orthotopic xenograft of pancreatic cells [285]. Unfortunately, onartuzumab phase III clinical trial was stopped because of lack of efficacy and further development of this antibody has been halted [286]. Emibetuzumab, alternative to onartuzumab, sequester HGF and binds MET to promote internalization and degradation [287]. In preclinical mouse xenograft models, emibetuzumab prevented HGF-dependent and independent tumor growth [287]. Emibetuzumab phase II clinical trial are ongoing and phase III have not started. Hence, it is too early to determine emibetuzumab effectiveness in patients.

8.3 MET kinase inhibitors

TKIs are the predominant MET inhibitor in clinical trials. MET TKIs fall into two categories, type I (AMG337, capmatinib, crizotinib) and type II (cabozantinib). Type I TKIs are ATP competitors while type II TKIs bind at allosteric position to prevent active conformation of ATP binding pocket [288]. To date, selective MET inhibitors have failed in clinical trial due to lack of efficacy; for example, AMG337 entered clinical trials because of its success in suppressing tumor growth in GBM, gastric cancer and hepatocellular xenografts in preclinical studies [289, 290]; however, AMG337 progress in clinical trial have halted due to lack of efficacy in phase II.

Unlike selective TKIs, non-selective have fared better in clinical trials with FDA approval of crizotinib and cabozantinib. Unfortunately, their approvals were for their ability to target another oncoprotein.

For example, crizotinib is approved for +ALK positive NSCLC while its utility in MET dependent tumor is being test in phase II in +MET NSCLC and gastric cancer [279, 291].

However, multiple reports have described resistance to crizotinib in MET-dependent tumors in patients and preclinical studies [292, 293]; in addition, emergence of resistance was due to activation of bypass RTK, such as EGFR, or mutation in kinase domain preventing crizotinib binding to MET [294].

Cabozantinib is a non-selective inhibitor for MET, VEGFR2, FLT3, c-KIT, and RET [295, 296]. It is approved as an anti-angiogenic drug due to its ability to block VEGFR2 [295]. Currently, this compound is being tested in early stages of clinical trials for +MET gliomas, NSCLC, liver, renal, colorectal and head and neck cancers. However, recent preclinical studies have already identified multiple mechanism of resistance to cabozantinib [297, 298]. For example, Fuse et al report IGF1R as a bypass pathway to evade cabozantinib treatment in colorectal KM12 cell line [297]. Furthermore, Wu et al identified multiple mutations in RET's kinase domain which prevents cabozantinib inhibition [298]. For this reason, it stands to reason that targeting MET-dependent tumor with cabozantinib will eventually develop resistance. Hence, novel alternative approaches (outline in following section) are necessary to inhibit MET receptor.

9. Alternative approach to targeting MET receptor

Multiple groups have utilized a recombinant MET extracellular domain to suppress MET activity in preclinical studies [53, 223, 299]. Because the lack of transmembrane and intracellular domains, this MET isoform is secreted into extracellular space and inhibits FL-MET by binding to HGF and dominant negative engagement of residual FL-MET (figure 1.18).

In my thesis, I demonstrate that this soluble decoy MET (sdMET) isoform is due to intronic polyadenylation (IPA); IPA is U1-snRNP-dependent mechanism for an alternative 3' pre-mRNA processing to express variety of natural isoforms from a single gene [300]. For MET, I describe nine sdMET isoforms generated from IPA. These isoforms are able to bind HGF and suppress MET signaling pathways. Importantly, activation of IPA is

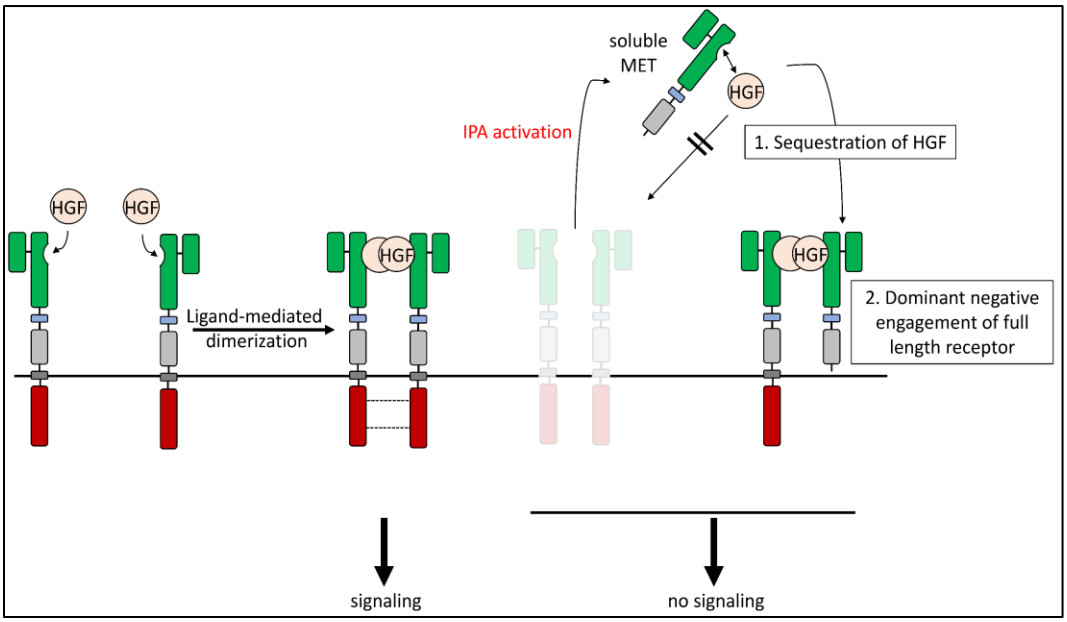

Figure 1.18. Activation of intronic polyadenylation (IPA) in MET receptor. IPA remove full-length (FL) MET and expresses soluble decoy MET which sequesters ligand and suppress activity of residual FL-ME**T.**

demonstrated by using splice switching anti-sense oligonucleotides (ASO). Hence, ASO can be used to covert oncogenic FL-MET to a therapeutic sdMET isoform.

The following chapter extensively describes constitutive and alternative pre-mRNA splicing and 3' processing. Examples of disease associate with aberrant splicing is described and how ASO is utilized to correct this molecular defect. Lastly, chapter 2

outlines pivotal preclinical studies conducted by Cartegni group and others who use ASO to generate isoforms for cancer therapeutics.

Chapter II

Therapeutic use of anti-sense compounds

1. Introduction

Genes are made up of exons and intervening introns. Pre-mRNA processing assists cells in understanding our transcribed genetic code. In eukaryotes, pre-mRNA processing consists of splicing and polyadenylation to produce exon containing mRNA; in addition to helping interpret genomic message, mechanism of pre-mRNA processing expand transcriptome and add cadre of proteins from a single gene [301-303]. If this mechanism is deregulated, it can have a devastating effect on mRNA or protein stability and lead to pathologies that can cripple life [303].

In this chapter, alternative splicing and polyadenylation is described with their emphasis on disease causing events that can be corrected by anti-sense-based approach. In the last section, a strategy is described that utilizes anti-sense oligonucleotides (ASO) to activate intronic polyadenylation to generate therapeutic isoform for cancer therapy.

2. pre-mRNA splicing

Pre-mRNA splicing removes introns and ligates exons to generate mRNA for ribosomal translation. Any error in the process causes disconnect between coding gene and their translated protein. For this reason, splicing must be efficient and accurate for proper gene expression and avoid producing non-functional or pathogenic proteins [303]. Spliceosome, a complex and dynamic macromolecule consisting of hundreds of proteins and small RNAs, catalyzes pre-mRNA splicing. Its complexity allows it to achieve specificity given diverse sequence elements that define exons and introns.

Conserved sequence motifs which define exons and introns are core cis signal elements comprised of 5'splice site (ss), 3'ss, branchpoint sequence (BS), and polypyrimidine tract (Figure 2.1). These sequence elements demarcate exons and are recognized through

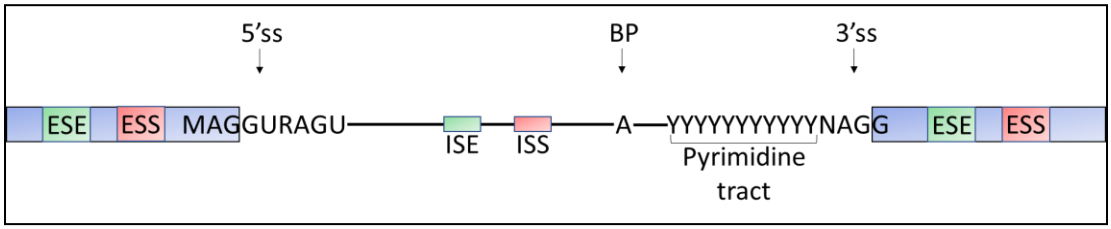

Figure 2.1. Schematic of two-exon gene with their consensus splice site and enhancers and silencers. Conserved motifs of 5' splice site (ss), and 3'ss. Both splice site consists of invariant dinucleotide (GU at 5'ss and AG at 3'ss) surrounds be consensus sequence. Also, shown are ESE – exonic splicing enhancer, ESS – exonic splicing silencer, ISE – intronic splicing enhancer, ISS – intronic splicing silencer, ss – splice site, BP – branch point adenine.

base-pairing interaction with small nuclear RNA of ribonucleoproteins (snRNPs), U1, U2, U4, and U5 [304]. These snRNPs are vital for orchestrating the splicing reaction (figure 2.2) [304]. U1 initiates splicing by binding to 5'ss. This is followed by U2 base pairing to BS and U4, U5, and U6 bridging 5' and 3' end of intron. In addition to snRNPs, other splicing factors, such as RNA binding proteins, regulate splicing by direct interaction with RNA is sequence-dependent manner. They can either enhance or silence splicing of exon and intron. Based on their location, these sequence elements are referred to as exonic or intronic splicing enhancer or silencers (ESE, ESS, ISE, ISS; figure 2.1) [302].

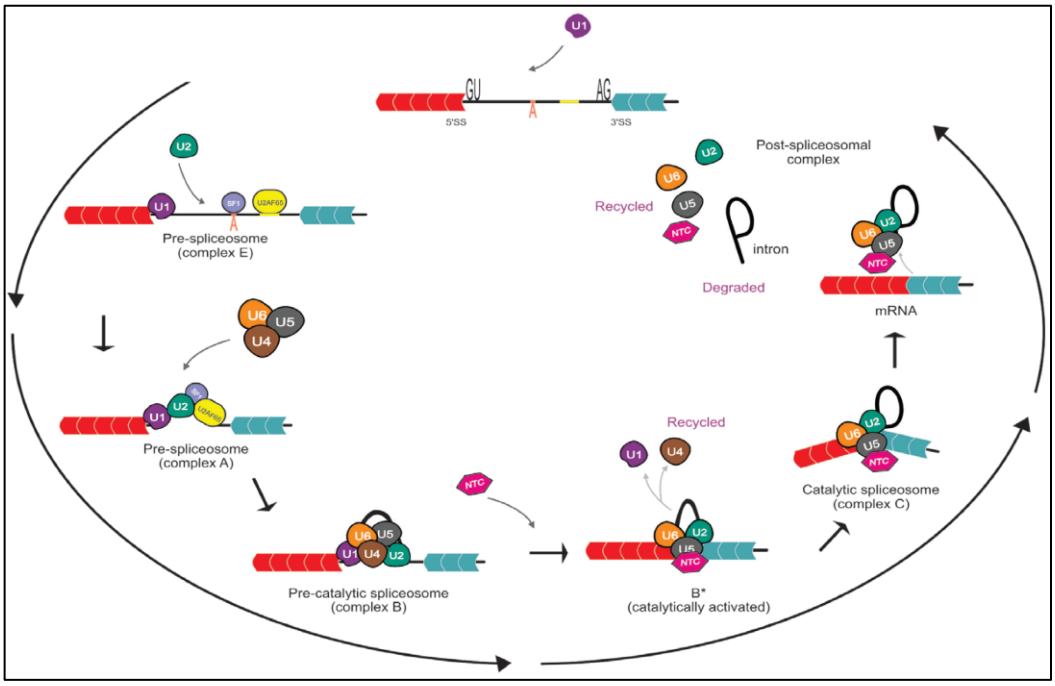

Figure 2.2. pre-mRNA splicing reaction. Splicing is initiated by U1 recognition of 5'ss and followed by U2AF binding to polypyrimidine tract to form complex E. U2 bridges U1 to U2AF to generate complex A. At this point, conformational change recruits U4, U5, and U6 to form complex B. Nineteen complex (NTC) binds complex B to form catalytically active complex B. U1 and U4 dissociate from splicing reaction to form complex C. the final catalytic step takes place in complex C which ligates exons together and splicing out intron as a lariat. Reprint with permission from [304].

2.1. Alternative splicing

Constitutive splicing predominates with strong splice sites. However, approximately 75% of exons are alternatively spliced to generate multiple distinct mRNA variants from a single gene (figure 2.3) [303, 305]. Most common form of alternative

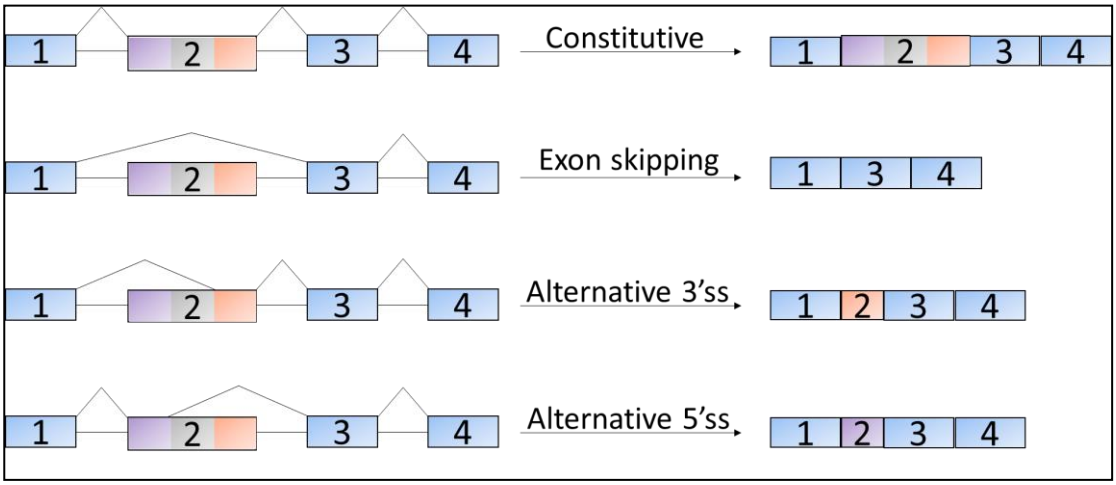

Figure 2.3. Examples of alternative pre-mRNA splicing.

splicing is exon skipping. Moreover, Spliceosome can also recognize alternative 5' or 3'ss in exon and intron [302]. In most scenarios, alternative spliced mRNA encodes proteins with either subtle or dramatic functional difference compared to wild type (WT) isoform [304]. Hence, alternative splicing plays a crucial role in contributing towards phenotypic diversity of higher eukaryotes [306]; it expands organism's proteomic profile without the need to increase overall number of genes. Because most pre-mRNA is alternatively spliced, it suggests most genes have intrinsic plasticity that helps modulate protein expression and their activity. Indeed, most exons are multiples of trinucleotide such that exon skipping maintains open reading frame (ORF) and contributes towards mRNA stability. This mRNA will encode for isoform with internal deletion of amino acids that were encoded by skipped exon. Many isoforms generated by alternative splicing have unique functions during developmental stages as well as in specific tissues- and cell type in adulthood [306]. Hence, precise regulation of pre-mRNA splicing is used to exploit functional variation of isoforms in spaciotemporal manner [306].

2.2. Splicing defects due to mutations

Mutations that disrupt splicing can lead to devasting diseases (table 2.1). It is estimated that such mutation account for third of all disease-causing mutations [303].

Table 2.1. Diseases due to splicing mutations

Disease	Gene	Mechanism	Splicing effect
Limb girdle muscular dystrophy	*LMNA*	5'ss mutation	Intron retention → PTC → NMD target
Familial dysautonomia	*IKBKAP*	ESE mutation	Exon skipping → frameshift → PTC → NMD target
Duchenne muscular dystrophy	*DMD*	Exon deletions and skipping	Exon skipping → frameshift → PTC → NMD target
Early-onset of Parkinson disease	*PINK1*	5'ss mutation; decrease U1 recruitment	Cryptic splice site usage → frameshift → PTC → NMD target
Frontotemporal dementia with parkinsonism	*MAPT*	5'ss mutation; increase U1 recruitment	Increase in exon 10 inclusion; altered 3R-Tau:4R-Tau
Spinal muscular atrophy	SMN2	Disruption of ESE sequence	Exon skipping → unstable isoform→ protein degradation

Because introns are non-coding, intronic mutations by default are categorized as splicing mutation. Majority of mutations in introns disrupt 5'-ss, 3'-ss, branch point sequence, or polypyrimidine tract in addition to creation of *de novo* alternative ss. Most intronic mutations usually cause exon skipping or intron retention. Furthermore, when WT-ss is mutated, cryptic-ss can be activated within juxtapose intron or exon [302]; cryptic ss is pseudo ss that are not recognized under normal context but can be used when surrounding sequence is altered [302]. Intronic mutation can also disrupt enchancer or silencer sequence and prevent their recognized by RNA binding proteins which contribute towards pre-mRNA splicing regulation (figure 2.4) [302, 305].

Exonic mutation can also affect pre-mRNA splicing. As in intronic mutation, mutations in exon can create *de novo* cryptic ss or disrupt enhancer or silencer sequences.

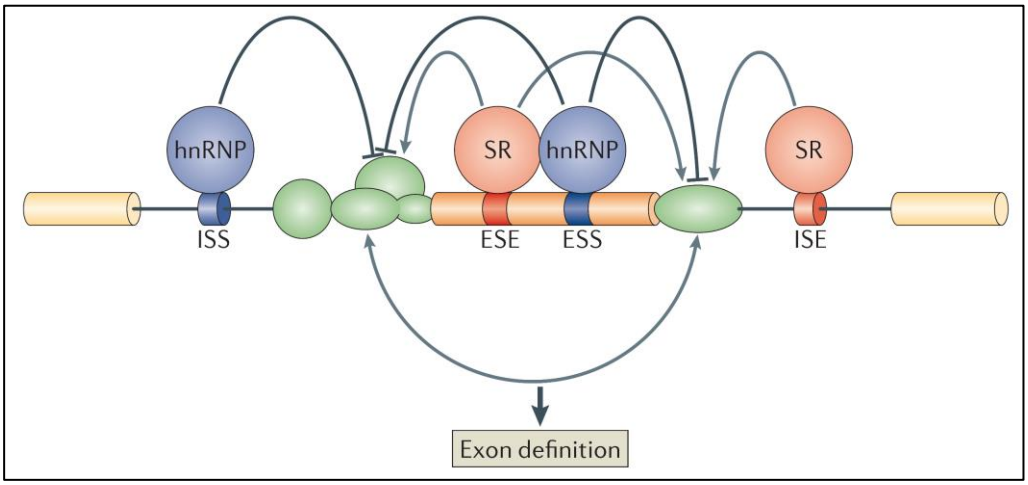

Figure 2.4. RNA binding protein recognize intronic or exonic enhancers and silencers to regulate pre-mRNA splicing. Reprint with permission from [305].

consequence of aberrant splicing is typically generation of unstable mRNA or quantitative switch from WT to alternative variant [303]. As in nonsense mutations, shift in ORF can possibly generate premature termination codon (PTC) that targets mutant transcript for degradation by nonsense mediated decay pathway (NMD), an mRNA surveillance mechanism that degrades PTC containing mRNA [307]. Hence, stability of mRNA with PTC is compromised and results in loss of WT protein. Furthermore, splicing mutation can possibly yield stable mRNA with deletion of vital coding sequencing that are required to produce functional protein [302]; in this scenario, as long as PTC is not included, ORF is maintained to generate NMD immune transcript resulting in a quantitative switch to a non-functional isoform [304]. Other culprit in aberrant splicing is non-functional splicing factors. In this case, splicing is deregulated in all RNA transcripts that require the affected factor for proper splicing [308].

For diseases due to splicing or nonsense/missense mutation, splicing redirection can prevent expression of pathogenic proteins [309]. For example, exon skipping can remove nonsense mutation and rescue protein expression even if the new transcript encodes isoforms with internal deletion; these isoforms may be partially functional

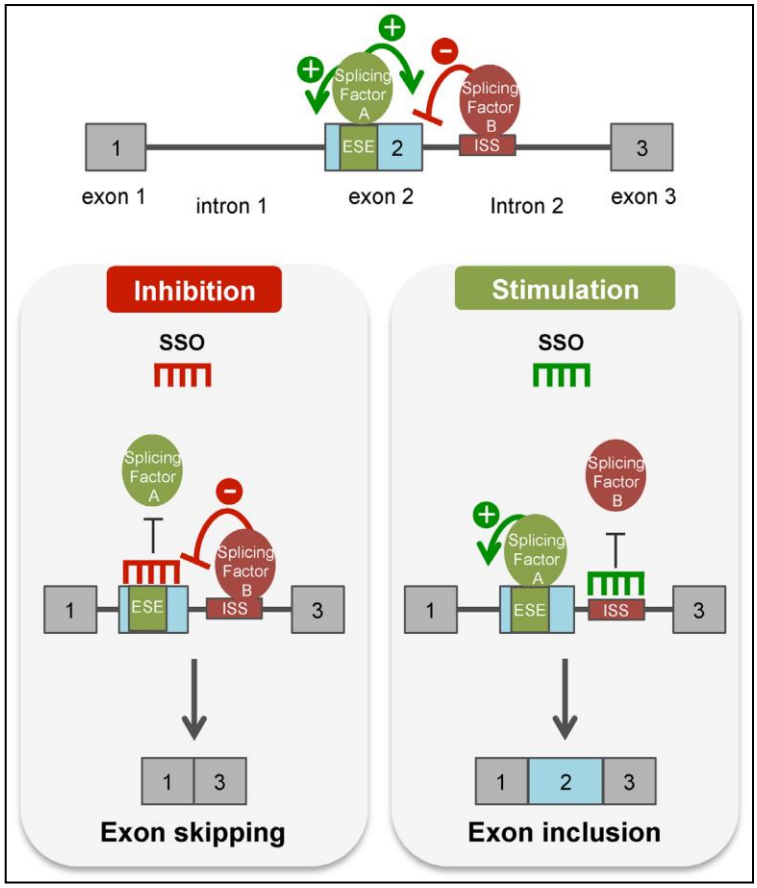

Figure 2.5. alteration of splicing with anti-sense oligonucleotides (ASO). Splice switching oligonucleotides (SSO) prevent splicing factors from recognizing their target sequence and can possibly induce exon skipping or exon inclusion. No shown are alternative events which can also occur, such as cryptic splice site activation or intron retentions. Reprint with permission from [310].

compared to WT but can alleviate disease phenotype. For this reason, anti-sense-based strategy can remove unwanted sequence or restore ORF and have significant impact in suppressing manifestation of otherwise devastating illness [310].

3. Splicing correction with anti-sense oligonucleotides

Anti-sense oligonucleotides (ASOs) are synthetic compounds made from nucleotides or their analogues that bind complementary sequence. The consequence of ASO base-pairing relies on chemistry of ASO and binding sequence [310]. Unlike RNA:DNA duplex that promotes RNAse H-mediated degradation of RNA, ASO nucleotides are chemically modified to prevent RNAse H recruitment and recognition [310]. This ASO feature is crucial since the goal is to alter splicing not promote mRNA degradation. ASOs are typically 15-35 nucleotides in length and sterically block splicing factors from interacting with their target sequence. Hence, ASOs alters ss recognition by spliceosome to generate mutant variant or restore WT mRNA (figure 2.5).

3.1. Type of anti-sense oligonucleotides

Natural oligonucleotides are unstable *in vivo* because they are degraded by nucleases in cells and serum [310, 311]; hence they are not useful for the purpose of splicing redirection. Chemically modified oligonucleotides improve base-pairing in addition to *in vivo* stability [310, 311]. Sugar components and/or phosphate backbone are common target for chemical modifications [312]. Phosphorothiate and phosphorodiamidate-based alterations are well studies form of synthetic

oligonucleotides and ASO with these modifications are currently approved for clinical use [312-314].

ASO with phosphorothioate modifications (figure 2.6, top) were the first to enter clinic for therapeutic purpose. Phosphorothioate-ASO have slightly less affinity to its target than its natural counterpart; however, it has better in vivo stability and greater resistance to nucleases [310, 315]. Furthermore, because phosphorothiate-ASO binds plasma proteins, it has improved retention and reduced clearance, thereby providing broad tissue distribution and increase in toxicity [312, 315]. Because phosphorothiate-ASO are not completely resistant to RNAse H, additional modifications are required; methyl or methoxyethyl modification at 2’ position on furanose sugar backbone is commonly used to prevent RNAse H-mediated degradation [314]. Furthermore, bridging of furanose sugar ring, referred to as locked nucleic acid, is another form of phosphorothiate-ASO modification [314]; LNA have higher binding affinity thereby allowing use of shorter sequence to minimize off target effect [311, 314]. All three modification are used in various combination to successfully alter splicing pattern for therapeutic purpose.

Another form of ASO modification is phosphorodiamidate morpholinos (MO) [312, 314, 315]. In this alteration, furanose sugar is replace by morpholine ring and negatively charge phosphodiester linkers are replaced by neutral phosphorodiamidate

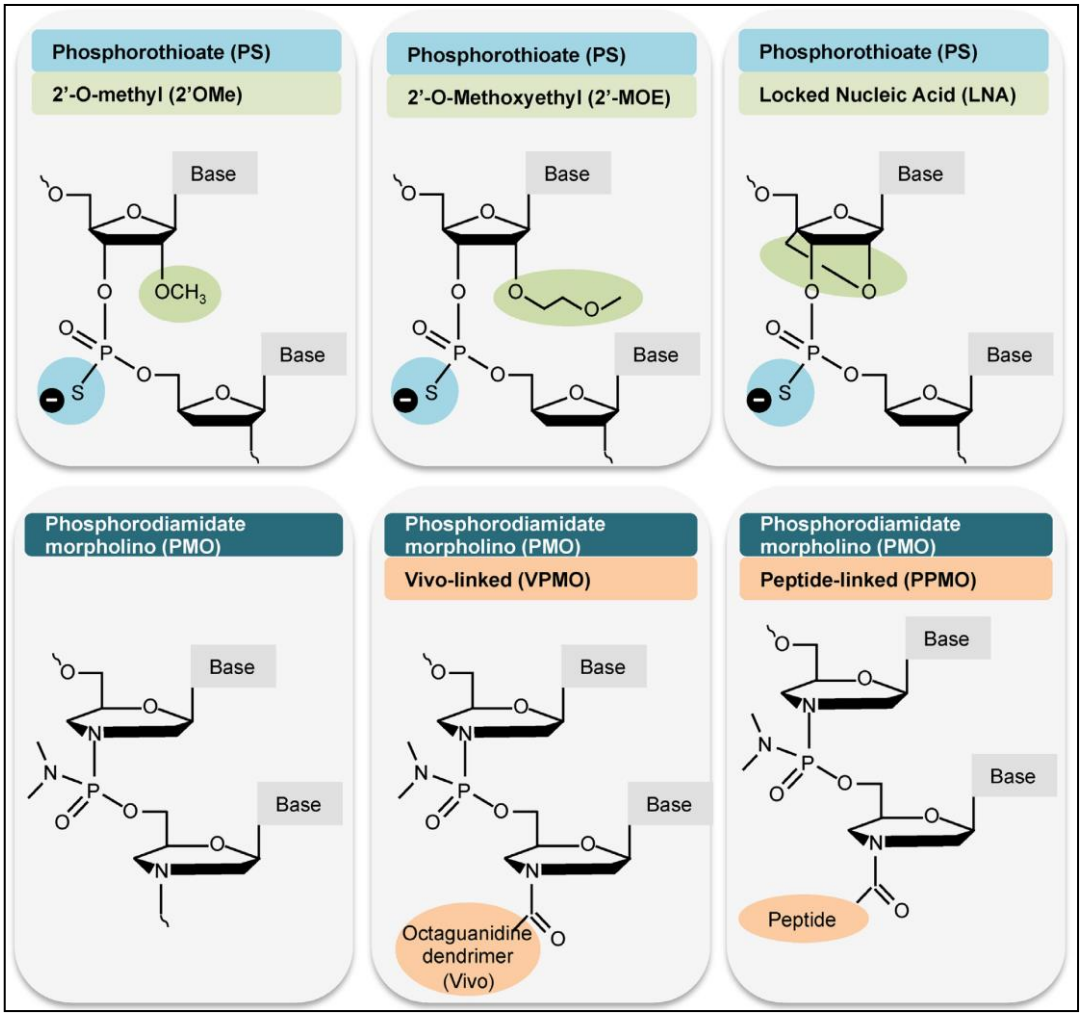

Figure 2.6. Types of ASO modifications. Reprint with permission from [310].

backbone (figure 2.6, bottom). MOs are better tolerated *in vivo* than phosphorothiate-ASO due to MO's neutral charge which prevents binding to plasma proteins; however, this property allows rapid clearance and high dose is required to achieve pharmacological response. To overcome this obstacle, further modification, such as conjugation of cell-penetrating peptides or octaguanidine dendrimer, is required to improve cellular delivery and efficacy.

The following two sections describe FDA approved ASOs that correct splicing to restore fully or partially functional protein and prevent disease manifestation.

3.2. ASO to treat Duchenne Muscular Dystrophy (DMD)

DMD is an X-linked neuromuscular disorder that affects 1 in 3,500 male births [316-319]. DMD is due to mutations in *dystrophin* gene that encodes structural protein in muscle cells. internal cytoskeleton is anchored to external microenvironment with molecular bridge provided by dystrophin, allowing tensile strength to maintain cellular morphology. Roughly 70% of patients suffering from DMD is due to mutation leading to exon skipping. Exon skipping in dystrophin pre-mRNA disrupts ORF and generates PTC

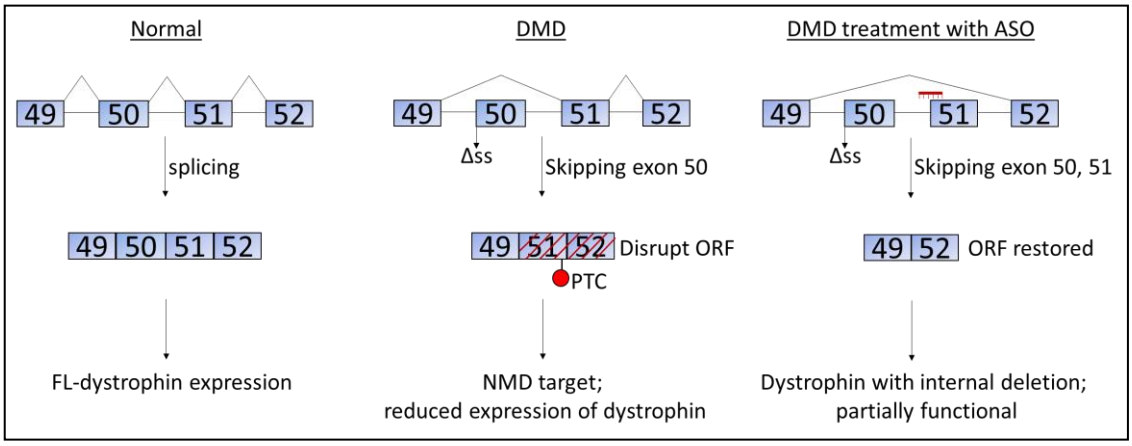

Figure 2.7. Dystrophin splicing in DMD and its correction with ASO. 3'ss mutation (Δss) promotes exon skipping which shifts ORF to generate PTC and target mutant transcript for degradation by NMD pathway. ORF can be restored by skipping exon 51 which can be induced by targeting 3'ss of exon 51.

that targets mutant transcript for degradation by NMD pathway, thereby reducing expression of WT protein (figure 2.7). Lack of dystrophin causes progressive muscle weakness beginning around 6 years of age and inability to walk by early teens. During their 20's, death can occur from respiratory muscle failure or cardiomyopathy.

Initially studies used *in vitro* minigene splicing assay to demonstrate ASO-induced exon skipping can restore ORF of RNA produced by minigene [320]. This was followed by ASO-mediated exon skipping to restore dystrophin expression in cells derived from DMD mouse model and DMD patient (figure 2.7, right) [321, 322]. Afterward, various groups used intramuscular, intravenous, and subcutaneous injections of ASOs with different chemistries to induce exon skipping in DMD mouse models to correct disrupted dystrophin ORF [317]. Importantly, weekly ASO injections were well tolerated and produced sufficient dystrophin protein to improve muscle functions.

Initiation of clinical trials with ASO in DMD patients followed promising preclinical studies. First compounded to be tested in clinical trial was 31-mer phosphorothioate-ASO which successfully induced exon skipping and increase in dystrophin protein [323]; unfortunately, phosphorothioate-ASO was sensitive to RNAse-mediated degradation lower its effectiveness. Ultimately in 2016, Sarepta's 30-nucleotide morpholino-based ASO, called exondys 51, was FDA approved for promoting exon 51 skipping to rescue dystrophin expression (figure 2.7, right) [324, 325]. In a four-year study of 12 patient treated with exondys 51, participants scored higher than patients created with placebo in 6-minute walk test and was accompanied by increase in dystrophin protein [324, 325].

3.3. ASO to treat Spinal Muscular Atrophy

ASO are also approved for spinal muscular atrophy (SMA). SMA is a degenerative disorder of motor neurons characterized progressive muscle weakness ultimately leading to respiratory failure [326]. SMA is a genetic disorder responsible for infant mortality and affects ~1:10,000 new born [326].

At the molecular level, SMA is due to inadequate expression of survival motor neuron (SMN) protein [326]. SMN is a pre-mRNA splicing factor which is highly conserved and ubiquitously expressed [327]. SMN protein can be produced by two genes, *SMN1* and *SMN2* [327]. Most SMN is made from *SMN1* because *SMN2* has exon 7 single nucleotide mutation that disrupts an ESE and allows ISE in intron 7 to repress and exclude exon 7 from mature transcript [327, 328]. Exon 7 skipping transcript produces an unstable isoform which is swiftly degraded; hence, *SMN2* gene makes little to no contribution toward levels of SMN protein (figure 2.8, middle). SMA patients do not have functional *SMN1* gene due to gene deletion or nonsense mutation [327, 328]; therefore, small amount of SMN protein produced from *SMN2* gene is insufficient to reverse debilitating symptoms of SMA.

Because lack of SMN protein in SMA patients is due to exon 7 exclusion in SMN2-generated transcript, use of ASO was extensively studied to correct *SMN2* pre-mRNA splicing (figure 2.8, right) [329]. Initial strategy included targeting 3'ss of downstream exon 8 resulting in increase in exon 7 inclusion. However, following studies identified splicing silencers around exon 7 which can serve as possible targets for ASO; among the

silencer sequences was an ISS (ISS-N1) near exon 7 – intron 7 boundary [327-329]. ISS-N1 was recognized by hnRNP which repressed exon 7 inclusion in mature SMN2 transcript. Indeed, using ASO to prevent hnRNP binding to ISS-N1, Cartegni et al successfully restored exon 7 inclusion [329]. Thereafter, ASO targeting ISS-N1 was shown to increase SMN expression in SMA mouse models [330]. With success in preclinical studies, SMA ASOs were shuttle along into phase I clinical trial in 2011 [331]; with intrathecal injection, treatment of 28 patients with SMA showed not only safety in route of delivery and desirable half-life in cerebrospinal fluid [331], it also demonstrated increase in SMN protein levels after 9-14 months on treatment [331]. Importantly, increase levels in SMN

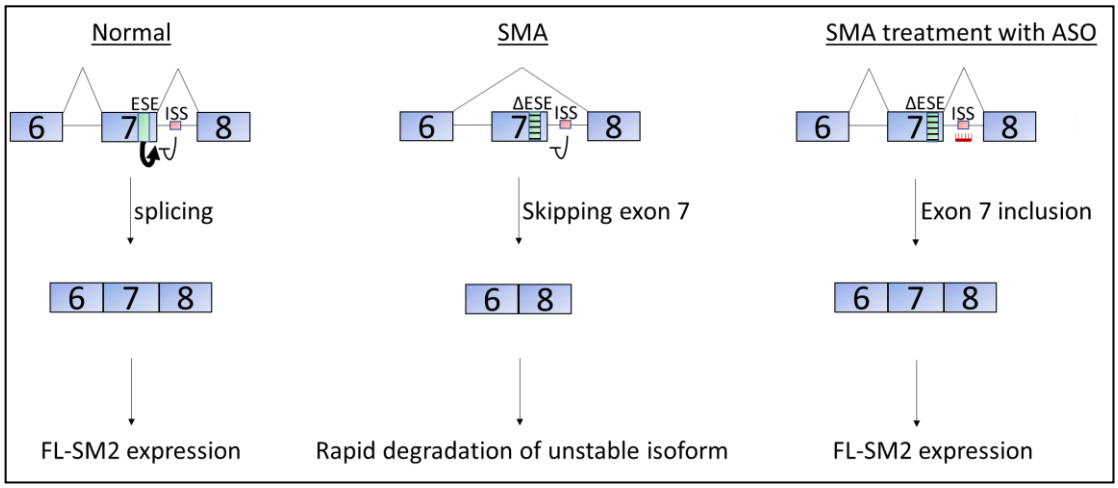

Figure 2.8. SM2 splicing in SMA and its correction with ASO. Left. Exon splicing enhancer (ESE) promote exon 7 5'ss definition in opposition of intronic splicing silencer (ISS). **Middle.** When ESE is mutated (ΔESE), ISS is able to silence exon 7 resulting in exon 7 exclusion from mature transcript which produces an unstable isoform which is swiftly degraded. **Right**. SMN2 splicing is corrected with ASO targeting ISS and promoting exon 7 inclusion to restore expression of FL-SMN2.

correlated with improvement in clinical assessment tests. A morpholino-based ASO targeting ISS-N1, referred to as nusinersen and developed by Ionis pharmaceutical, was approved for clinical use in late 2016 [332] and more ASO or splicing modifying compounds are currently in trial and may enter the clinic soon [326].

In addition to DMD and SMA, ASO are also utilized in preclinical and clinical studies to prevent cancer progression. Indeed, Zammarachi et al successfully promoted usage of

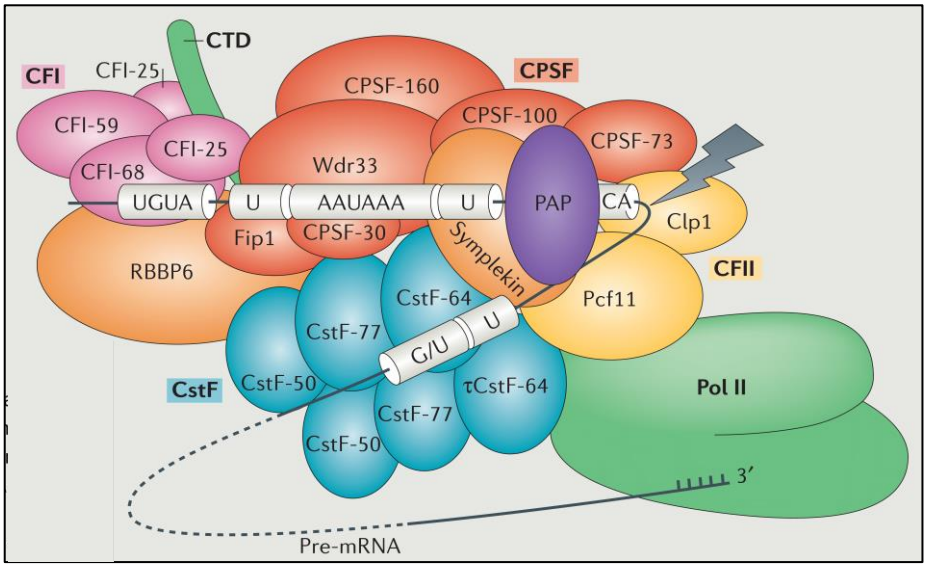

Figure 2.9. *Cis* and *trans*-acting elements involved in cleavage and polyadenylation. Reprint with permission from [301].

alternative 3'ss in STAT3 pre-mRNA by targeting WT 3'ss with ASO; this strategy switches oncogenic STAT3-α with an antitumorigenic β-form [333].

As in splicing redirection, ASO-pre-mRNA base-pairing can also be exploited to alter 3' processing. Alternative polyadenylation (APA) can generate stable mRNA variants which can produce c-terminal truncated isoform with possible dominant negative

functions [300, 333-335]. The following section describes APA and how it can be modulated with ASO for therapeutic purpose.

4. Alternative polyadenylation

mRNA synthesized by RNA polymerase II are co-transcriptionally processed at the 3' end; this step is important for mRNA stability and is considered a key mechanism of gene regulation [301]. The process entails pre-mRNA cleavage and polyadenylation by 3' processing complex (PC). 3'PC includes CstF (cleavage stimulation factor), CPSF (cleavage and polyadenylation specificity factor), PAP (polyA polymerase) and numerous other factors important for pre-mRNA processing (figure 2.9). Along with *trans*-acting factors, cleavage and polyadenylation (poly A) at CA sequence is regulated by *cis* elements located upstream and downstream of cleavage site; upstream elements include hexameric polyA signal (PAS), UGAU and U-rich sequences, while G-rich elements are found approximately 40 nucleotides downstream of cleavage site (figure 2.9) [301]. 3' processing is initiated by CPSF recognition of hexameric polyA signal (PAS) and polyadenylation by PAP with 200-250 nucleotide polyA tails [301].

Most eukaryotic genes use more than one of twelve possible PAS demonstrating that pre-mRNA undergo alternative polyadenylation (APA) [301, 335]. To date, most studies about APA are usually about selection from multiple PAS embedded within 3' UTR following terminal exon. Choice of PAS with 3' UTR can have dire effect mRNA stability; for example, mRNA shorter 3'UTR may exclude miRNA-binding site that can regulate post-transcriptional mRNA stability, translation, or cellular localization [301, 335].

In addition to APA in 3’ UTR, intronic PAS can also be recognized, cleaved and polyadenylation (IPA) [335]. Unlike APA that only effect of protein expression levels, IPA generates a shorter stable mRNA variant and thereby shorter ORF. These shortened transcripts express truncated isoforms with distinct C-terminal domain [300, 335]. For this reason, IPA can generate isoforms with vastly different properties relative to WT protein and may even possess dominant negative functions.

As with alternative splicing, 3’UTR and IPA expand transcriptome and proteome without increase number of genes. Mechanism controlling APA rely on levels of polyadenylation factors and RNA binding proteins that can regulate PAS selection [301, 335]. To add level of complexity to APA, recent studies have implicated epigenetic modification and chromatin structure in PAS usage [336, 337].

Global and specific APA and IPA regulation are important in multiple normal biological functions; however, their dysregulation can contribute to various disease, such as cancer. Recent studies have associated a switch towards shorter 3’UTR to cancer progression [338]; oncogenes with truncated 3’UTR may lack miRNA binding site that are required for mRNA degradation and proper post-transcriptional regulation, thereby increasing levels of oncoprotein and promoting tumorigenic transformation [338, 339].

IPA activation is also regulated in cancer. Generation of truncated isoforms can possess oncogenic or antitumorigenic functions. For example, cancer cells can activate specific IPA in cyclin D1 pre-mRNA; this generates a constitutive active cyclin D1 that promotes cell cycle progression and oncogenic transformation [340]. On the over hand,

tumors can inhibit IPA in VEGFR2 pre-mRNA thereby suppressing expression of soluble extracellular decoy version of VEGFR2 which are endogenous inhibitors of VEGF-VEGFR signaling pathway [300, 335].

Even though mechanism governing APA in 3'UTR and IPA are poorly understood, recent evidence has identified a crucial role of U1 snRNP in both these processes.

4.1. U1 snRNP and IPA

U1 snRNP (U1) was initially identified as a splicing factor that is responsible for defining 5'ss and initiating splicing reaction (figure 2.10). in addition, U1 was implicated in APA when cells treated in vitro with antibody against U1 interfered with polyadenylation [300, 335]. Thereafter, multiple reported described U1 ability to inhibit polyadenylation [341]; for example, studies examining 3' processing of human and bovine papillomavirus transcripts showed that U1 can suppress polyadenylation by binding to

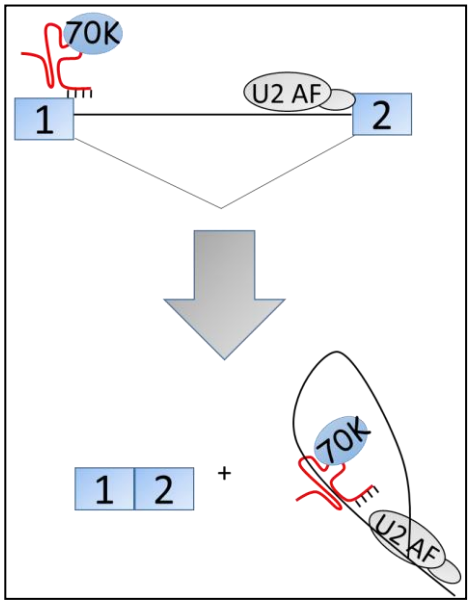

Figure 2.10. simplified schematic of canonical functions of U1 snRNP (U1). U1 initiates splicing by defining 5'ss while other splicing factors identify 3'ss. After series of reactions, exons are ligated together and intron is splicing out as a lariat.

upstream 5'ss [342]. Specifically, it was demonstrated that a component of U1, U1-70K, directly inhibit polyA polymerase (PAP) [341]. Thereafter, recent reports have described a protective function of U1 whereby U1 prevents recognition of intronic PAS and blocks IPA activation to protect WT-mRNA expression (figure 2.11, top) [343]; hence, U1 prevents aberrant IPA, prevents expression of unwanted mutant mRNA and suppress

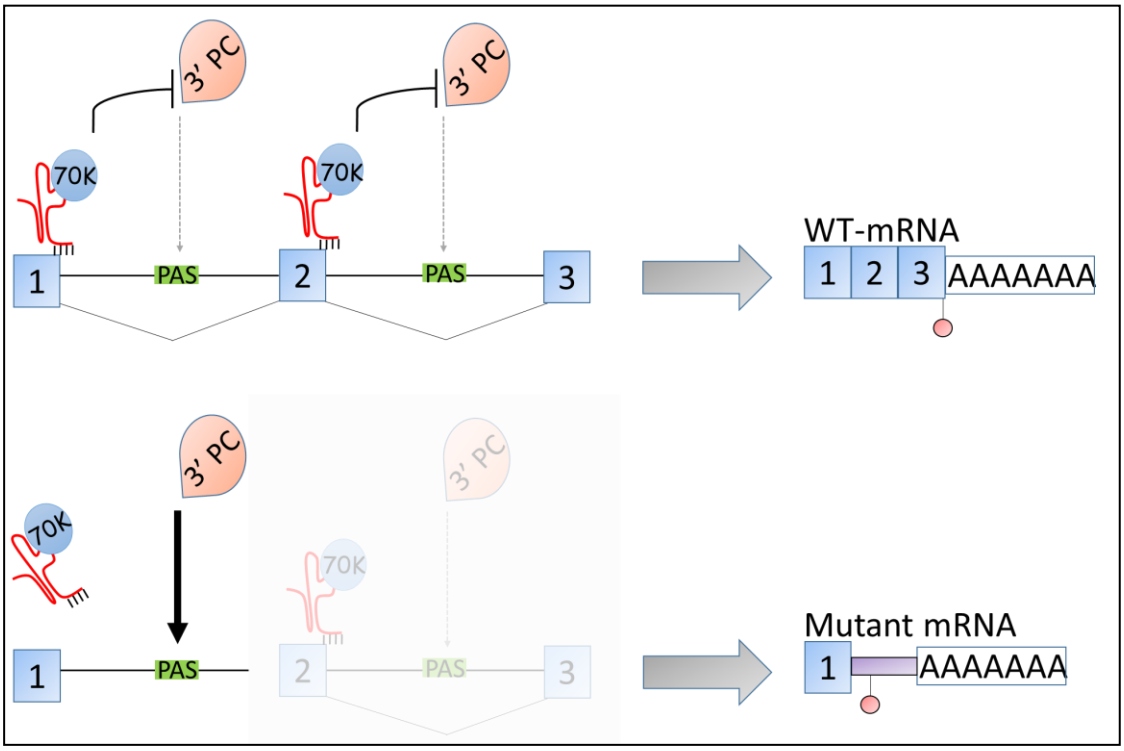

Figure 2.11. U1 suppression of IPA. **Top**. U1 binds to 5'ss and inhibits component of 3' PC, PAP, prevents PAS recognition and suppress IPA activation. **Bottom**. Under condition that prevent U1 binding to 5'ss, inhibition of 3'PC is relieved and pre-mRNA is cleaved and polyadenylation to form a mutant mRNA that retains intronic sequence. If the intronic sequence incorporate in-frame stop codon, IPA can generate a stable mRNA which can express non-functional or dominant negative isoform.

expression of non-functional isoform. For these reasons, 5'ss mutations reduces its affinity to U1 and activates downstream IPA and possibly express deleterious or dominant negative isoform (figure 2.11, bottom). Hence, 5'ss mutation or mutations to splicing signal motifs responsible for U1 recruitment can have similar effect as non-sense mutations or gene deletion [335].

Because IPA activation produces stable mRNA variant that can express dominant negative isoforms, multiple groups have tried to exploit U1 mechanism for therapeutic

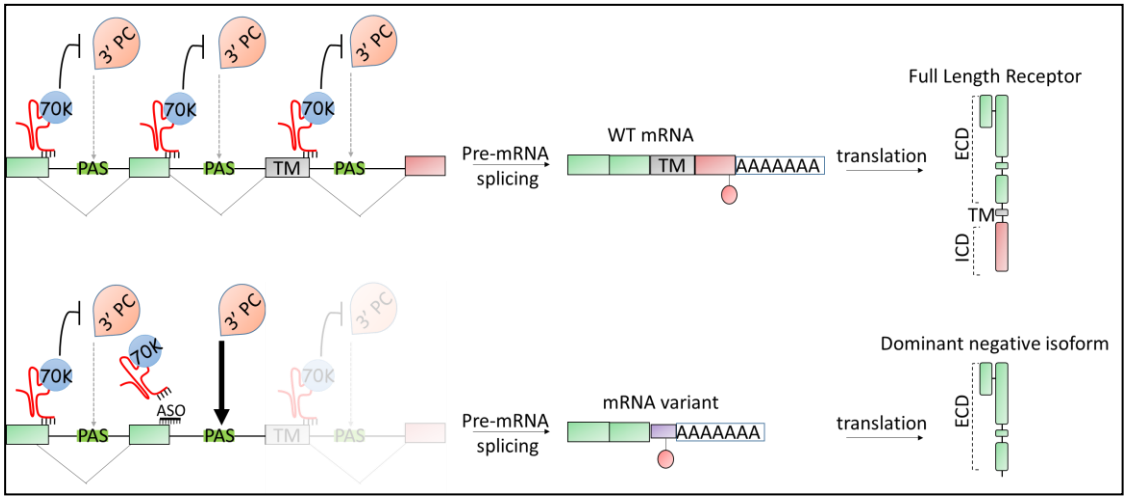

Figure 2.12. Expression of dominant negative isoform with ASO. **Top**. U1 binds to 5'ss and inhibits premature cleavage and polyadenylation and thereby expressing full length oncogenic receptor. **Bottom**. Activation of intronic polyadenylation by targeting specific 5'ss upstream of transmembrane domain (TM) with ASO. this IPA mRNA variant expresses isoform lacking TM and intracellular domain which can possible have dominant negative function.

purpose [300, 344]. The following section describes studies which generate possible therapeutic isoform with ASO.

4.2 Use of ASO to activation intronic polyadenylation

In the initial study that described U1's role in preventing premature cleavage and polyadenylation, Dreyfuss group demonstrated global IPA activation with treatment of ASO mimicking 5'ss [343]. Unfortunately, even though this approach can decipher U1 mechanism, it is futile for therapeutic use due to pleiotropic effect of their ASO. Thereafter, Vorlova et al successfully demonstrate use of ASO targeting 5'ss to inactivation of IPA and express dominant negative isoforms for receptor tyrosine kinase (RKT) [300]. This strategy involves targeting specific 5'ss upstream of transmembrane (TM) coding exon (figure 2.12) thereby expression truncated isoform which lacks TM and intracellular domains (ICD). More importantly, these isoforms are secreted into extracellular space and behave as decoy receptor (sdRTK) to sequester ligand and engage residual receptors in a dominant negative manner. Furthermore, the same report described existence of low levels of multiple endogenous sdRTK IPA variant, such as AXL, FGFR, and MET. Because many sdRTKs are naturally expressed, its rational to strategize similar approach to increase their expression for cancer therapy.

For this reason, work in this thesis exploits U1 mechanism in a similar manner to activation IPA and express soluble decoy form of MET RTK. A recombinant form of sdMET corresponding to intron 12 IPA was previously described. Importantly, this recombinant form was shown to behave in a dominant negative manner to suppress HGF signaling in

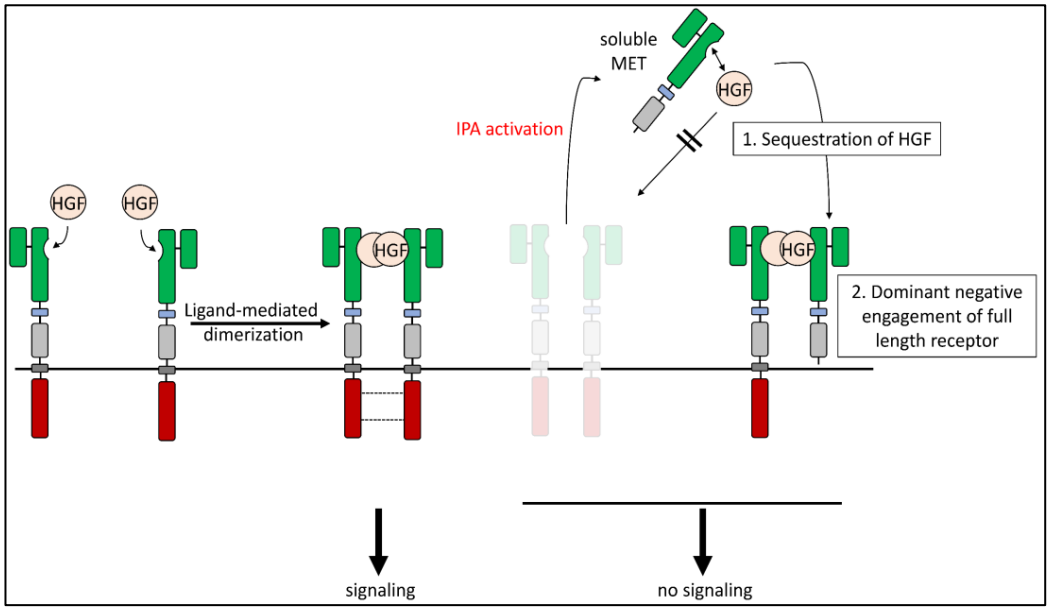

Figure 2.13. Activation of intronic polyadenylation (IPA) in MET receptor. IPA remove full-length (FL) MET and expresses soluble decoy MET which sequesters ligand and suppress activity of residual FL-ME**T.**

preclinical studies. In the following chapter, we present data that demonstrate IPA variants are naturally expressed and correspond to IPA of MET pre-mRNA; importantly, we show that these isoforms are secreted into extracellular space and sequester HGF (figure 2.13) and can be expressed by targeting specific 5'ss with ASO.

Chapter III

Generation of Anti-tumorigenic MET Receptor Variants by Splicing Interference

1. Introduction

Proto-oncogene MET, a receptor tyrosine kinase (RTK), is important for multiple biological processes during embryonic development and adulthood [5]. Along with its ligand hepatocyte growth factor (HGF), MET activity is critical for formation of placenta and limb buds at early development stage and liver regeneration in adulthood [10, 130, 345]. However, aberrant MET activation is tumorigenic and its role in tumors is extensively studied for multiple forms cancers [15]. Indeed, constitutively active MET due to activating mutations or gene amplification is frequently observed in MET dependent lung, gastric, pancreatic and brain cancers [9, 18, 346]. The consequence of constitutive MET activation is an increase of oncogenic signaling in downstream pathways, mainly RAS-MAPK, PI3K-AKT and STAT3; this allows MET-dependent cancers to maintain tumor growth [18], initiate migration and invasion [347], and sustain antiapoptotic signals [25].

Moreover, multiple reports have described functional crosstalk of MET with other RTKs, such as EGFR, HER2 and IGF1R [101]. For this reason, in tumors undergoing treatment with inhibitor for other RTKs, MET is frequently activated to serve as alternative bypass track to maintain cell survival, growth and eventually cause tumor relapse [19, 23, 348]. Because MET has emerged both as a driver and one of the primary mechanisms of resistance, multiple approaches are employed to inhibit MET activity for cancer treatment, such as, small molecule tyrosine kinase inhibitor and antibodies against MET or HGF [15].

Notably, multiple groups have suppressed MET activity with the use of soluble isoform of MET which consist solely of ligand binding extracellular domain [53, 223, 299, 300]. This soluble MET decoy (sdMET) was identified as a possible endogenous isoform encoded in mRNA variant from intronic polyadenylation (IPA) in Intron (In) 12 of MET's pre-mRNA [300]. During pre-mRNA splicing, IPA is suppressed by U1-snRNP (U1) from its 5' splice site (ss) binding site to prevent premature cleavage and polyadenylation [343]. However, Vorlova, S. et al. publish a strategy to overcome U1 mediated IPA inhibition; morpholino (MO) based antisense oligonucleotides were used to block U1 binding to 5'ss upstream of poly (A) site and selectively increase expression of sdRTK IPA isoform of choice [300].

To utilize this approach to generated sdMET isoforms, we searched for actionable 5'ss to target with MOs. To be included as a 5'ss target, the downstream intron must consist of in-frame stop codon, hexamer poly (A) signal, validated with 3' race assay, and be dominant negative over the FL-MET. Our pursuit led us to the identification of 3 natural sdMET IPA isoforms with inhibitory properties. Our results will show that 5'ss specific MOs can increase expression of IPA variant at the expense of FL-MET and generate sdMET which is secrete into extracellular space. importantly, cells which did not uptake MOs can be also affected due to presence of dominant negative sdMET in the microenvironment.

Hence, our work along with previous study served a blueprint to target RTK or other disease-causing membrane bound proteins. Controlled modulation of U1 with MOs to activate IPA in cancer or other disease can be a powerful tool to generate therapeutic isoforms.

2. Material and Methods

2.1. Sources for Cell lines

A549 lung cancer cells with KRAS G12C mutation (#CLL-185), BEAS-2B normal lung bronchial epithelial cells (#CRL-9609), H1792 lung cancer cells with KRAS G12C mutation (#CRL-5895), Hek293T cells (#CRL-3216), HeLa cervical cancer cells (#CCL-2), HPAF-II pancreatic adenocarcinoma cells (#CRL-1997), Hs738 normal gastrointestinal fibroblast cells (#CRL-7869), and Hs746T gastric cancer cells with MET amplification (#HBT-135) were obtained from American Type Culture Collection (ATCC, Manassas, VA, USA). EBC-1 lung cancer cells with MET amplification (#JCRB0820) were obtained from Japanese Collection of Research Bioresources cell bank (JCRB cell bank, Ibaragi City, Osaka, Japan). MKN-45 gastric adenocarcinoma cells with MET amplification were kind gift from Dr. Maurizio Scaltriti (Memorial Sloan Kettering Cancer Center, New York, NY, USA).

2.2 Cell culture conditions

All cell culture reagents were purchased from Thermo Fisher Scientific (Waltham, MA, USA). A549, EBC-1, H1792, and MKN-45 cells were cultured in 2mM L-Glutamine containing RPMI-1640 (#11875093) supplemented with 10% heat inactivated fetal bovine serum (FBS), and 1% Penicillin/Streptomycin (P/S). BEAS-2B, HEK293T, HeLa, Hs738, and Hs746T were cultured in 4.5 g/L D-Glucose, 2 mM L-Glutamine, and 110 mg/L Sodium Pyruvate containing DMEM (#11995065) supplemented with 10% FBS, and 1% P/S. HPAF-II cells were cultured in EMEM (#11095080) supplemented with 10% FBS and 1% P/S. Cells were maintained in humidified incubator with 5% CO_2 and 37^{o}C.

2.3 Sources for antibodies, growth factors, and inhibitor

From Cell Signaling Technology (CST, Danvers, MA, USA), rabbit anti-phospho MET Try1234/1235 (#3077), rabbit anti-MET (#8198), rabbit anti-phospho AKT Ser473 (#4060), rabbit anti-AKT (#4685), rabbit anti-phospho Erk1/2 Thr202/Try204 (#4370), rabbit anti-Erk1/2 (#4695), rabbit anti-flag (#2368) and rabbit anti-HGF β (#52445). All antibodies from CST were used at 1:1,000 dilution in 5% BSA in TBS-tween (TBS-T). Rabbit anti-MET N-terminal antibody was (#ab51067, Abcam, Cambridge, MA, USA) used at 1:1,000 dilution in 5% non-fat milk in TBS-T. Mouse anti-alpha tubulin was (#T9026, Sigma Aldrich, St. Louis, MO, USA) used at 1:10,000 in 5% non-fat milk in TSB-T. Horseradish peroxidase (HRP) conjugated goat anti-rabbit secondary (#31460) and HRP conjugated goat anti-mouse secondary (#32430) were from Thermo Fisher Scientific and used at 1:10,000 dilution in TSB-T.

Recombinant Human HGF (#294-HG, R&D systems, Minneapolis, MN, USA) was reconstitutes in 0.1% BSA in PBS. MET selective inhibitor, AMG337 (#S8167, Selleck Chemicals, Houston, TX, USA) was reconstitutes in DMSO.

2.4 Western blotting

Cell lysates were collected with radioimmunoprecipitation assay (RIPA) buffer containing 1x phosphatase inhibitor (#4906845001, Roche, Madison, WI, USA) and protease inhibitors (#11697498001, Roche). Cell lysates were cleared of debris and membranous material by centrifugation at 13,000 x g for 5 minutes and supernatant

transferred to a sterile tube. 10 uL of sample was used to measure protein concentration with BCA protein assay (#23224, Thermo Fisher Scientific).

10ug – 20ug of cell lysates were resolved in 6% or 10% SDS-PAGE gel. To detect MET intronic polyadenylation (IPA) isoforms in conditioned medium (CM), 45uL of CM was resolved in SDS-PAGE gel. Samples from SDS-PAGE gel were transferred to polyvinylidene difluoride (PVDF) membrane (#IPVH00010, Millipore, Burlington, MA, USA). Following transfer, PVDF membranes were blocked with 5% non-fat milk in TBS-tween for 1 hour at room temperature (RT) then incubated with primary antibodies at 4^{o}C overnight. The following day, PVDF membranes were incubated in HRP conjugated secondary antibody in 5% non-fat milk in TBS-tween at room temperature for 1 hour. Proteins were detected with SuperSignal^{TM} west femto maximum sensitivity substrate (#34095, Thermo Fisher Scientific) and visualized with GeneGnome XRQ Chemiluminescence imaging system (Syngene International Limited, Frederick, MD, USA). Image-J software (National Institutes of Health, Bethesda, MD, USA) was used for protein quantification and normalized to alpha-tubulin.

2.5 Detection and analysis of intronic polyadenylation sites

2-primer PCR assay was used to detection of natural IPA mRNA variants. Briefly, 5ug of human universal total RNA (#338112, Qiagen), or RNA from BEAS-2B and Hs738 cells was reverse transcribed with SuperScript^{TM} first-strand synthesis kit according to manufacturer's protocol (#18080051, Thermo Fisher Scientific). 4uL of cDNA was used to amplify MET IPA variants with a common MET Exon 2 forward primer and intron specific

primer upstream of the 1st poly (A) signal (PAS) using GoTaq® Flexi DNA polymerase (#M8291, Promega, Madison, WI, USA) with the following conditions:

1. Initial denaturation at 95°C for 2 minutes
2. 35 cycles of denaturation for 30 seconds at 95°C, annealing for 30 seconds at 60°C, extension for 45 seconds at 72°C
3. Final extension for 5 minutes at 72°C

PCR reactions was resolved on 2% agarose gel, post-stained with ethidium bromide and imaged with Gel Doc™ EZ Gel Documentation System (Bio-Rad Laboratories, Hercules, CA, USA). Expected PCR products were gel purified with QIAquick gel extraction kit (#28115, Qiagen, Germantown, MD, USA) according to manufacturer's instructions, cloned into TA cloning vector (#K202020, Thermo Fisher Scientific) which was then used to transform DH5α competent bacterial cells (#18258012, Thermo Fisher Scientific). Plasmid was extracted from transformed colonies with QIAprep® spin miniprep kit (Qiagen) according to manufacturer's instructions and sequence analyzed with MacVector alignment software (MacVector, Inc, Apex, NC, USA).

2.6. 3' RACE assay

5ug of human universal RNA (#338112, Qiagen) was reverse transcribed with 3' RACE kit according to manufacturer's protocol (#18373010, Thermo Fisher Scientific). Forward intron specific primer upstream of 1st PAS and reverse adapter primer were used to amplify specific MET IPA variants with GoTaq® Flexi DNA polymerase (#M8291, Promega) with the same PCR protocol as 2-primer PCR assay described in section 2.5. 2uL

of PCR product was cloned into TA cloning vector (#K202020, Thermo Fisher Scientific) and used to transform DH5α competent bacterial cells (#18258012, Thermo Fisher Scientific). Plasmid was extracted from more than 50 transformed colonies with QIAprep® spin miniprep kit (Qiagen) and sequence analyzed with MacVector alignment software (MacVector, Inc, Apex, NC, USA).

2.7. Cloning of flag-tag MET IPA Isoforms

cDNA for all MET IPA variants were amplified with Phusion® high-fidelity DNA polymerase (#M0530S, New England Biolabs) according to manufacturer's instructions with two specific primers: forward-MET Exon 2-ATG HindIII primer and reverse MET intron primer containing last amino acid codon followed by NotI site. cDNA variants were cloned as HindIII and NotI fragment into 3xflag-CMV-14 expression vector (#E7908, Sigma Aldrich). A non-tag version of selected MET IPA isoforms was cloned into pcDNA^{TM} 3.1(+) mammalian expression vector (#V79020, Thermo Fisher Scientific) as HindIII and NotI fragment. All plasmids were verified by sequence analysis with MacVector alignment software to confirm absence of mutations.

2.8. Detection of flag-tag isoforms in Lysate and culture medium

To detect flag-tag MET IPA isoforms in lysate and conditioned medium (CM), $3.5x10^6$ Hek293T cells were seeded in 6 cm cell culture dish. After 24 hours, 10 ug of plasmid was transfected with lipofectamine® LTX according to manufacturer's protocol (#15338100, Thermo Fisher Scientific). After 6 to 8 hours, culture medium was replaced with 3 mL of 0.1% FBS containing Opti-MEM^{TM} I (#31985062, Thermo Fisher Scientific).

After additional 72 hours, cell lysate and approximately 3 mL CM were collected. CM was centrifuged 2,000 x g for 5 minutes to remove floating cells and debris and transferred to sterile 15 mL tube. To detect flag-tag MET IPA isoforms, 20 ug of lysate and 45 uL of CM were subjected to western blot analysis with rabbit anti-flag antibody as described in section 2.4.

2.9. PNGase F treatment

To remove N-linked oligosaccharides from flag-tag MET IPA isoforms, 20 ug of lysate from HEK293T cells transfected with In12, In8, or In6 flag constructs were treated with PNGase F (#P0704S, New England Biolabs) under reducing and non-reducing conditions according to manufacturer's instructions. Following treatment, reactions were resolved on 10% SDS-PAGE and subjected to western blot analysis with rabbit anti-flag antibody (#2368, CST).

2.10. Conditioned medium (CM) assay

1 mL of CM was used to demonstrate activity of MET IPA isoforms. Briefly, $2x10^5$ of HeLa or A549 cells were seed in 12 – well dish. After 24 hours, culture medium was replaced with 1 mL of CM containing 10 ng of recombinant human HGF (#294-HG, R&D Systems) for 5 minutes. Following 5 minutes of stimulation with HGF, cells were washed with ice cold 1x PBS and cell lysates were collected for western blot analysis for phosphorylation of MET Try1234/1235, AKT Ser473, and Erk1/2 Thr202/Try204.

2.11. Conditioned medium depletion assay

To deplete flag-tag MET IPA isoforms from CM, 100 uL of mouse anti-flag antibody conjugated to sepharose beads (#5750, CST) or mouse IgG conjugated to sepharose beads (#3420, CST) was added to 1.2 mL of CM and incubated with rotation overnight at 4oC. Following day, CM with sepharose beads were centrifuged at 3,000 x g for 3 minutes and flow through CM was transferred to sterile tube. Sepharose bead pellet was washed 2x with 1 mL of ice cold Opti-MEM I and pellet from final wash was resuspended in SDS-PAGE loading buffer for western blot analysis alongside 45 uL of flow through CM with rabbit anti-Flag antibody. To test flow through CM's activity, 10 ng/ml of recombinant human HGF (#294-HG, R&D Systems) was added to 1 mL of flow through CM. HeLa cells were treated with HGF/depleted CM mixture for 5 minutes. After 5 minutes, cells were washed with ice cold PBS and cell lysate were collected for western blot analysis for phosphorylation of MET Try1234/1235, AKT Ser473, and Erk1/2 Thr202/Try204.

2.12. Co-immunoprecipitation assay

To demonstrate that HGF binds MET flag-tag IPA isoforms, 5 ng/ml of human recombinant of HGF was added to 1.2 mL of CM and incubate for 4 – 6 hours with rotation at 4^{o}C. Thereafter, mouse anti-flag antibody conjugated to sepharose bead (#5750, CST) or moues IgG conjugated to sepharose bead (#3420, CST) were added to CM/HGF mixture and incubated with rotation overnight at 4^{o}C. Following day, CM with sepharose beads were centrifuged at 3,000 x g for 3 minutes and flow through was transferred into sterile tube. Sepharose bead pellet were wash 2x with 1 mL of ice cold Opti-MEM I and pellet

from final wash was resuspended in SDS-PAGE loading buffer for western blot analysis alongside with 45 uL of flow thorough with rabbit anti-flag antibody followed by rabbit anti-HGF antibody

2.13. Biological *in vitro* assay

Anchorage – independent growth assay was performed as previously described [223, 349]. Briefly, $5x10^3$ A549 cells were suspended in culture medium containing 10% FBS and 0.5% noble agarose (J1090722, Thermo Fisher Scientific) and seeded on top of 1% noble agarose in complete medium. CM containing MET IPA isoforms plus 20 ng/ml of HGF were added twice weekly. After 14 days, cells were stained with nitroblue tetrazolium blue chloride (#N6876, Sigma Aldrich) in 1X PBS and colonies were quantified with Image-J software.

Cell scatter assay was performed as previously described with slight modification [223]. 5 x 10^4 HPAF-II cells were seeded in 24 well dish. After 24 hours, culture medium was replaced with 1 mL of CM containing MET IPA isoforms. after additional 6 hours, cells were stimulated with 10 ng/mL of HGF. After another 24 hours, cells were image with Nikon inverted microscope (Nikon Instruments).

Invasion assay was performed as previously described with slight modification [223]. 1.5 x 10^5 HPAF-II cells were suspended in CM containing MET IPA isoforms and seeded in upper compartment of transwell insert (#3472, Corning Life Sciences, Corning, NY, USA) pre-coated with 30 ug of matrigel matrix (#356230, Corning Life Sciences). Culture medium supplemented with 2% FBS and 10 ng/mL of HGF was added in the lower

compartment. After 24 hours, cells were mechanically removed from upper side of the transwell membrane. Cells which migrated to lower side of the transwell insert were washed with 1x PBS, fixed with ice cold methanol for 20 minutes and stained with 0.1% crystal violet. Image of migrating cells were acquired with Nikon inverted microscope. Furthermore, crystal violet was eluted with 10% acetic acid and optical density was measured at 590nM with SpectraMax^{M} microplate reader (Molecular Devices, San Jose, CA, USA).

For migration assay, transwell inserts without pre-coat Matrigel matrix were used with similar protocol as described for invasion assay.

2.14. Morpholino treatment assay

For western blot analysis, EBC-1 ($3x10^5$), MKN-45 ($4x10^5$), Hs746T ($2x10^5$), BEAS-2B ($2x10^5$), Hs738 ($2x10^5$), or H1792 ($2x10^5$) cells were seeded in 12 – well dish. After 24 hours, culture medium was replaced with medium containing CTRL-MO, MET targeting MOs (MET-MOs) or AMG337. After additional 48 hours, cell lysates were collected for western blot analysis for phosphorylation of MET Try1234/1235, AKT Ser473, and Erk1/2 Thr202/Try204.

To collect CM from morpholino treated cells, mutant $3x10^6$ H1792 cells were seeded in 6cm dish. After 24 hours, culture medium was replaced with medium containing CTRL-MO or MET-MOs. After additional 12 hours, medium was replaced with Opti-MEM^{TM} I supplemented with 0.1% FBS. After 48 hours, Lysates and CMs were

collected for western blot analysis and CM collected was used for conditioned medium experiment and in vitro biological assays.

For analysis of IPA activation post morpholino treatment, cells were treated as descried above for 48 hours and analyzed with three primer PCR strategy as previously described. Briefly, total RNA from treated cells was extracted with TRIzol™ reagent according to manufacturer's protocol (#15596026, Thermo Fisher Scientific). Extracted RNA samples were treated with Turbo™ DNase (#AM1907, Thermo Fisher Scientific) to remove any residual DNA carry over. 1ug of extracted RNA was reverse transcribe with SuperScript™ first-strand synthesis kit. 2 uL of cDNA samples were used in a 3-primer PCR assay as previously described[300, 350]. Briefly, forward primer was place one or two exons upstream of intron of interest, first reverse primer was place in the intron upstream of 1st PAS, and second reverse primer was place one or two exons downstream of PAS. With these three primers, 2ul of cDNA was amplified with GoTaq® flexi DNA polymerase (#M8291, Promega) with the following conditions:

1. Initial denaturation at 95°C for 2 minutes
2. 30 cycles of denaturation for 30 seconds at 95°C, annealing for 30 seconds at 60°C, extension for 45 seconds at 72°C
3. Final extension for 5 minutes at 72°C

PCR reactions were resolved on 3% agarose gel and imaged with Gel Doc™ EZ Gel Documentation System (Bio-Rad Laboratories).

All cloning primers are listed in supplemental table 2.1

2.15. Cell viability assay

EBC-1 ($4x10^4$), MKN-45 ($4x10^4$), Hs746T ($2x10^4$), BEAS-2B ($2x10^4$), Hs738 ($2x10^4$), and H1792 ($2x10^4$) cells were in 48 – well dish. After 24 hours, culture medium was replaced with medium containing CTRL-MO, MET-MOs, or AMG337. After additional 72 hours, viable cells were quantified with Cell Counting Kit – 8 according to manufacturer's instructions (CK04-05, Dojindo Molecular Technologies) using Tecan microplate reader at 490 nM wavelength (Morrisville, NC, USA).

3. Results

3.1. Identification of intronic polyadenylation (IPA) mRNA variants

Multiple reports have demonstrated that existence of a C-terminal truncated soluble decoy form of MET (sdMET) which is secreted into extracellular space, trap HGF and suppress MET activation [223, 299, 300]. We hypothesized that this isoform is a byproduct of intronic polyadenylation of introns which consist of in-frame stop codon (IFSC) followed by a poly (A) signal (PAS), a hexamer sequence 5' to polyadenylation site. In a U1 dependent manner, these PAS are recognized, cleaved and polyadenylated 15 – 30 nucleotides downstream at a CA sequence to generated a mature IPA mRNA. Because these IPA variants lacks transmembrane (TM) and intracellular domain (ICD) coding exons, the translated C-terminal truncated isoforms are secreted into extracellular space and trap ligand (figure 3.1A). For this reason, we did a systematic search in all introns 5' to TM coding exon 13 for IFSC followed by one of the 12 consensus PAS. In our search, we found IFSC and PAS in all introns except intron 7 (figure 3.1B).

When RT-PCR was done with a common forward primer in exon 2 and specific reverse primer for introns with IFSC and PAS, we detected product corresponding to predicted IPA variants for all introns (figure 3.2A). To rule out false positive due to alternative splicing or intron retention which can include primer binding site, we

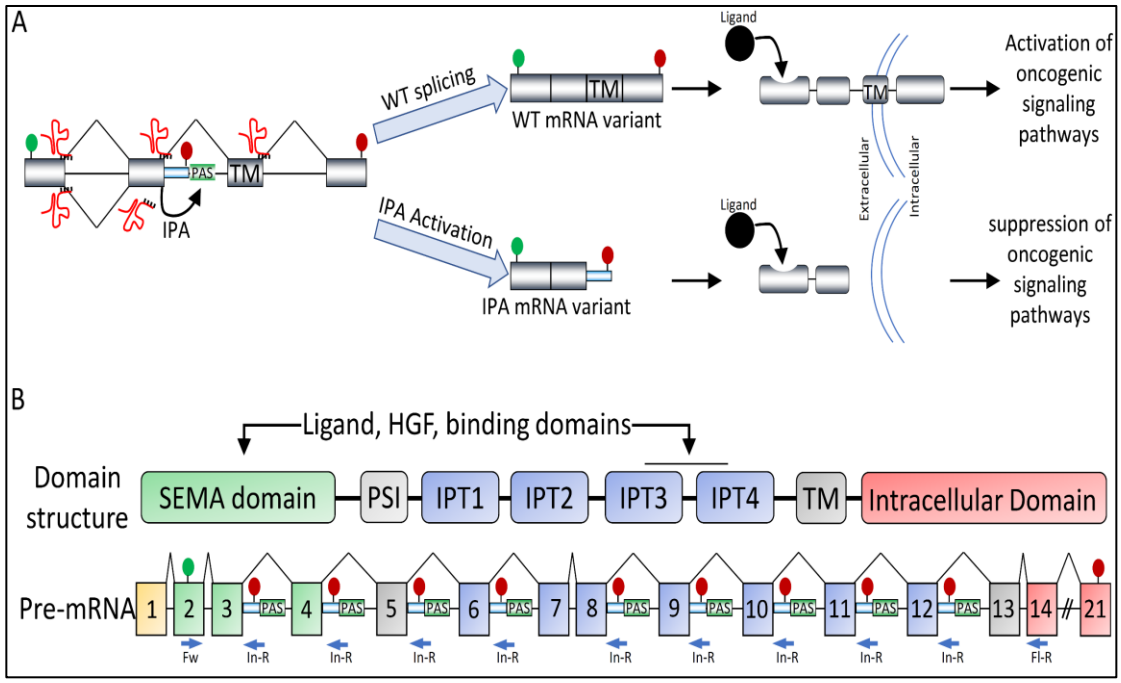

Figure 3.1: **A. Schematic of wild type (WT) splicing or IPA.** Hypothetical 4 exon pre-mRNA can be subjected to WT splicing or recognition of poly (A) signal (PAS) followed by cleavage and polyadenylation of intron 5' to transmembrane (TM) coding exon. The resulting mRNAs can express oncogenic membrane bound receptor (WT mRNA variant) or therapeutic ligand trapping soluble decoy (IPA mRNA variant). **B**. poly A signals in MET pre-mRNA introns. MET protein topology and pre-mRNA. Top: Domain structure of full-length MET protein; bottom: MET pre-mRNA with annotation of in-frame stop codon followed by PAS. Also, indicated are primer positions for 2 primer PCR assay for IPA detection in figure 3.2A.

performed 3’ RACE assay and validated the previously described In12 IPA and identified novel In8 and In6 IPA mRNA variants (figure 3.2B).

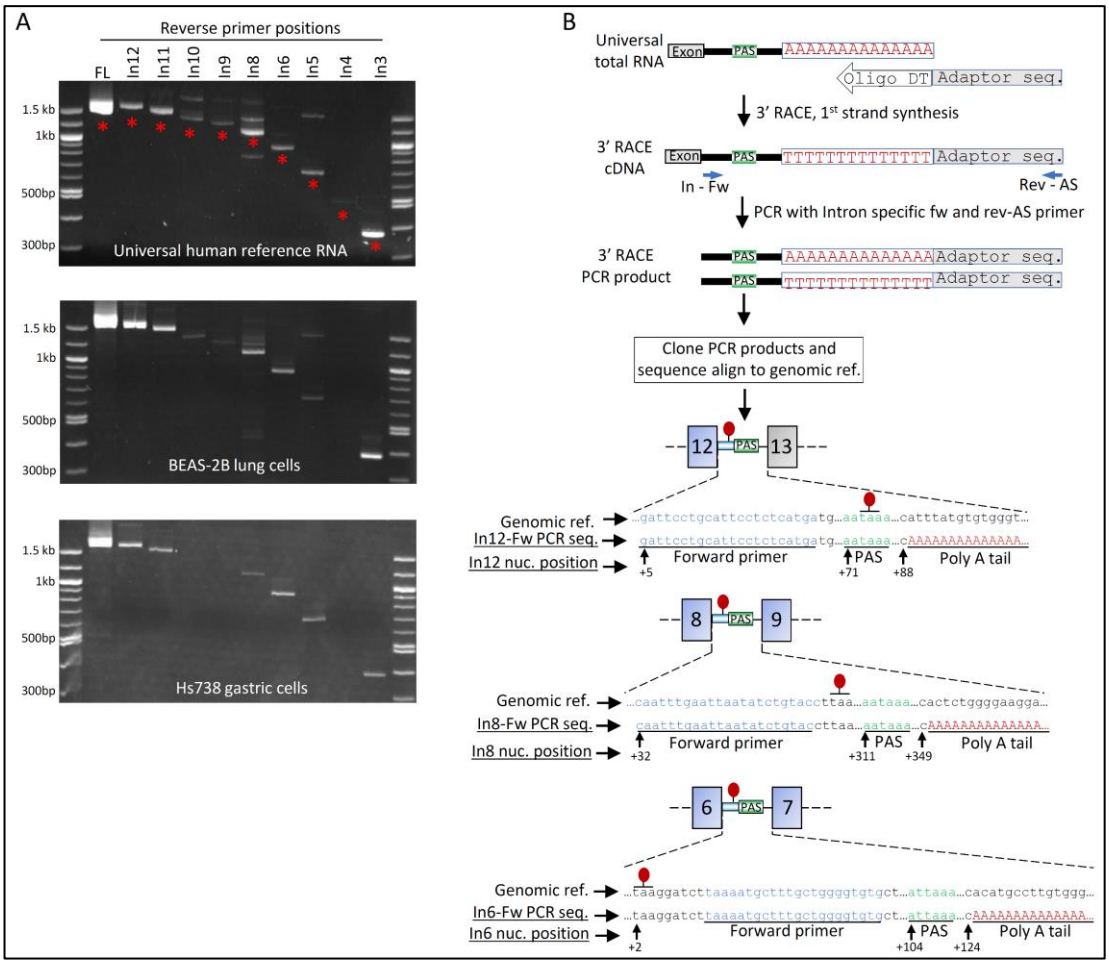

Figure 3.2: **Detection of endogenous MET IPA variants**. **A.** 2-primer PCR assay for IPA detection**.** IPA variants in total RNA from universal human reference, normal lung cells, or normal gastric cells. Primer positions are annotated in pre-mRNA schematic in figure 3.1B. **B.** 3’ RACE assay to validate existence of soluble decoy MET (sdMET) IPA mRNA variants. top: overview of 3’ RACE assay with universal human total RNA reference with intron specific forward primer. Bottom: sequence alignments from cloned 3’ RACE PCR products to genomic reference along with nucleotide position for forward primer position, PAS, and cleavage and polyadenylation.

Together, our identification and validation assay identified three MET IPA variants. The lack of TM and ICD allows these variants to be secreted, bind ligand and prevent MET activity.

3.2. Characterization of sdMET and their inhibitory properties

sdMET IPA variants corresponding to all intron IPAs (figure 3.1B, 3.2A) were cloned as C-terminal flag tag recombinant isoforms (figure 3.3A) to study their ability to inhibit MET activity. As predicted, flag tagged sdMET isoforms were secreted and conditioned the culture medium when expressed in HEK293T cells (figure 3.3B).

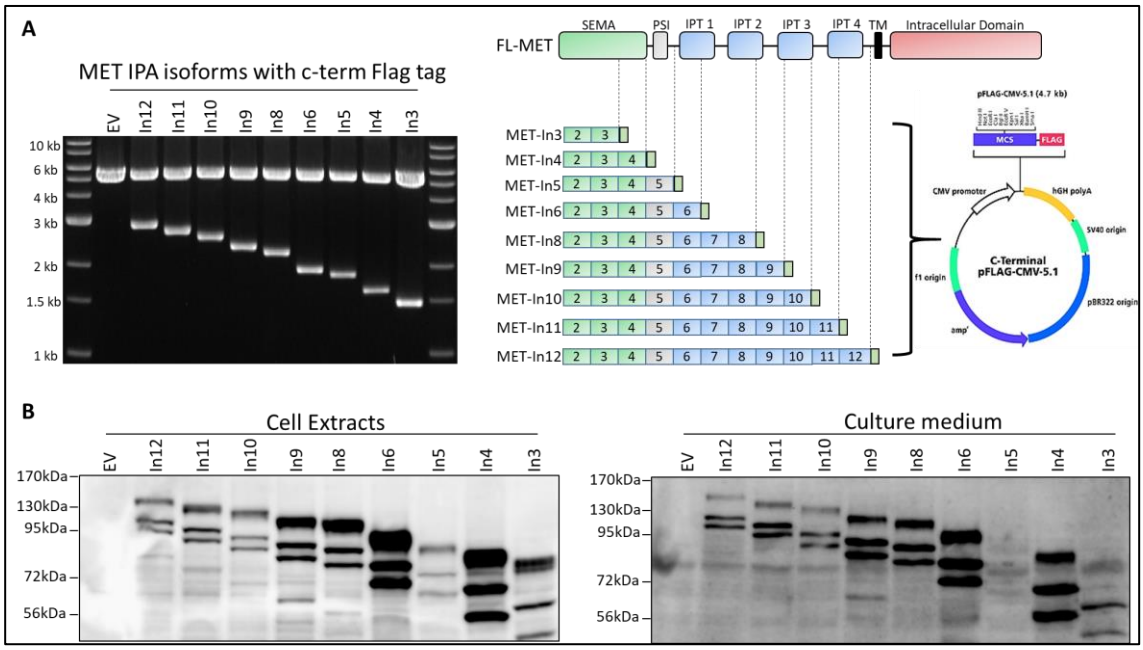

Figure 3.3: **Secretion of flag tagged sdMET IPA isoforms into culture medium. A.** Truncated isoform corresponding to each intron IPA was cloned in a c-terminal flag tagged recombinant protein. **B.** Overexpression of sdMET IPA isoforms in HEK293T cells. After 72 hours transfection, cell extract and culture medium were subjected to western blot analysis with flag antibody.

Next, we ask if sdMET isoforms are N-linked glycosylated and undergo other post-translation modification just as full-length (FL) MET. For our analysis, we selected In12, In8, In6 sdMET IPA isoform to demonstrate glycosylation and disulfide bond formation. As expected, sdMET isoform migrated faster in SDS-PAGE analysis after treatment with N-linked oligosaccharides removing enzyme, PNGase F demonstrating that sdMETs have similar post translation modification as FL-MET (figure 3.4B). Furthermore, three bands observed in lysates and CM (figure 3.3B, 3.4A) were resolved to a single band with absence of reducing agent, DTT, from sample buffer suggesting sdMETs are heterodimer composed of two polypeptides joined together with disulfide bonds just as FL-MET (figure 3.4).

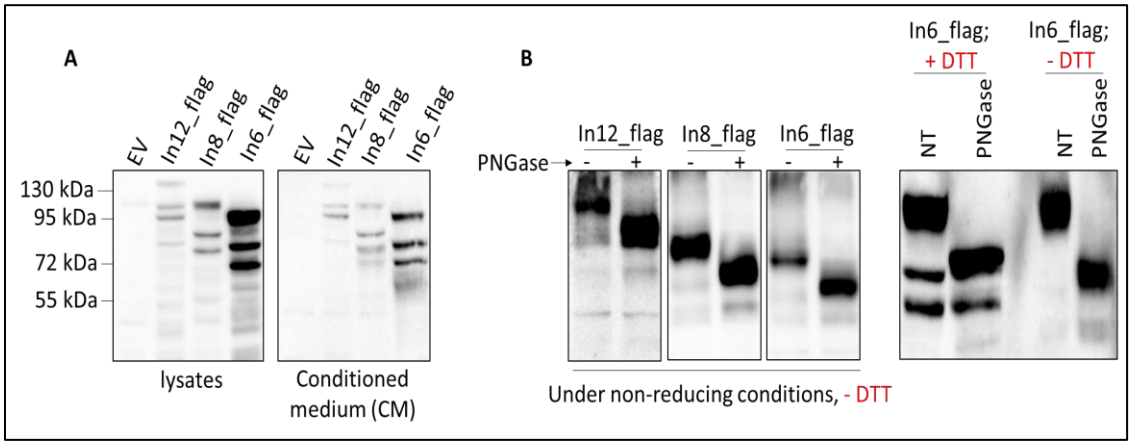

Figure 3.4: **Post-translation modification of sdMET IPA isoforms. A.** Expression of In12, In8, In6 sdMET IPA isoforms in cells and culture medium from HEK293T cells. **B.** Post-translation modification of sdMET IPA isoforms. 20ug of lysates from panel A were treated with or without PNGase F to remove N-terminal glycosylation under reducing (+DTT) or non-reducing (-DTT) conditions and subjected to western blot analysis with anti-flag antibody.

Next, we asked if sdMET isoforms are able to bind its ligand HGF. To address this question, we performed co-immunoprecipitation (Co-IP) assay of HGF with flag tagged sdMET isoforms. As predicted, we were able to Co-IP HGF along with sdMETs demonstrating that HGF is able to bind sdMET isoforms (figure 3.5).

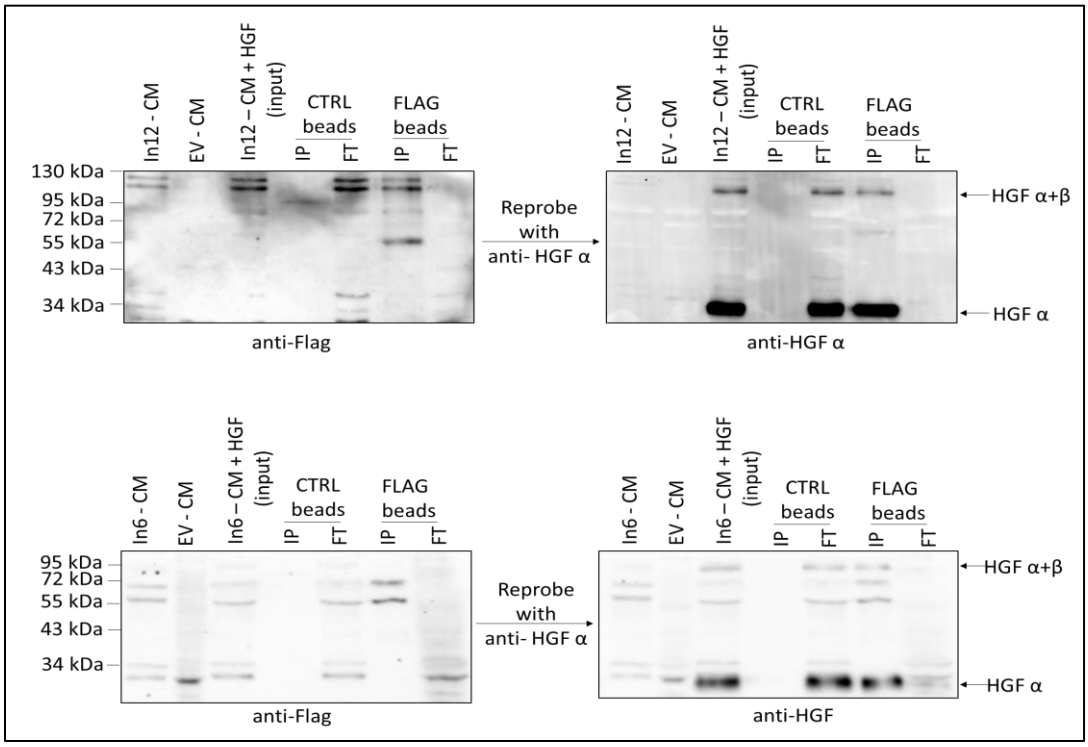

Figure 3.5: **HGF binds sdMET IPA isoform.** Co-immunoprecipitation of HGF with flag tagged sdMET In12 (top) and In6 (bottom). HGF was added to CM from HEK293T transfected with In12 or In6 flag tag sdMET and subjected to overnight co-immunoprecipitation (IP) with sepharose beads conjugated with anti-flag antibody. IP and flow through (FT) were subjected to western blot analysis with anti-flag antibody followed by anti-HGF α antibody.

because sdMET isoforms are able to bind HGF, we asked if sdMETs can block MET activation and its downstream signaling pathways in our conditioned medium (CM) test (figure 3.6).

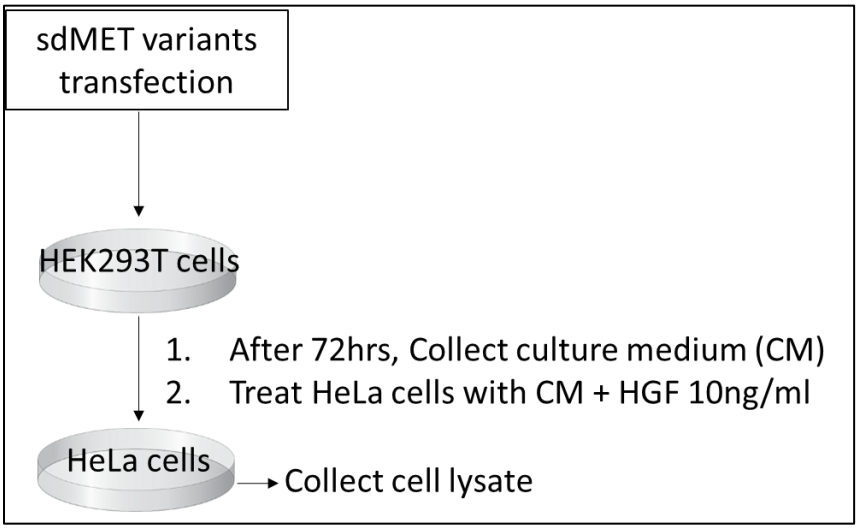

Figure 3.6: **Schematic of conditioned medium (CM) test**. HeLa cells were stimulated with or without 10 ng/ml of HGF for 5 minutes in presence of fresh medium (FM) or CM containing flag tag sdMET isoforms.

In our CM test, we treated HeLa cells with HGF in presence of CM containing sdMETs and there was significant reduction of MET phosphorylation and perturbation of downstream AKT and ERK signaling pathways (figure 3.7A, B).

Collectively, our sdMET are processed similarly as FL-MET, sequester HGF, prevent MET activation, suppress oncogenic signaling pathways.

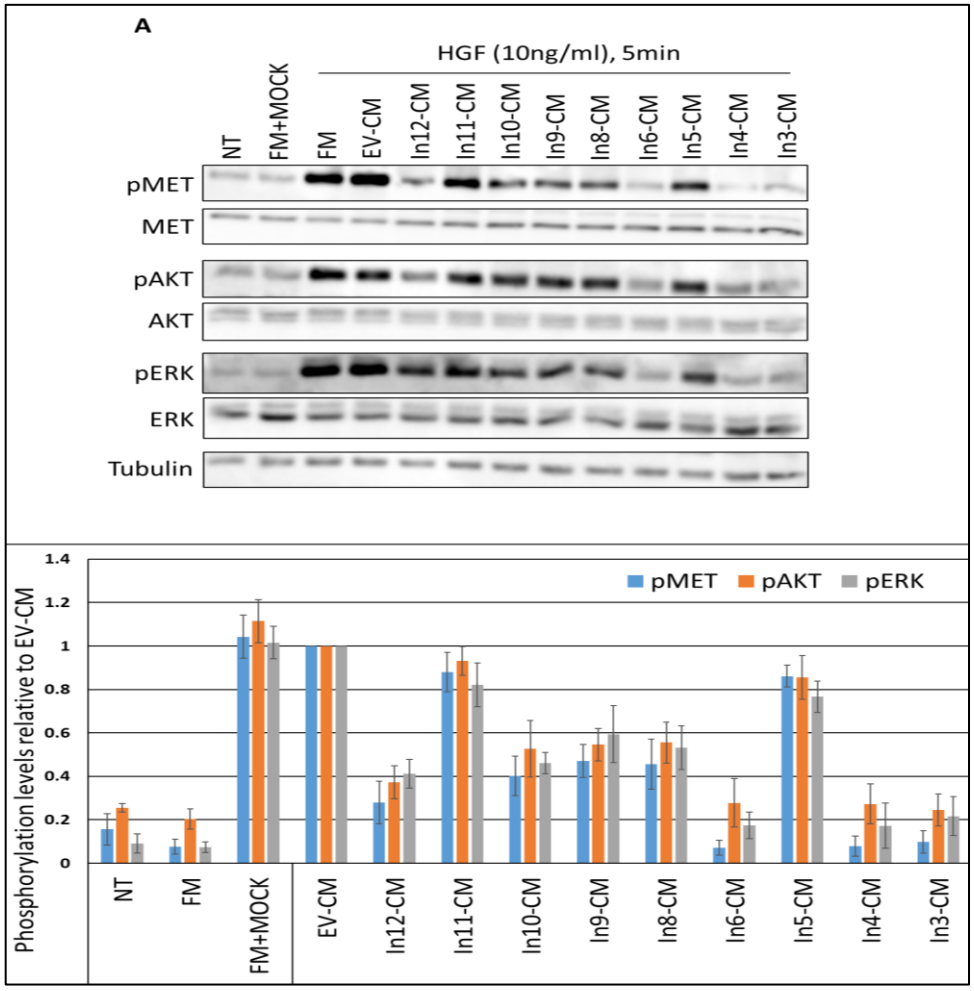

Figure 3.7: **Inhibitory activity of sdMET isoforms**. **A.** samples from CM test subjected to western blot analysis for pMET, pAKT, pERK. **B**. bands in panel A were quantified, normalized to tubulin and represented as percentage to FM + HGF. Each point represents mean of values in triplicate ± standard deviation [SD; error bars].

3.3 Validation of inhibitory properties of sdMET isoforms

It is possible that sdMET inhibitory activity observed in figure 3.7 can be artifact from experimental conditions, such as cell line specific effect, non-specific HGF binding to

flag tag, or transfection conditions that introduced factors into CM that inhibits MET. To negate the possibility that activity is due to cell line specific effect, we treat A549 cells with HGF in presence of CM containing sdMET. As expected, we observed similar MET inhibition in A549 cells as observed in HeLa cells (figure 3.8A). furthermore, to rule out cell culture conditions during CM test, we starved A549 cells for 24 hours before CM test. As expected, sdMETs were able to suppress MET phosphorylation and downstream pathways irrespective of starved or non-starved conditions of A549 cells (figure 3.8B).

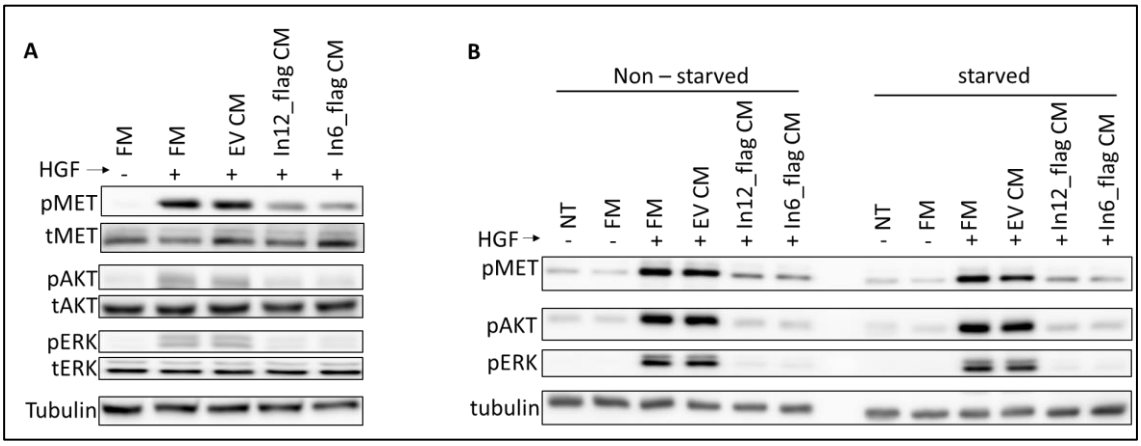

Figure 3.8: **Flag tag sdMET isoforms can block MET activation in A549 cells**. **A**. A549 cells were stimulated with 10 ng/ml of HGF for 5 minutes in presence of CM containing flag tagged sdMET isoforms. Following HGF stimulation, A549 cell lysate were subjected to western blot analysis for phosphorylation of MET and activation of downstream AKT and ERK pathways. **B**. A549 cells are 24 hours starved or non-starved before CM test as in panel A.

To rule out non-specific interaction between flag tag and HGF, we remove flag from sdMET (figure 3.7A) and perform CM test. As predicted, the presence or absence of flag tag did not make a difference in sdMET ability to block MET activation (figure 3.9B).

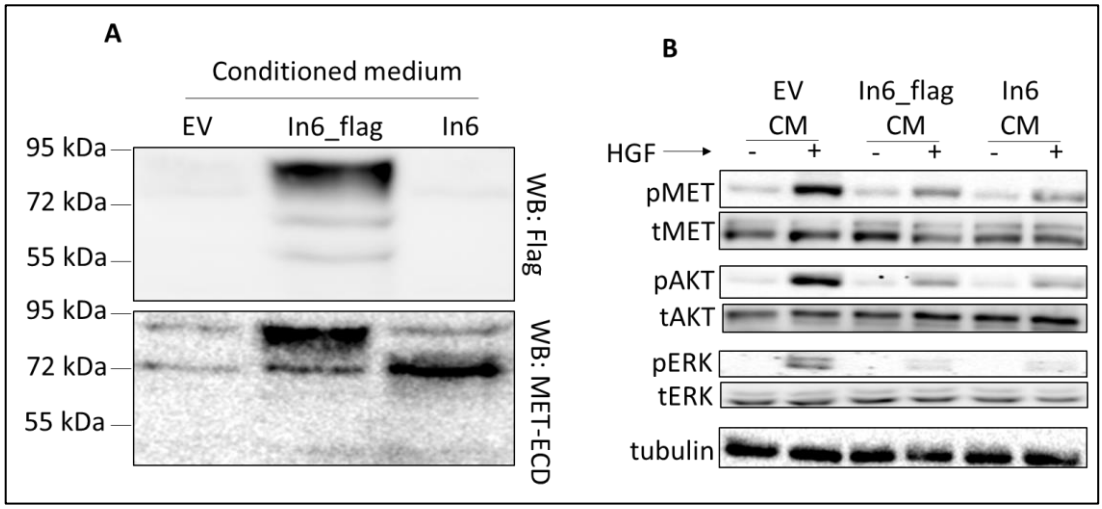

Figure 3.9: **Removal of flag tag does not affect sdMET inhibitory activity**. **A**. sdMET In6 isoform with or without flag tag were expressed in HEK293T cells for 72 hours. Top: western blot with anti-flag antibody; bottom: western blot with anti-MET extracellular domain (ECD) antibody **B**. HeLa cells treated with 10ng/ml of HGF for 5 minutes in presence of CM from panel A.

Finally, we perform a CM depletion assay to rule of effect of transfection conditions (figure 3.10).

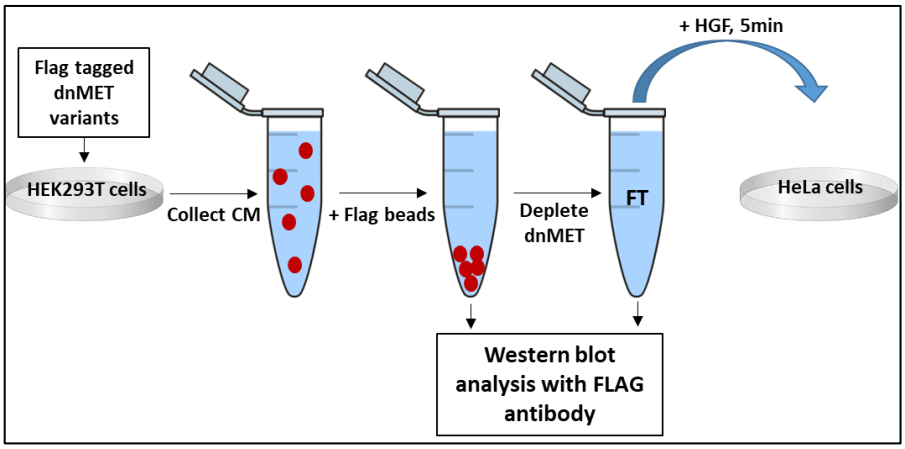

Figure 3.10: **Schematic of sdMET depletion from CM**. Sepharose beads conjugated with anti-flag antibody is added to CM containing flag tagged sdMET isoforms. After overnight immunoprecipitation (IP), flow through (FT) is collected and added to HeLa cells in presence of 10 ng/ml of HGF for 5 minutes. After 5 minutes, lysates are collected and analyzed for MET activation.

In our CM depletion assay, we depleted sdMET from CM by immunoprecipitation (figure 3.11, left) and performed CM test with flow through (FT) from IP. As expected, removal of sdMET from CM, restored MET phosphorylation and activation of downstream pathway (figure 3.11, right).

Together, our data demonstrates that MET inhibition and suppression AKT and ERK pathways is due specifically to presence of sdMET in CM rather than artifact in experimental conditions.

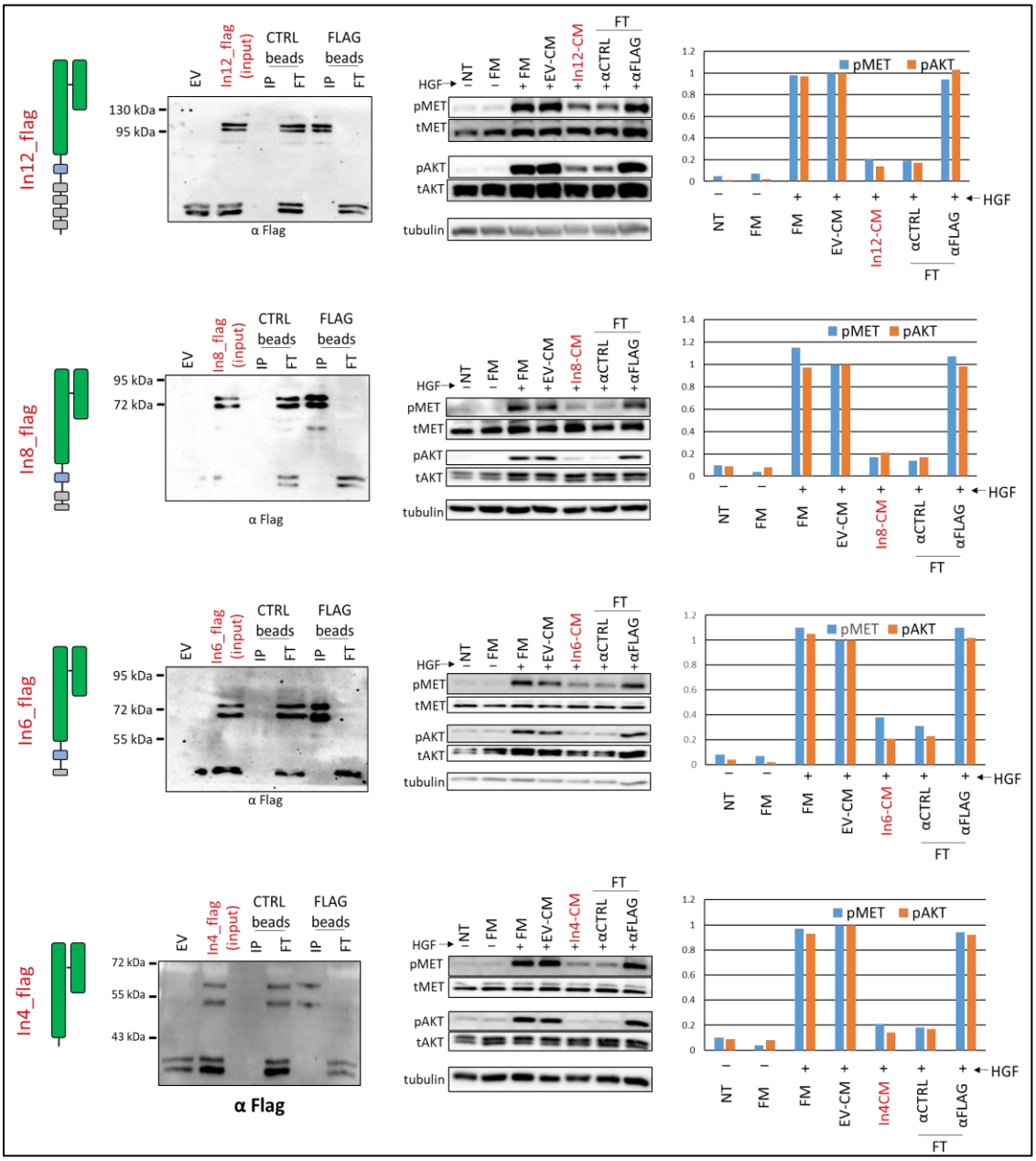

Figure 3.11: **Depletion of sdMETs from CM restores MET activity**. Depletion assay was performed as outlined in figure 3.10 for In12, In8, In6, and In4 flag isoforms.

3.4. Biological activity of MET is suppressed in presence of sdMET isoforms

After we established that sdMET IPA isoforms can inhibit MET activity at the molecular level, it stands to reason that sdMETs can also suppress MET's biological

activity. Recent studies have described in vitro biological assay for MET, such as, cell scattering, migration, invasion, and anchorage independent assay.

To demonstrate that sdMETs can suppress cell scattering, we treated HPAF II pancreatic adenocarcinoma cells with HGF in presence of CM containing sdMETs. As expected, sdMETs isoforms were able to suppress scatter effect of HGF-MET activation (figure 3.12).

Next, we asked whether sdMET IPA isoforms can prevent MET-dependent migration and invasion. To address this question, we utilized transwell migration and

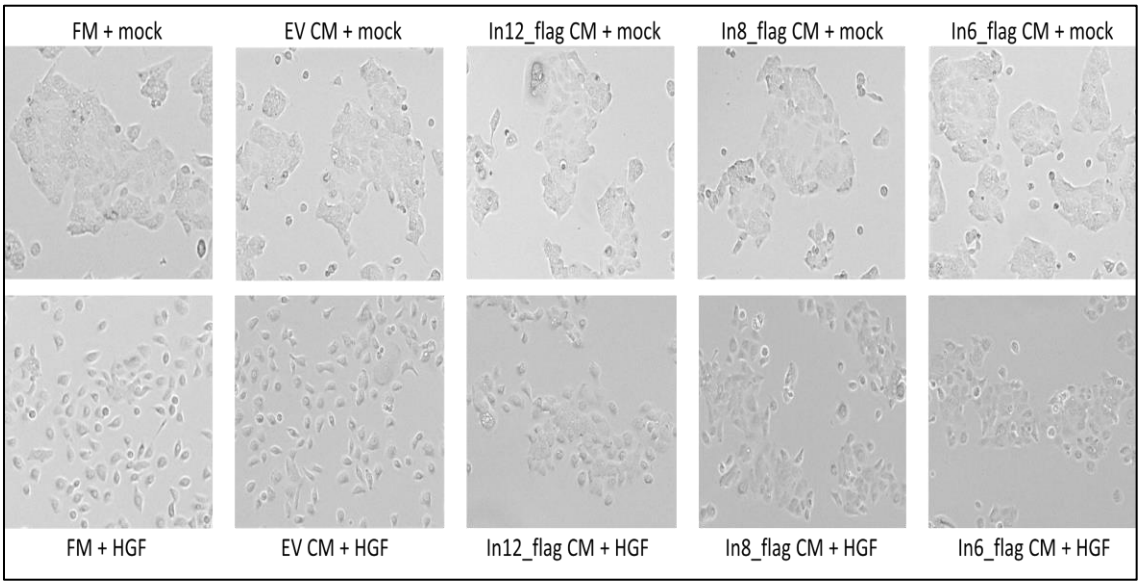

Figure 3.12: **sdMET isoform prevents scattering in HPAF-II pancreatic cancer cells**. HPAF II cells were treated with 10 ng/ml of HGF for 24 hours in presence of fresh medium (FM) or CM containing sdMET isoforms.

invasion assay. In the presence of CM containing sdMETs, there is a significant reduction of migrating and invading HPAF II cells (figure 3.13).

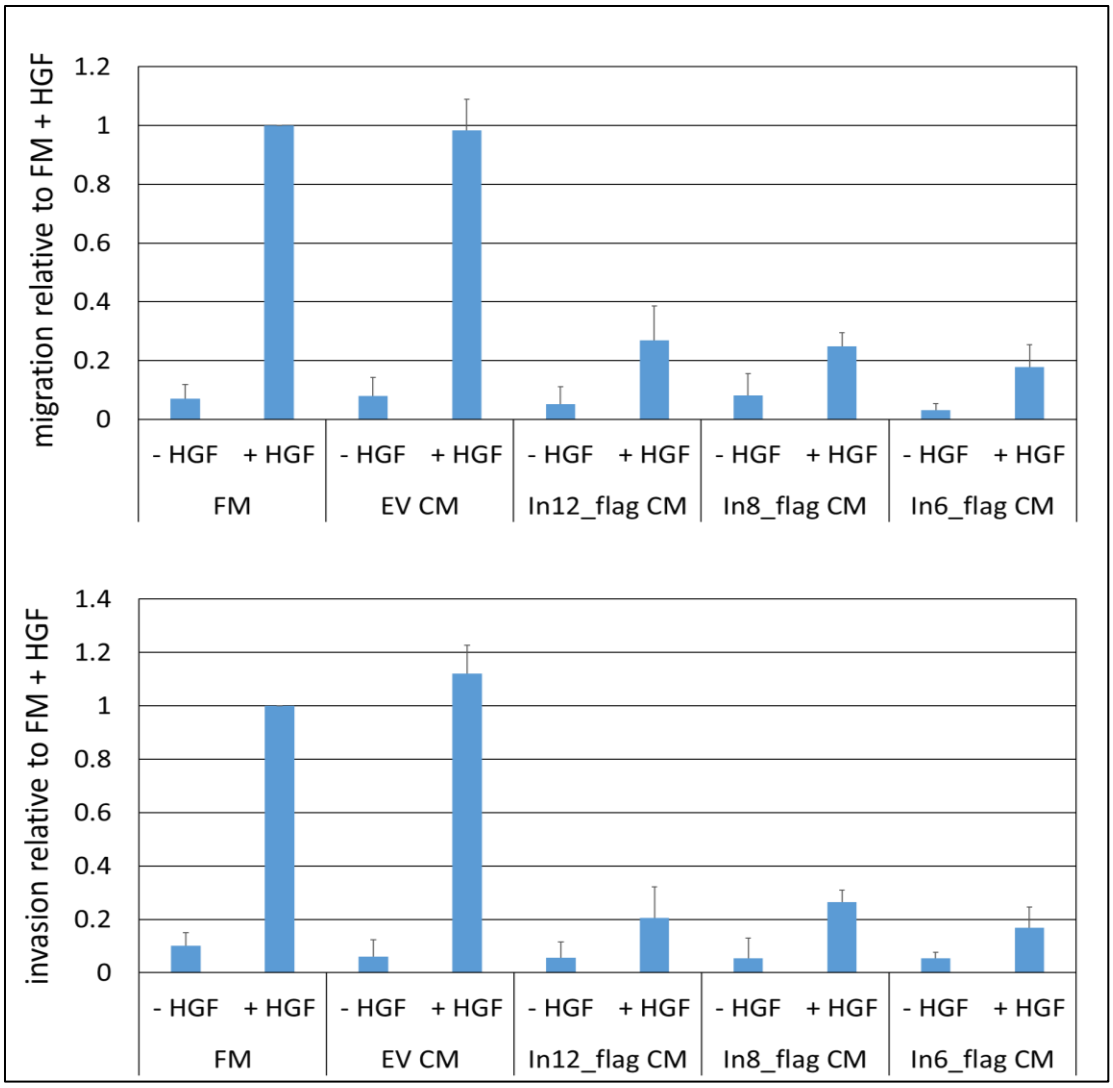

Figure 3.13: **sdMET isoforms prevents cell migration (top) and invasion (bottom).** HPAF II cells were treated for 24 hours with HGF (10ng/ml) in presence of FM or CM containing sdMETs in a transwell migration or invasion assay. After 24 hours, cells were stained with 0.1% crystal violet, eluted, quantified at 590 nm and represented as percentage of FM ± HGF. Each point represents mean of values **in** triplicate ± standard deviation [SD; error bars].

To test if sdMETs can inhibit anchorage independent growth, we seeded A549 cells in soft agar. For two weeks, cells treated with HGF in presence of CM containing sdMET. As shown in figure 3.14, sdMET was able to prevent colony formation compared to control conditions.

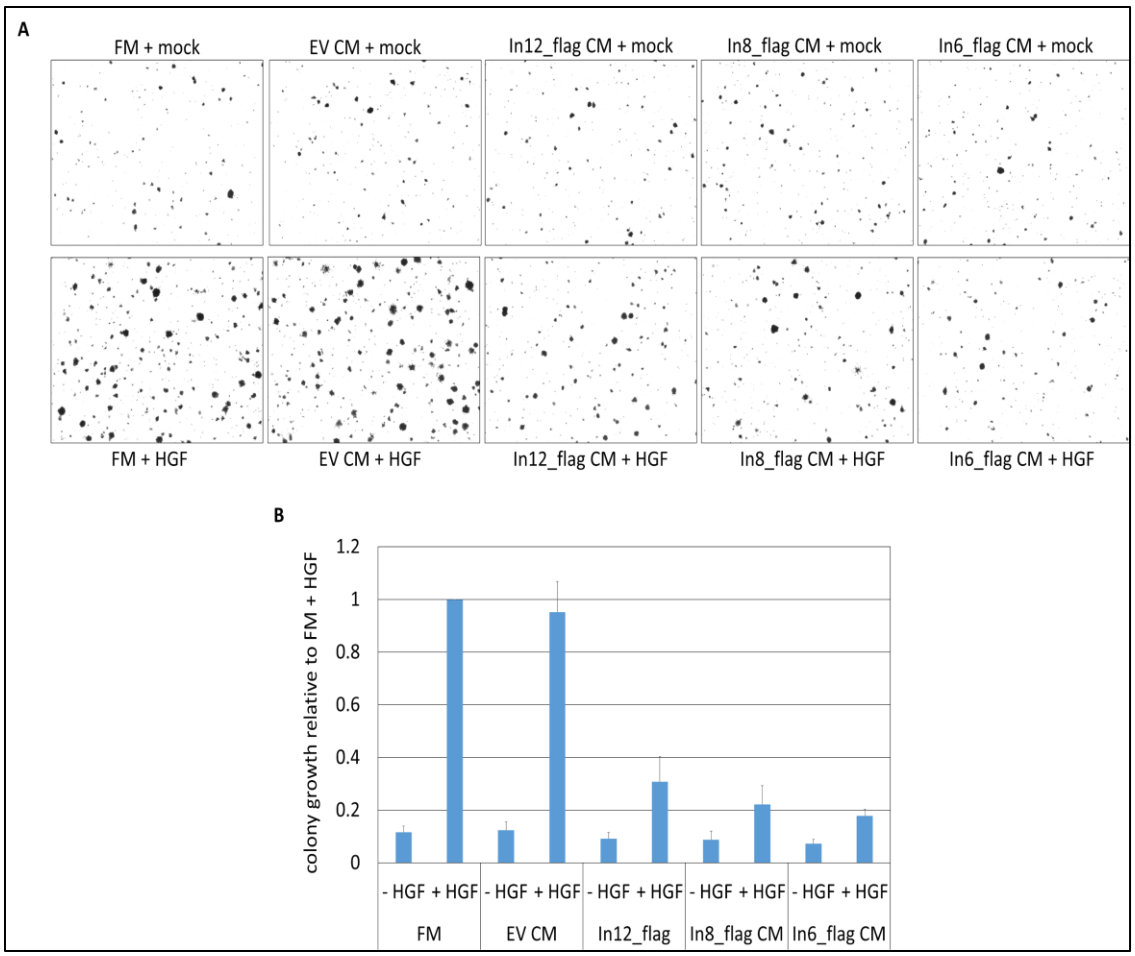

Figure 3.14: **sdMET isoform inhibits anchorage-independent colony formation**. **A**. After seeding A549 cells in soft agar, cells were treated with 10 ng/ml of HGF in presence of FM or CM containing sdMETs for 14 days. **B**. Colonies were quantified and represented as percentage of FM + HGF (bottom). Each point represents mean of values in triplicate ± standard deviation [SD; error bars].

Overall, our data demonstrate that sdMET IPA isoforms can block MET activation and suppress is biological activity by preventing cell movement, migration and invasion.

3.5. Targeting 5' splice site specific exons with anti-sense morpholino compounds to activation intronic polyadenylation

Based on our results of inhibitory properties with sdMET IPA isoforms, we used an anti-sense base approach using morpholino (MO) oligonucleotides coupled to dendritic transporter to activate IPA in selected introns. We designed MOs to bind to specific upstream exon's 5' splice site (ss) to prevent U1 snRNP binding thereby activating IPA in intron immediate downstream of target 5'ss (figure 3.15A). For example, to activate IPA in In12, designed MO binds to Ex12.5'ss. Furthermore, as a control, we designed a MO to Ex2.3'ss to knockdown MET. With this rational, we initially targeted 5'ss of exon 2, 4, 6, 9, and 12 (figure 3.15B). As a control, we also targeted 3'ss for exon 2 (figure 3.15B).

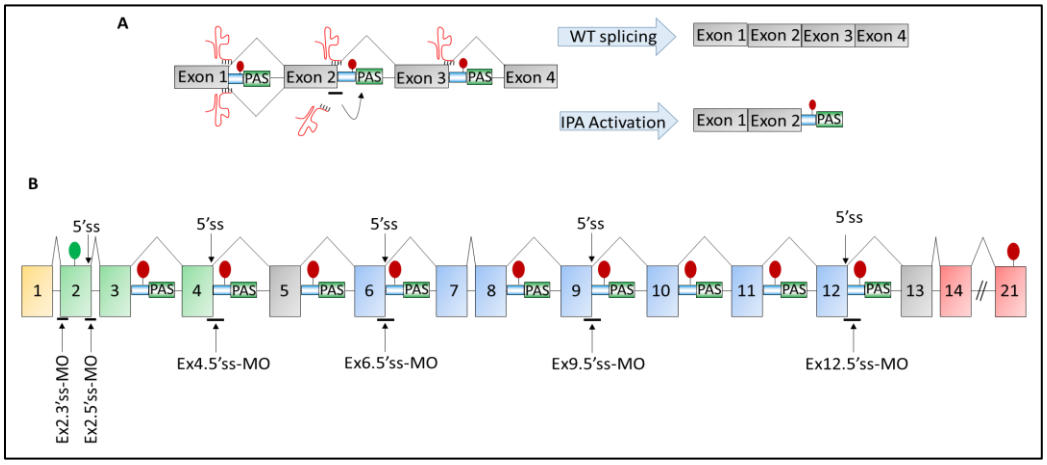

Figure 3.15: **Selective targeting with MO to activate IPA**. **A**. Schematic of activating IPA with anti-sense compounds in hypothetical 4 exon pre-mRNA**. B**. Antisense morpholino compounds is designed to target specific exon 5' splice site (ss) for Ex12, 9, 6, 4, 2. In addition, we also targeted exon 2.3'ss as a control.

3.6. Activity of anti-sense morpholino targeting exon 4 or exon 9 5' splice site

For test our strategy, we initially targeted Ex4.5'ss and Ex9.5'ss. To detect IPA mRNA, we utilized a previously described 3-primer RT-PCR strategy. In this RT-PCR assay, a common forward primer is used with two reverse primers: one intronic reverse primer to detect IPA mRNA and second exonic reverse primer to detect WT or other alternative splicing events (figure 3.16A). Unfortunately, after 48hr treated in EBC-1 cells with

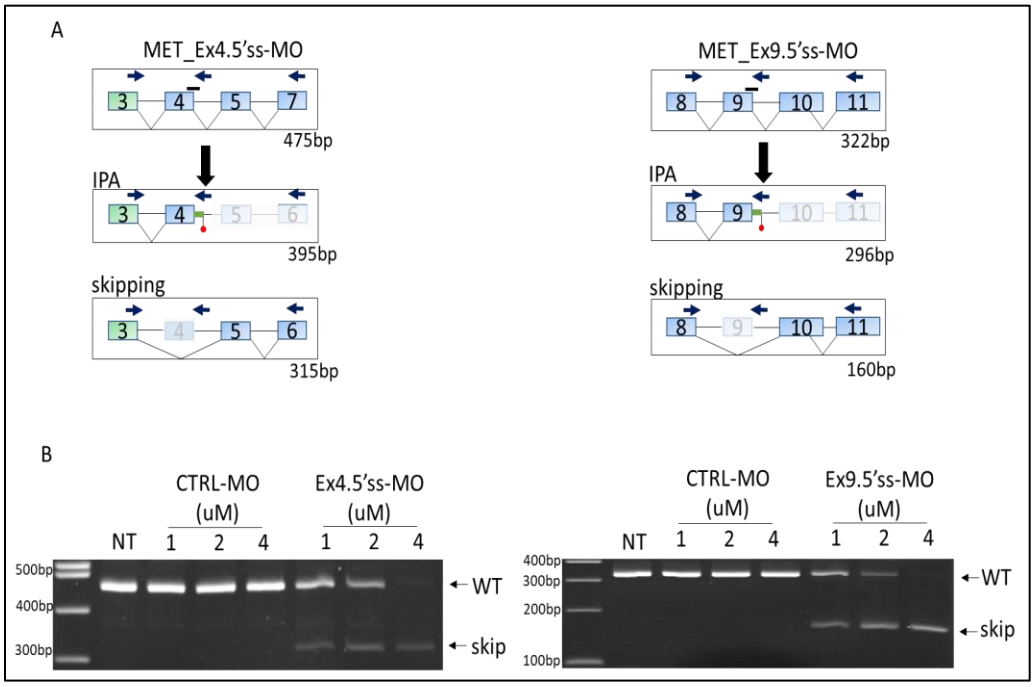

Figure 3.16: **Schematic of 3-primer RT-PCR assay for Ex4.5'ss-MO and Ex9.5'ss-MO. A**. Switch from wild type mRNA to IPA variant is detecting in 3-primer PCR assay; a common forward primer is paired with two reverse primers: a reverse intronic primer to detect IPA variant and a reverse exonic primer to detect WT mRNA or other splicing events, such as exon skipping. **B**. EBC-1 cells were treated with 1uM, 2uM or 4uM of CTRL-MO, Ex4.5'ss-MO or Ex9.5'ssMO for 48 hours. 3-primer assays were performed as described in panel A.

Ex4.5'ss-MO and Ex9.5'ss-MO with increasing concentration, we were only able to induce exon skipping. (figure 3.16B).

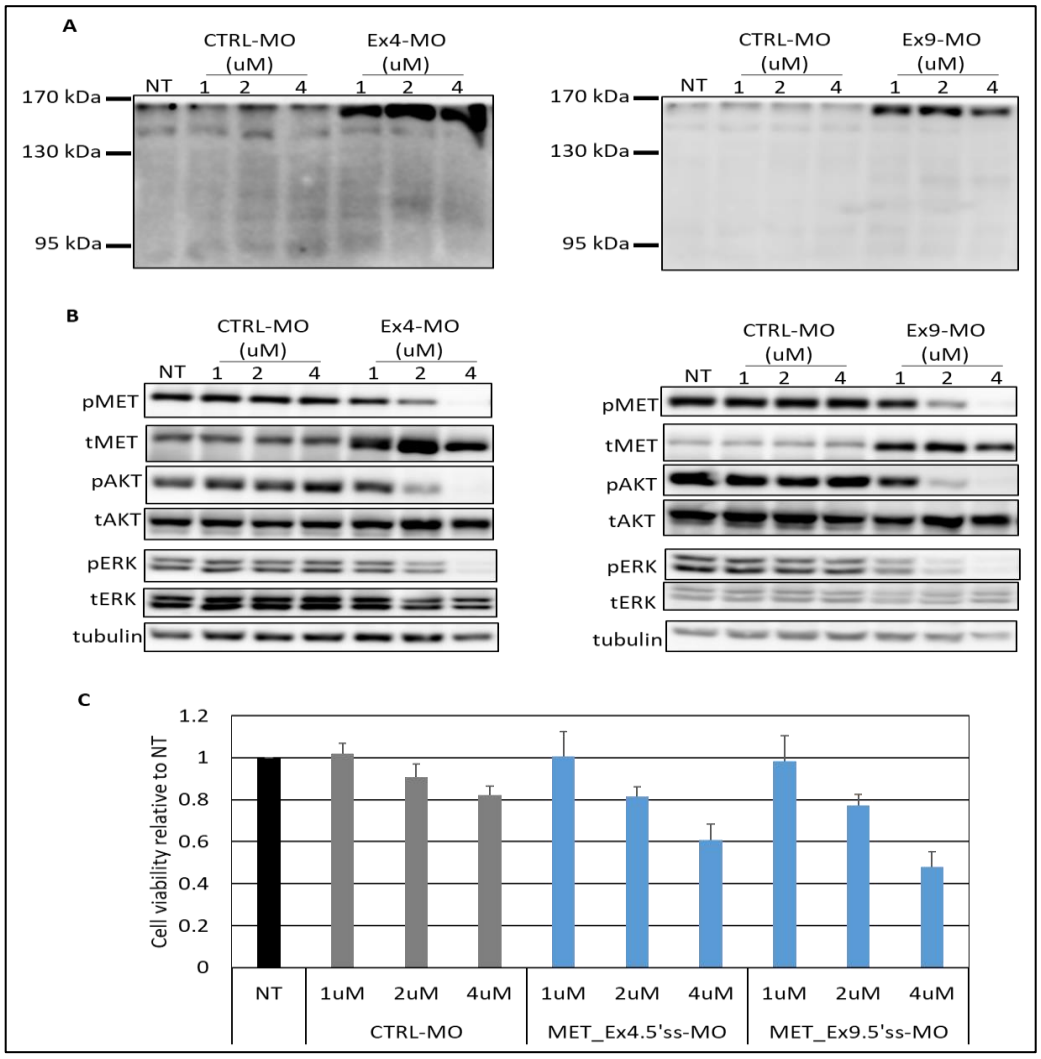

Figure 3.17: **Ex4.5'ss-MO and Ex9.5'-MO generate inactive exon skipping isoform.**

A and B. EBC-1 cells were treated with 1uM, 2uM or 4uM of CTRL-MO, Ex4.5'ss-MO or Ex9.5'ssMO for 48 hours. Lysates were analyzed with MET extracellular (ECD) antibody (A) or activation of AKT or ERK pathways (C). EBC-1 cells treated similarly to panel A and B for 72 hours. Cell viability was measured and represented as percentage of non-treated (NT) group. Each point represents mean of values in triplicate + standard deviation (error bars).

mRNA without exon 4 or 9 retains open reading frame and codes for isoform similar to FL-MET with the exception amino acids (AA) encoded by skipped exon. For this reason, we analyzed treated EBC-1 cells for Ex4 or Ex9 skpping corresponding isoforms, 145 kDa and 140 kDa respectively. As expected, western blot analysis with N-terminal extracellular domain (ECD) or C-terminal MET antibody detected slower migrating band corresponding to Ex4 and Ex9 skipped isoforms (figure 3.17 A, B). Furthermore, based on their expression pattern, it suggests that these isoforms are stabilized and are expressed at higher levels than FL-MET (figure 3.17 A, B). However, the lack of Ex4 or Ex9 coding AA prevented activation of downstream ERK and AKT pathway and significantly reduced cell viability (figure 3.17 B, C). From these results, the utility of Ex4.5'ss-MO and Ex9.5'ss-MO can be exploited when inactive intracellular MET is required.

3.7. Activity of anti-sense morpholino targeting 5' and 3' splice site of exon 2

The next set of anti-sense MOs tested were targeting exon 2 5'ss and 3'ss. These MOs are designed to serve as control for IPA generating compounds. As previously with Ex4 and Ex9 MOs experiment, we treated EBC-1 with increasing concentration of Ex2.5'ss-MO or Ex2.3'ss-MO for 48 hours and performed 3-primer RT-PCR assay. As predicted, targeting 5'ss of exon 2 generated IPA variant at mRNA level, whereas Ex2.3'ss produced exon skipping variant (figure 3.18A, B).

To analyze protein generated with Ex2.5'ss-MO or Ex2.3'ss-MO, we again treated EBC-1 cells with Ex2 targeting MO compounds. After 48 hours of treatment, we performed western blot analysis with antibodies against the extracellular domain and C-

terminal domain of MET. With Ex2.5'ss-MO, we detected faster migrating isoform corresponding to In2 IPA which is predicted to be 38 kDa in higher MO treated samples (figure 3.19A). Furthermore, EBC-1 cells treated with Ex2.3'ss-MO knockdown FL-MET (figure 3.19B); importantly, C-terminal MET antibody did not detect any isoform with Ex2.3'ss-MO ruling out usage of alternative splice site which retains open reading frame. Moreover, Ex2.3'ss-MO and Ex2.5-MO perturbed AKT and ERK pathways and induced cytotoxicity in EBC-1 cells (figure 3.19C, D).

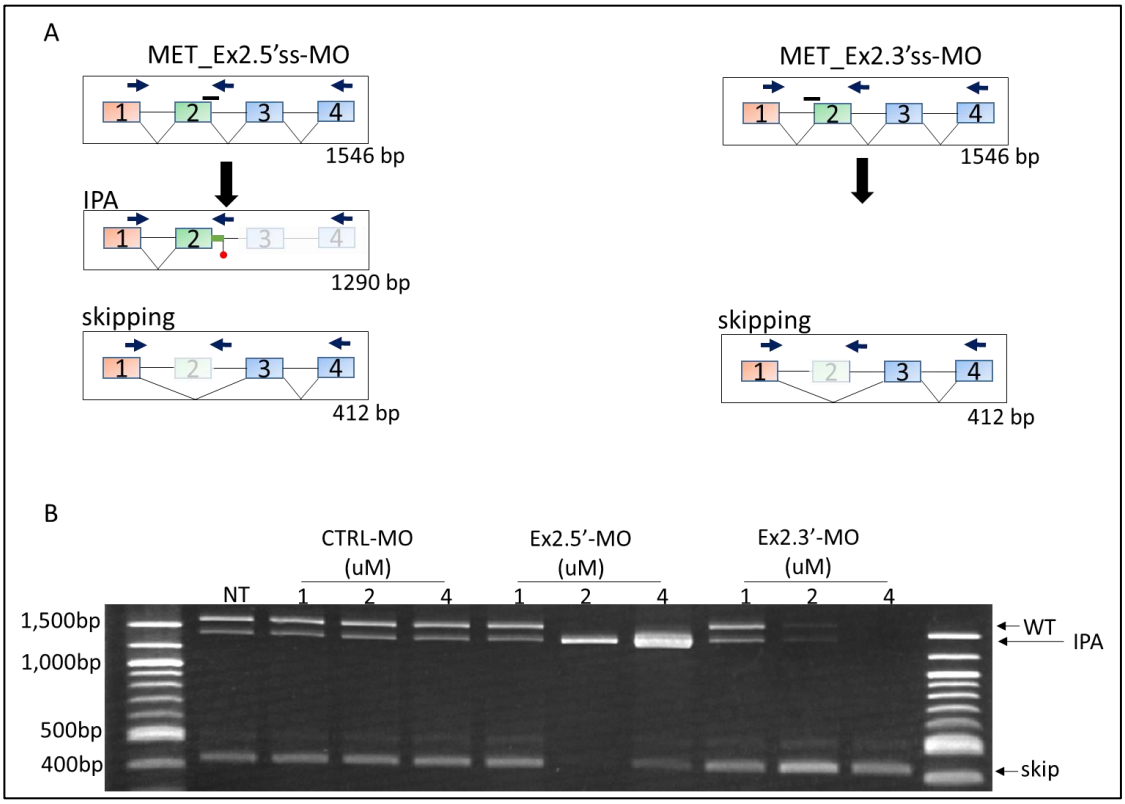

Figure 3.18: **Schematic of 3-primer RT-PCR assay for Ex2.5'ss-MO and Ex2.3'ss-MO.** **A**. Targeting exon 2 with .5'ss-MO and 3'ss-MO and predicted splicing event. **B**. EBC-1 cells were treated with 1uM, 2uM or 4uM of CTRL-MO, Ex2.5'ss-MO or Ex2.3'ssMO for 48 hours and 3-primer RT-PCR assays were performed as in panel A.

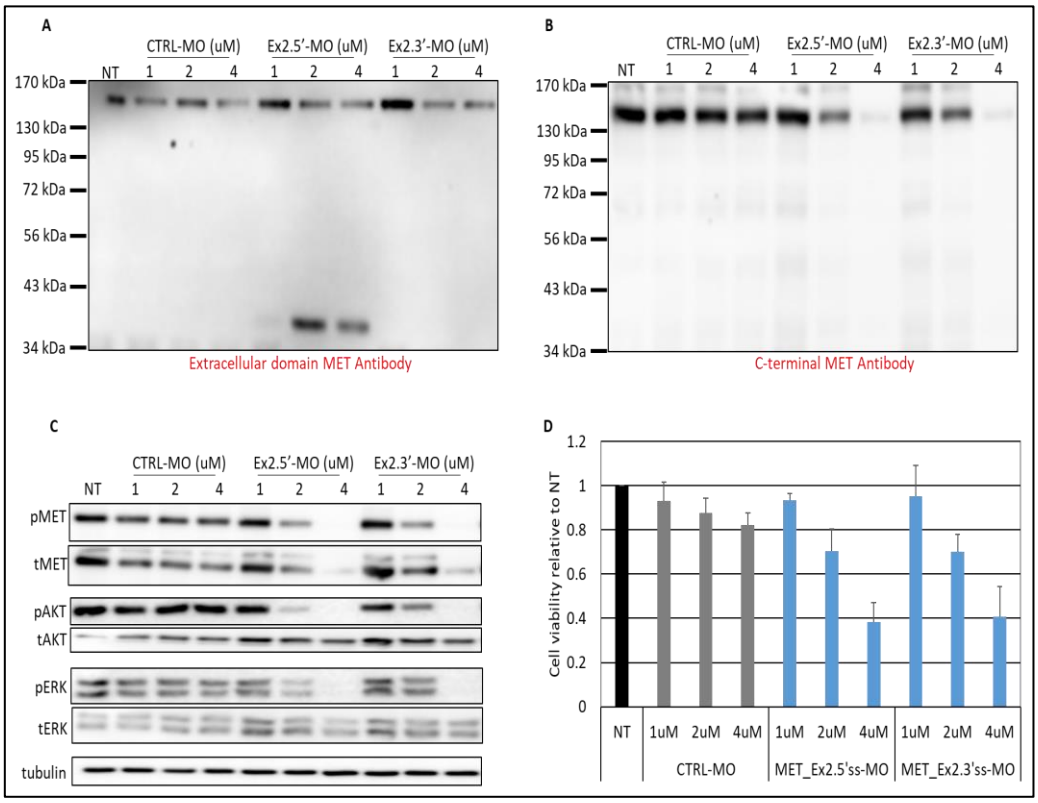

Figure 3.19: Activity of Ex2.5'ss-MO and Ex2.3'ss-MO. A and B. EBC-1 treated with 1uM, 2uM, or 4uM with CTRL-MO, Ex2.5'ss-MO or Ex2.3'ss-MO. Western blot analysis with ECD MET antibody (**A**) or C-terminal MET antibody (**B**). **C**. sample from panel A and B were analyzed for activation of AKT or ERK pathways. **D**. EBC-1 treated similarly as panel A and B for 72 hours. Cell viability was measured after 72 hours and represented as percentage of non-treated (NT) group. Each point represents mean of values in triplicate ± standard deviation (error bars).

3.8 Activation of intronic polyadenylation (IPA) with Ex12.5'ss-MO and Ex6.5'ss-MO to generate soluble decoy MET

To screen for molecular activity of Ex12.5'ss and Ex6.5'ss MO compounds (figure 3.20A), we utilized a cell line which is independent of MET activity: KRAS G12C mutant

H1792 cells. With our 3-primer RT-PCR assay, we were able to detect increasing level of sdMET In12 and In6 IPA mRNA in dose dependent manner where we observed a switch to therapeutic variants at highest concentration exclusively in MET 5'ss specific MO and not CTRL-MO (figure 3.20B).

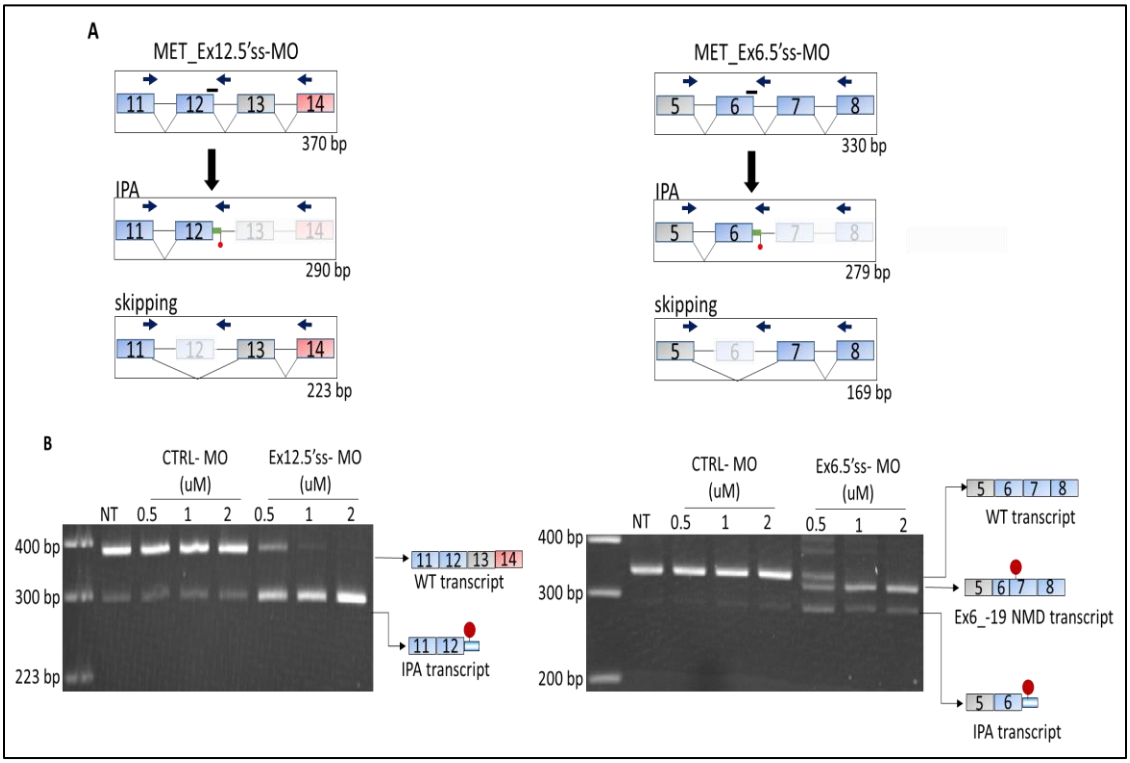

Figure 3.20: Schematic of 3-primer RT-PCR assay for Ex12.5'ss-MO and Ex6.5'ss-MO. **A**. Targeting exon 12.5'ss or 6.5'ss with anti-sense morpholinos and predicted splicing event. **B**. H1792 cells were treated with 0.5uM, 1uM or 2uM of CTRL-MO, Ex12.5'ss-MO or Ex6.5'ssMO for 48 hours and 3-primer RT-PCR assays.

After observations of complete reduction of FL-MET at RNA level, we hypothesized that FL-MET protein should also be removed with our MO compounds. As expect, treatment of H1792 cells for 48 hours with Ex12.5'ss-MO and Ex6.5'ss-MO remarkably reduced FL-MET when using antibodies against the C-terminus (figure 3.21A). Moreover, since H1792 harbor KRAS G12C mutation, reduction of FL-MET marginally effected the downstream AKT and ERK pathways (figure 3.21A) and had no consequence on cell viability (figure 3.21B).

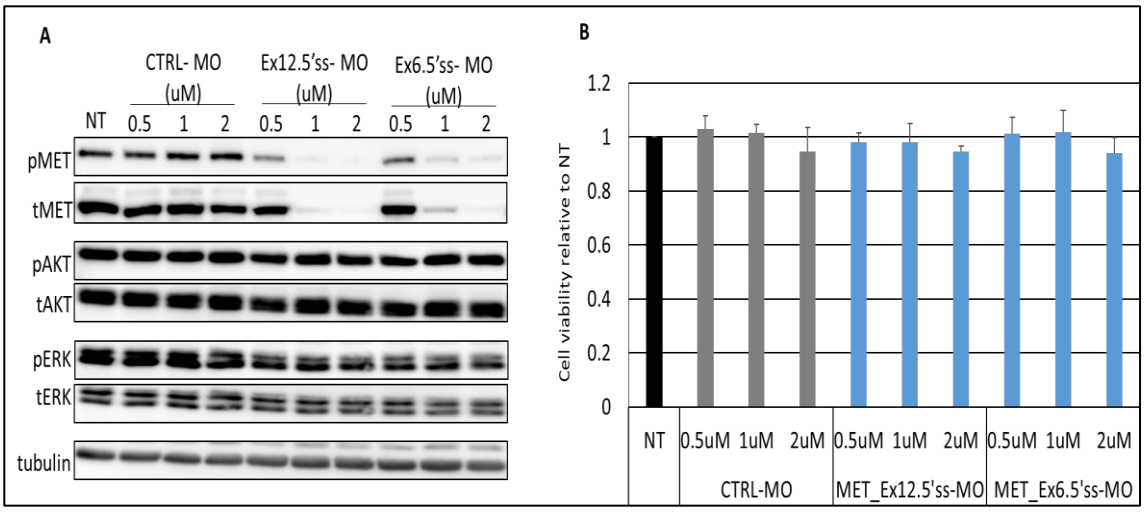

Figure 3.21: Targeting Ex12 and Ex6 5'ss with MOs reduces full length (FL) MET and does not affect cell viability in H1792 cells. A. analysis of FL-MET and AKT and ERK pathway activation after 48-hour treatment. B. 72-hour cell viability was measured and expressed as percentage of NT group. Each point represents mean of value in triplicate ± standard deviation (error bars).

With our Ex6.5'ss-MO, we also detected an alternative splicing event corresponding to usage of cryptic 5'ss splice site located 19 nucleotides within Exon 6 (figure 3.20B right, figure 3.22A) leading to frameshift and generation of premature termination codon (PTC) in exon 7 (figure 3.22A).

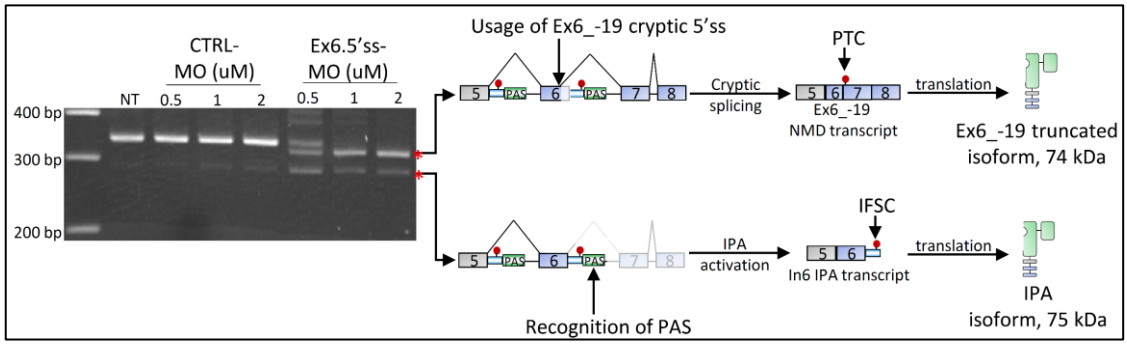

Figure 3.22: characterization of sdMET mRNA variants generated by Ex6.5'ss-MO. A. same PCR gel as figure 3.20B right. For 2uM Ex6.5'ss-MO lane, slower migrating PCR product is Ex6_-19 NMD transcript which has a premature termination codon (PTC) due to shift in open reading frame; the faster migrating PCR product is In6 IPA variant which includes in-frame stop codon (IFSC). However, if Ex6_-19 NMD transcript is expressed, it will generate a C-terminal truncated sdMET similar to sdMET In6 IPA isoform.

Due to the PTC in reading frame, Ex6_-19 transcript is target for nonsense mediate decay (NMD) pathway which is an RNA surveillance mechanism to degrade mRNA with PTC. Nevertheless, if low levels of Ex6_-19 transcript were to escape NMD mediated degradation, the expressed protein is similar in activity to sdMET In6 IPA isoform (figure 3.23A, B).

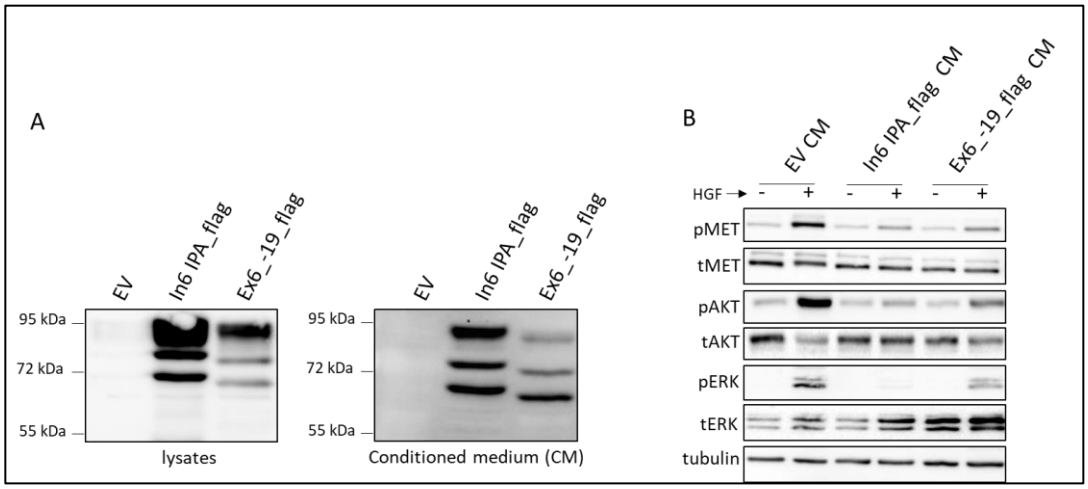

Figure 3.23: In6 IPA and Ex6_-19 NMD isoform have similar inhibitory activity. **A**. Ex6_-19 variant and ex6_skipping isoform was cloned as C-terminal flag tag recombinant protein similarly to sdMET In6 IPA (figure 3.3). sdMET Ex6_-19 and sdMET In6 IPA isoforms were transfected into HEK293T cells. After 72 hours, lysate and conditioned medium (CM) were collected and subjected to western blot analysis with anti-flag antibody. **B**. sdMET Ex6_-19 and sdMET In6 IPA flag tagged proteins have comparable inhibitory activity. Conditioned medium test with HeLa cells and lysates were collected for western blot analysis for phosphorylation of MET and activation of AKT and ERK pathways.

More importantly, since MOs did not affect H1792 cell viability, we hypothesized that the switch from FL-MET to MET IPA variants we observed at the RNA level will also be detect at the protein level. Furthermore, MET IPA In12 and In6 isoform should condition the culture medium just the recombinant flag tag isoforms (figure 3.3B) due to the lack of TM and ICD domains. As expected, when using N-terminal ECD MET antibody to detect both FL-MET and sdMET IPA isoforms, we observed substantial conversion of

FL-MET to IPA proteins and IPA proteins were overwhelmingly secrete into extracellular space in cells treated with Ex12.5'ss and Ex6.5'ss MOs (figure 3.24A). Next, we asked whether sdMET IPA isoform generated with our MO compounds can inhibit MET activation. To test for inhibitory activity, we perform CM test with CM collected from MET MOs treated H1792 cells. As anticipated, when HeLa cells were treated with HGF for 5 minutes in the presence of CM containing MET IPA isoforms expressed via our anti-sense-based approach, there was a significant reduction of MET phosphorylation and suppression of AKT and ERK pathways (figure 3.24B).

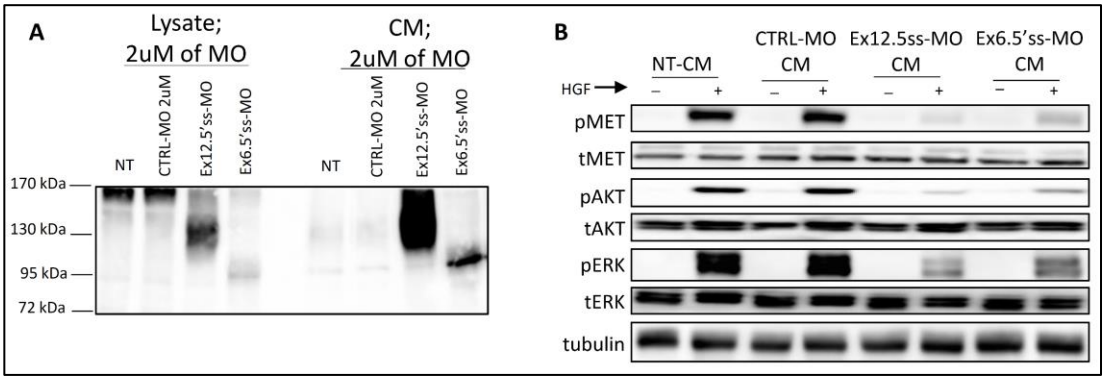

Figure 3.24: Ex12.5'ss and Ex6.5'ss MOs convert FL-MET to sdMET IPA isoforms.

A. H1792 cells were treated with 2uM of MOs targeting Ex12.5'ss or Ex.6.5'ss. After 72 hours, lysate and conditioned medium (CM) was collected for western blot analysis with anti-MET ECD antibody to detect sdMET IPA isoforms. **B**. sdMET IPA isoform generated with 5'ss specific antisense MOs can block MET activation. HeLa cell were stimulated with 10ng/ml of 5 minutes in presence of CM from panel A. after 5 minutes stimulation, lysates were collected for western blot analysis for activation of MET and downstream pathways, AKT and ERK.

Collectively, our Ex12.5'ss and Ex6.5'ss MOs demonstrates that targeting specific 5'ss can generate sdMET isoforms of choice at the expense of FL-MET protein. Moreover, these C-terminal truncated sdMET IPA isoforms are released into extracellular space and behave in a dominant negative manner over its FL-MET counterpart.

3.9. MET anti-sense compounds leads to sdMET expression and toxicity in MET dependent cancer cells

Next, we tested MET 5'ss-MOs activity in cells lines dependent on MET activity. We utilized cells lines with MET amplification (MET^{amp}.), EBC-1, MKN45 and Hs746T, which are sensitive to MET inhibition. Furthermore, as a control for MET inhibition, selective small molecule tyrosine kinase inhibitor, AMG337, was used in parallel with MET MOs. First, we treated MET^{amp} cells with increasing concentration of MET Ex12.5'ss-MO and Ex6.5'ss-MO for 48 hours and performed 3 primer RT-PCR assay. As expected, FL-MET mRNA was completely removed at 2uM of MOs and replaced with sdMET mRNA (figure 3.25).

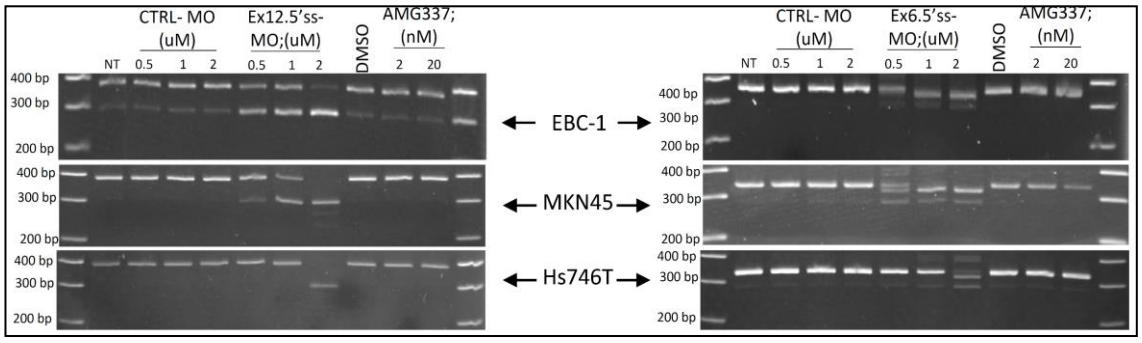

Figure 3.25: Ex12.5'ss and Ex6.5'ss MOs convert FL-MET to sdMET IPA at mRNA level. EBC-1, MKN45, or Hs746T, were treated with CTRL-MO, Ex12.5'-MO, Ex6.5'ss-MO, or AMG337. After 48 hours, 3-primer RT-PCR assay as described in figure 3.20.

Second, we asked if MET^{amp} cell lines treated with MET 5'ss MOs for 48 hours can generate sdMET In12 and In6 IPA proteins. When cells extracts were resolved in SDS-PAGE and probed with N-terminal MET antibody, we detected expression of MET In12 and In6 IPA isoform solely in cells treated with MET 5'ss MOs and not in CTRL-MO or AMG337 treatment groups (figure 3.26).

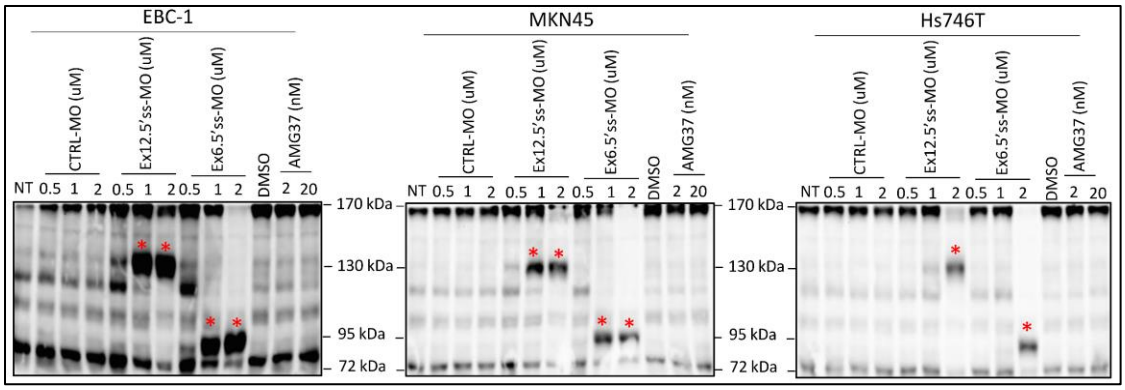

Figure 3.26: Ex12.5'ss and Ex6.5'ss MOs convert FL-MET protein and generates sdMET IPA isoform. EBC-1, MKN45, and Hs764T cells were treated similarly as figure 3.25 for 48 hours. Thereafter, cell lysates were subjected to western blot analysis with MET ECD antibody. Red asterisks are predicted IPA isoforms.

Furthermore, when lysates were probed with C-terminal MET antibodies, FL-MET was significantly reduced which led to suppression of downstream signaling AKT and ERK pathways (figure 3.27).

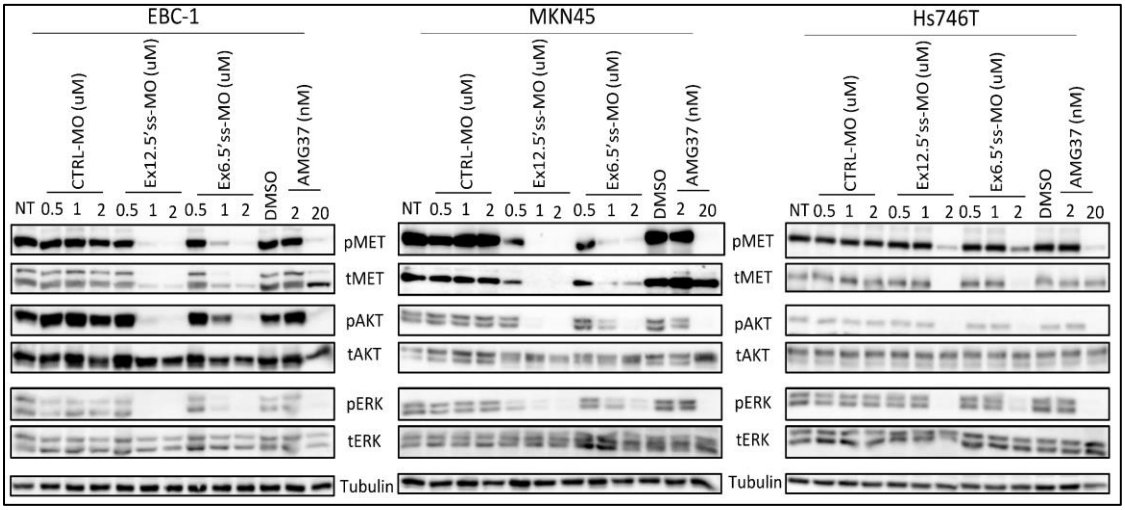

Figure 3.27: Ex12.5'ss and Ex6.5'ss MOs reduced FL-MET and perturbs downstream signaling pathways. EBC, MKN45, Hs746T cells were treated with Ex12.5'ss-MO, Ex6.5'ss-MO or AMG337 for 48 hours and analyzed for pMET, pAKT, and pERK.

Finally, we tested MET 5'ss MOs' ability to induced cellular toxicity in METamp. cells that are dependent of MET activity. When METamp. cells were treated with Ex12'5ss-MO and Ex6.5'ss-MO for 72 hours, we observed increase in cellular toxicity in dose dependent manner upon MET 5'ss MOs treatment and not CTRL-MO (figure 3.28). furthermore, the increase in toxicity correlate with increase in sdMET IPA isoform and reduction of FL-MET (figure 3.25,26,27).

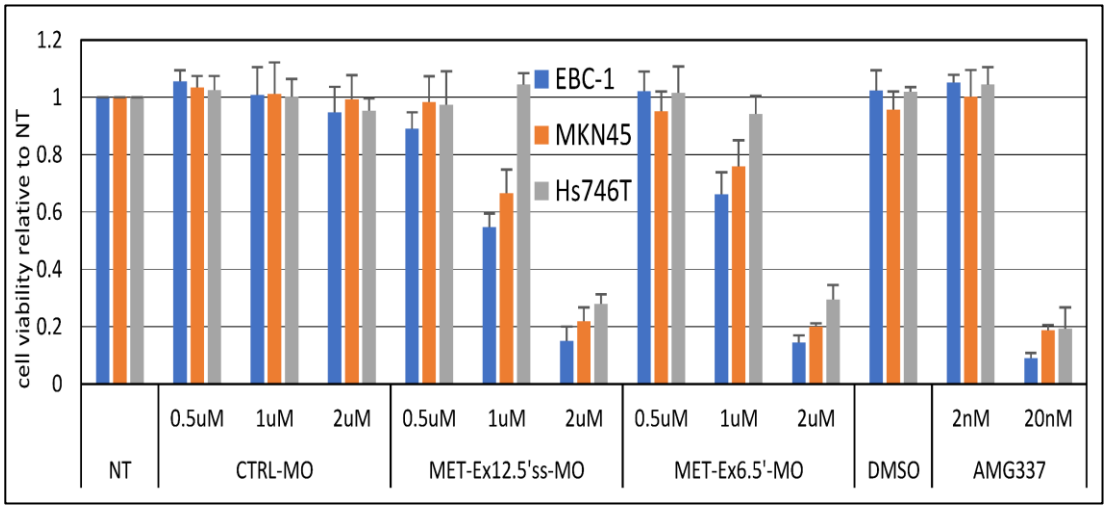

Figure 3.28: cytotoxic effect of Ex12.5'ss and Ex6.5'ss MOs treatments. MET dependent cells treated with Ex12.5'ss and Ex6.5'ss MOs leads to cellular toxicity. EBC-1, MKN45, and Hs746T were treated with increasing concentration of CTRL-MO, Ex12.5'ss-MO, Ex6.5'ss-MO or AMG337. After 72 hours, cell viability was measured and represented as a percentage of non-treated group. Each point represents mean of values in triplicate ± standard deviation [SD; error bars].

In addition to testing MET MO compounds in MET dependent cells, normal lung BEAS-2B and normal gastric Hs728 cells were treated with MET 5'ss MOs. As predicted, we observed reduction of FL-MET proteins (figure 3.29A). however, because these cells are not dependent on MET activity, MET MOs did not affect downstream pathway, AKT and ERK (figure 3.29A). Furthermore, Ex12.5'ss and Ex6.5'ss MOs did not induce cell viability (figure 3.29B).

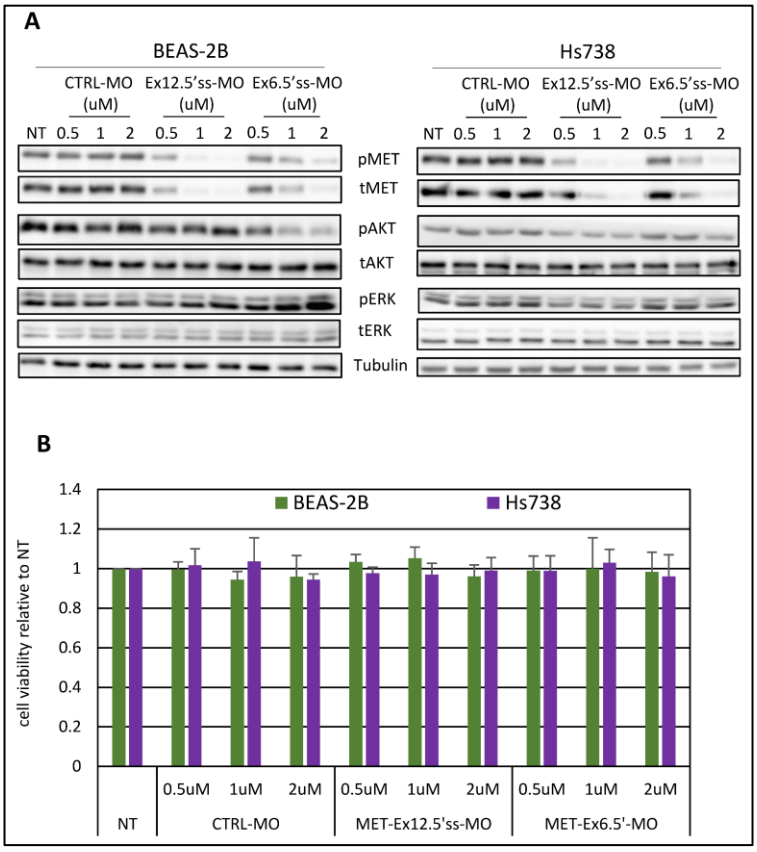

Figure 3.29: Activity of MET Ex12.5'ss-MO and Ex6.5'ss-MO in normal cells. **A**. Treatment of normal lung BEAS-2B and normal gastric Hs738 cells with MET 5'ss MOs reduced FL-MET but marginally effect AKT and ERK pathways. B. After 72 hours, cell viability was measured and represented as a percentage of non-treated group. Each point represents mean of values in triplicate ± standard deviation [SD; error bars].

Overall, these data demonstrate that MET specific 5'ss MOs are active in MET dependent cells. MOs are able to re-direct FL-MET pre-mRNA splicing towards generation of sdMET mRNA variants which are expressed at protein level. Furthermore, the switch from FL-MET to sdMET isoform perturbs downstream AKT and ERK pathways and leads to cytotoxic effect in MET dependent cells.

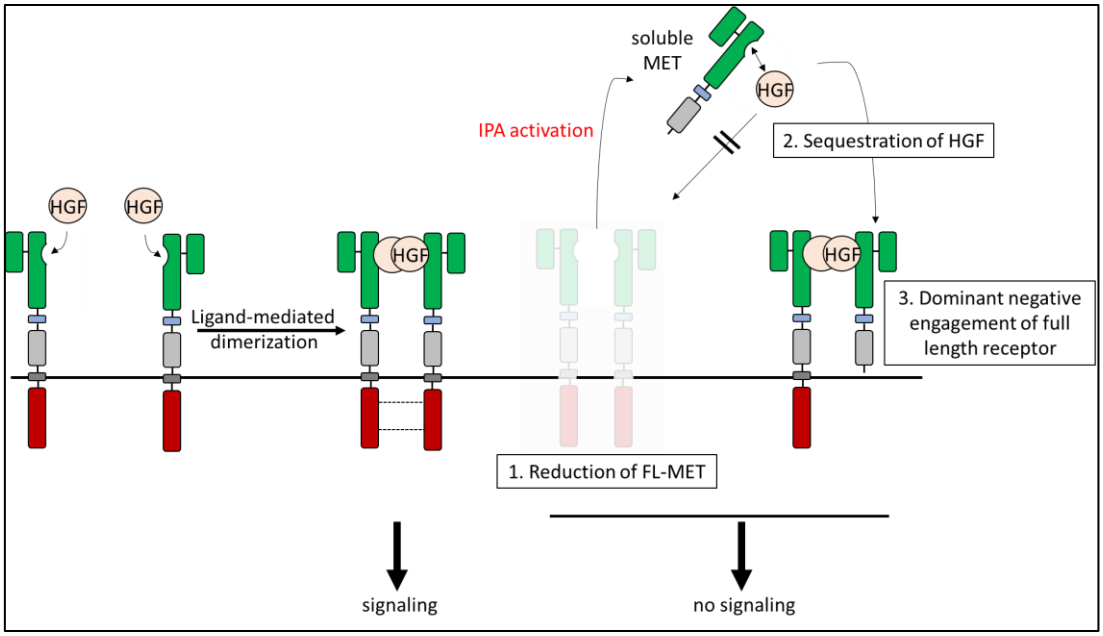

Figure 3.30: Advantage of targeting MET with anti-sense-based approach. Use of anti-sense compounds has a three-pronged effect: 1. Removal of oncogenic FL-MET receptor, 2. Release of soluble decoy MET (sdMET) into extracellular space to trap HGF, 3. sdMET engages residual FL-MET in effected and naïve cells in a dominant negative manner.

4. Discussion and future perspectives

Aberrant MET activation is involved in various aspects of cancer biology, including tumor initiation, progression, maintenance, angiogenesis, and metastasis. Hence, multiple groups have employed strategies to target MET receptor for cancer therapy. Current approaches include:

1. Ligand neutralizing antibodies
2. MET targeting antibodies to prevent ligand interaction and/or induce receptor degradation

3. Recombinant dominant negative MET ectodomain to sequester ligand and form non-functional dimer with Full length (FL) MET
4. Selective or non-selective small molecule tyrosine kinase inhibitors (TKIs)

Unfortunately, tumors activate mechanisms of resistance to maintain cancer progression, such as:

1. alternative RTK activity as a bypass track
2. Mutations to prevent drug-receptor interactions
3. Activating mutations in downstream signaling factors to prevent reliance on upstream receptor
4. Cell transformation to prevent drug uptake
5. Secretion of excess ligand from stromal cells to outnumber neutralizing antibodies

For these reasons, in this thesis, a novel method was described for targeting MET receptor (figure 3.30). Our anti-sense oligonucleotides (ASO) induces alternative intronic polyadenylation (IPA) with specific intron of choice in a U1-snRNP dependent manner. Hence, within a single ASO, we accomplish three-prong approach to inhibit MET activity at multiple levels:

1. Reduction of FL-MET oncoprotein similarly to RNAi-mediated knockdown
2. Expression and secretion of therapeutic soluble decoy MET (sdMET) into tumor microenvironment to trap MET ligand, hepatocyte growth factor (HGF)

3. Possibly engage residual FL-MET on targeted or naïve cells to form a non-productive dimer

Because of multifaceted role of MET in cancer progression, our approach can be useful in MET dependent or independent tumors. For example, patients under treatment with angiogenic inhibitors can relapse due to hypoxia inducible factor 1α (HIF1α) – mediated expression and secretion of HGF from tumor associated fibroblast [218]. This HGF activate MET on remaining blood vessel endothelial cells and rescue angiogenesis, thus allowing cancer to progress. Furthermore, MET signaling cascade can modulate and induce epithelial to mesenchymal transition (EMT), hence promoting metastases [202]. For these reasons, while there are short-term benefits with angiogenic inhibitors, their long-term use can have dire consequences. Due to this sequence of events under angiogenic inhibitors, addition of MET-ASO can have a synergistic effect to eradicate MET-dependent or independent tumors.

As with other reports, our strategy can be applied to other RTKs. indeed, our group previously generate sdVEGFR2 by targeting VEGFR2 to block tubulogenesis in huvec cells *in vitro*. Furthermore, Thomas Rando group recently therapeutic use ASO to generate membrane bound C-terminal truncated PDGFRα which can bind PDGF but lack kinase domain; their strategy activated IPA of PDGFRα in resident stem cells to attenuate muscle fibrosis. In addition to targeting RTKs or other membrane bound protein, ASO-mediated IPA can potentially target cytoplasmic protein. In protein which pathogenic domain is in C-terminus, IPA activation can remove C-terminus while preserving N-terminus which might be required for normal biological functions.

The approach described in this thesis has successfully targeted MET to generated therapeutic decoys; even though further work is needed to address tumor specific delivery of ASO, this work provides proof of principle that ASO can generated MET decoys while removing oncogenic MET. Moreover, this thesis is expected to serve as a blueprint for useful assays to describe and activate decoys for others RTKs.

Appendix

Alternative Splicing Generates p53 isoform with Possible Metastatic Function

1. Abstract

Transcription factor p53 plays a vital part in maintenance of genome stability and avoiding tumorigenesis. p53 gene encodes twelve isoforms because of alternative splicing, alternative promoter usage, and alternative initiation sites of translation. p53 isoforms can modulate cell-fate in stress response by regulating p53 transcriptional activity in a promoter and stress dependent manner. However, p53 isoforms are aberrantly expressed in multipe types of cancers, signifying their importance to cancer formation. Recently, laboratory of R. Sordella described a novel isoform for p53, p53ψ. Rather than preventing tumorigenesis, it contributes to cancer formation. p53ψ is a byproduct of the usage of alternative 3' splice site with intron 6 that generated a C-terminal truncated 27 kDa protein. p53ψ lacks oligomerization, DNA binding and nuclear localization domain. Hence, it is primarily localized in the cytoplasm where it alters mitochondrial permeability to increase reactive oxygen species (ROS). Increase in ROS promotes epithelial to mesenchymal transition (EMT) and induces metastasis. Because intronic and exonic mutation can promote alternative splicing, we, we explored existence other alternatively splice isoform due to mutation in 5'ss or codon juxtapose to 5'ss of exon 6 that will generate similar truncation with tumorigenic function. For our purpose, we employed an minigene splicing assay and usage of alternative 5'ss to generate truncated variant which should express truncated C-terminal isoform with similar topology as p53ψ.

2. Introduction

p53 is a key tumor suppressor inactivated in nearly all form of cancers [351]. p53 avoids tumorigenesis by modulating multiple pathways including cell cycle or cell death (appendix figure 1) [352]. p53 oligomerizes and binds p53- responsive elements (p53REs) in the genome to regulate gene expression. For instance, p53 promotes cell cycle arrest by activating genes such as BTG2, GADD45 or the cyclin-dependent kinase inhibitor, p21 [353]. On the other hand, p53 promotes apoptosis by activating pro-apoptotic genes such as Puma, Bax, Apaf1, Noxa and suppressing the anti-apoptotic gene - Bcl-2 [353]. However, how p53 decides to initiate with define cellular responses to promote cell death or cell survival to variable stress signals remains poorly understood. It has been

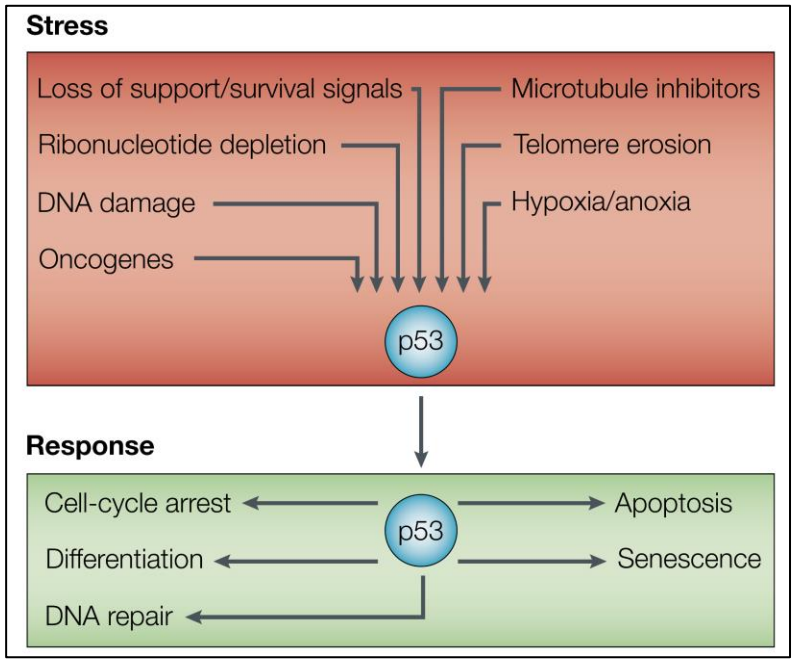

Appendix figure 1. P53 responses to stress signals.

Reprint with permission from [2].

demonstrated in tissue and cell type dependent manner that different p53 isoforms can regulate cellular responses to stress signals [351].

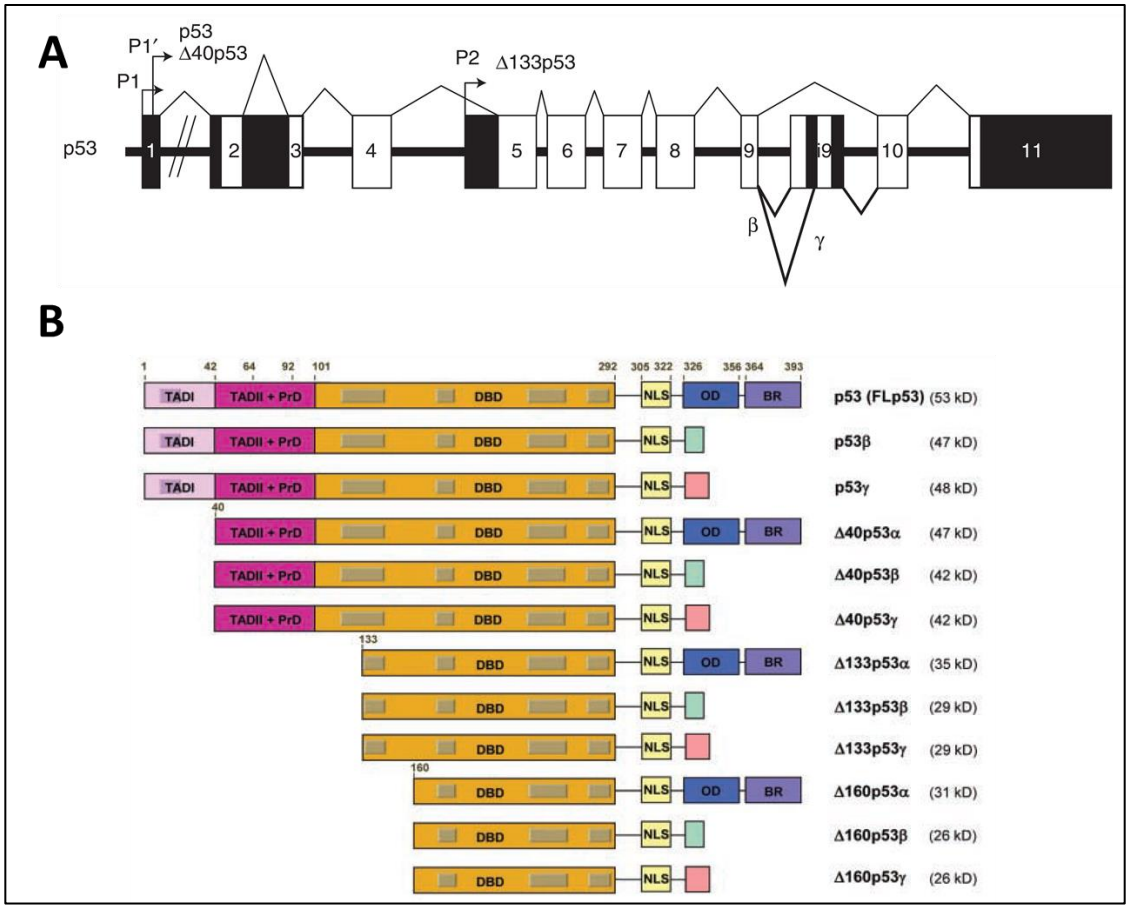

Appendix figure 2. 12 isoforms of P53. A. Schematic of *p53* gene of Homo sapiens. Promoters are indicated with forward arrows, exons are numbered. White box exons are coding and black box noncoding. **B**. **Schematic representation of 12 isoforms of p53**. TADI and TADII: transactivating domains; DBD: DNA binding domains; NLS: nuclear localization signal; OD: oligomerization domain; BR: basic region. Reprint with permission from [351 and 354].

Before the discovery of p53ψ, 12 distinct human p53 isoform were characterized (appendix figure 2) [351, 354, 355]. These Isoform are due to alternative splicing, promoter usage or AUG; thus, each p53 isoform have distinct topological layout. These isoforms are expressed in normal tissues but can be aberrantly expressed in in cancer [356]. Indeed, the response to genotoxic damage can be switched from senescence to apoptosis by modulating p53 isoform expression [357].

The following sections give a brief description of p53 isoforms.

2.1. Δ133p53α

In response to DNA damage or embryonic defect, usage of internal promoter in intron 4 leads to expression of Δ133p53α that prevented p53-mediated apoptosis [358]. Indeed, selective knockdown of Δ113p53α with morpholino injection in Zebrafish embryos increase sensitivity to ionizing radiation and promoted embryonic defect [358, 359]. Thereafter, re-expression of morpholino resistant Δ113p53α mRNA induced expression of MDM2, cyclin G, p21, and Bcl-xL leading to rescue of development of embryo [358, 360-364]. Therefore, in addition to behaving in a dominant negative manner, Δ113p53α differentially modulates p53 responsive genes profile at the physiological level and thereby demonstrating its intrinsic biological activity.

2.2. Δ133p53β and Δ133p53γ

p53 mRNAs produced from usage of internal promoter in intron 4 are also alternatively spliced in intron 9 to generate 2 other isoforms, Δ133p53β and Δ133p53γ [351, 365]. Expression of Δ133p53β or Δ133p53γ in cells with endogenous p53 does not

affect p53-mediated apoptosis [355, 365, 366]. While these two isoforms are expressed in normal tissue, analysis of tumor samples revealed abnormal expression of Δ133p53β and Δ133p53γ suggesting that they some play a role in tumorigenesis [365, 366].

2.3. Δ160p53α, Δ160p53β, and Δ160p53γ

These three isoforms lack first 159 amino acids because the use of alternative AUG from Δ133p53α, Δ133p53β, and Δ133p53γ mRNA [351, 356]. Interestingly, this alternative AUG 160 is conserved across all mammals while the 133 AUG is only found in primates [356, 367]. Of note, upon hemin-mediated erythroid differentiation of K562 cells, Δ160p53β was reduced, while Δ160p53α expression was constant, signifying the role of Δ160p53β in erythroid differentiation [351].

2.4. p53β

Intron 9 can be alternatively spliced to generate 2 different truncated isoforms: p53β and p53γ [351, 368, 369]. Both lack oligomerization domain due to inclusion of in-frame stop codon carried over from alternatively spliced intron 9 [353, 354, 356, 368, 369]. p53β can selectively bind to promoter of p53 transcriptional targets [351, 368, 369]; for example, it can bind Bax promoter while weakly binding to MDM2 promoter [368-370]. Laboratory of JC Bourdon has demonstrated that p53β has residual transcriptional activity by using artificial p53 response element driving luciferase expression [354]. Moreover, p53β expression promotes apoptosis independent of p53, although with a decreased efficiency than p53 possibly due to direct interaction of p53β with p53 [368-370]. Furthermore, p53-mediated cellular senescence is accelerated in the presence of

p53β in human normal fibroblasts by upregulating p21 and miR-34a [368-370]. Overall, this proposes that p53β helps regulate p53 transcriptional targets in a promoter-dependent manner in addition to having it owns residual transcriptional activity.

2.5 p53γ

p53γ isoform is byproduct of alternative splicing of intron 9 and expressed in normal tissue [351, 368, 370]. The subcellular localization of p53γ and p53β are different from each other. p53β is in the nucleus, while p53γ can be found in the nucleus or the cytoplasm [369]. p53γ induce p53-mediated transcriptional targets Bax but not on the p21 [369].

2.6. Δ40p53α, Δ40p53β, and Δ40p53γ

Δ40p53 isoforms lacks the first transactivation domain due to alternative splicing of intron 2 [351]. Recent evidence has established the existence of internal ribosome entry site (IRES) sequence that allows usage of alternative AUG initiation at position 40 rather than 1st AUG [351, 354, 355, 371]. p53 IRES sequences are modulated by various IRES transacting factors (ITAFs) including polypyrimidine tract binding protein (PTB), dyskerin, and hnRNP C1/C2 [372]. All regulate expression of p53 and Δ40p53 isoforms and thereby p53 tumor suppressor activity.

2.7. p53ψ

Recently, Dr. Raffaella Sordella's lab identified a thirteenth p53 isoform which has metastatic functions called p53ψ [373]. This isoform is produced due to usage of

alternative 3' splice within intron 6. This new transcript has a shift in open reading frame (ORF) that introduces stop codon in exon 7 to generate a C-terminal truncated p53ψ isoform (appendix figure 3). ψ is mainly expressed under conditions of chronic stress and

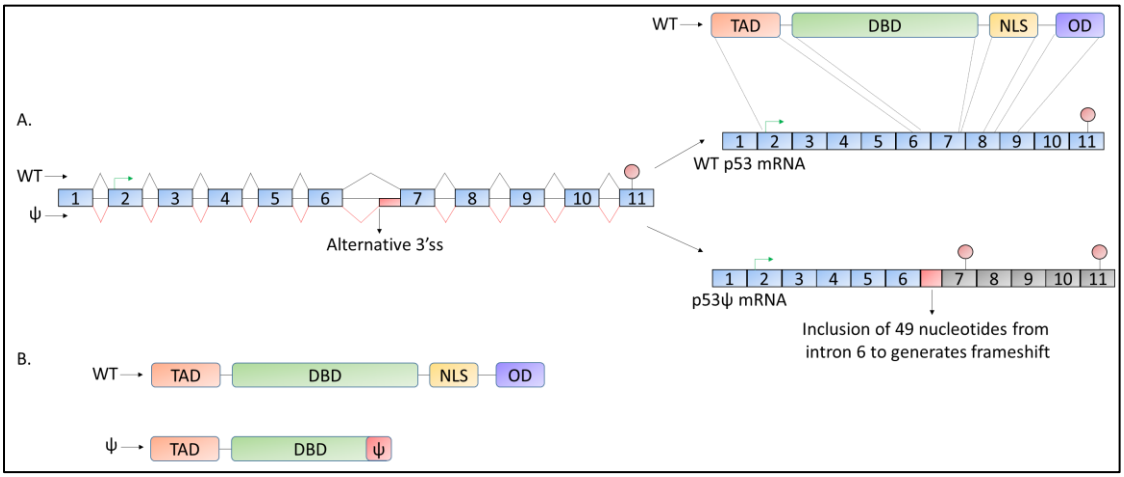

Appendix figure 3. P53ψ isoform. A. Usage of alternative 3' splice site to generate p53ψ mRNA variant**. B.** p53ψ domain topology relative to p53-WT. TAD: transactivation domain; DBD: DNA binding domain; NLS: nuclear localization signal; OD: oligomerization domain; ψ: specific amino acids.

in tumors with high metastatic potential. ψ lacks a portion of DNA binding domain, nuclear localization signal, and oligomerization domain. p53 transcriptional activity and tumor suppressor function is not present in ψ. On the other hand, ψ localized to the mitochondria and associates with cyclophilin D, regulator for mitochondrial permeability. Thus, ψ increase reactive oxygen species, induces EMT through regulation of EMT related genes (appendix figure 4).

In addition to splice site mutations, Cartegni et al. have suggested that silent and nonsense mutation can alter pre-mRNA splicing [302]. Hence, it is possible to generate ψ-like isoforms with 5'splice site (ss) mutation for intron 6 or mutation to codon juxtapose Exon 6 5'ss. For this reason, I performed a mutational screen for Ex6'ss and the juxtapose

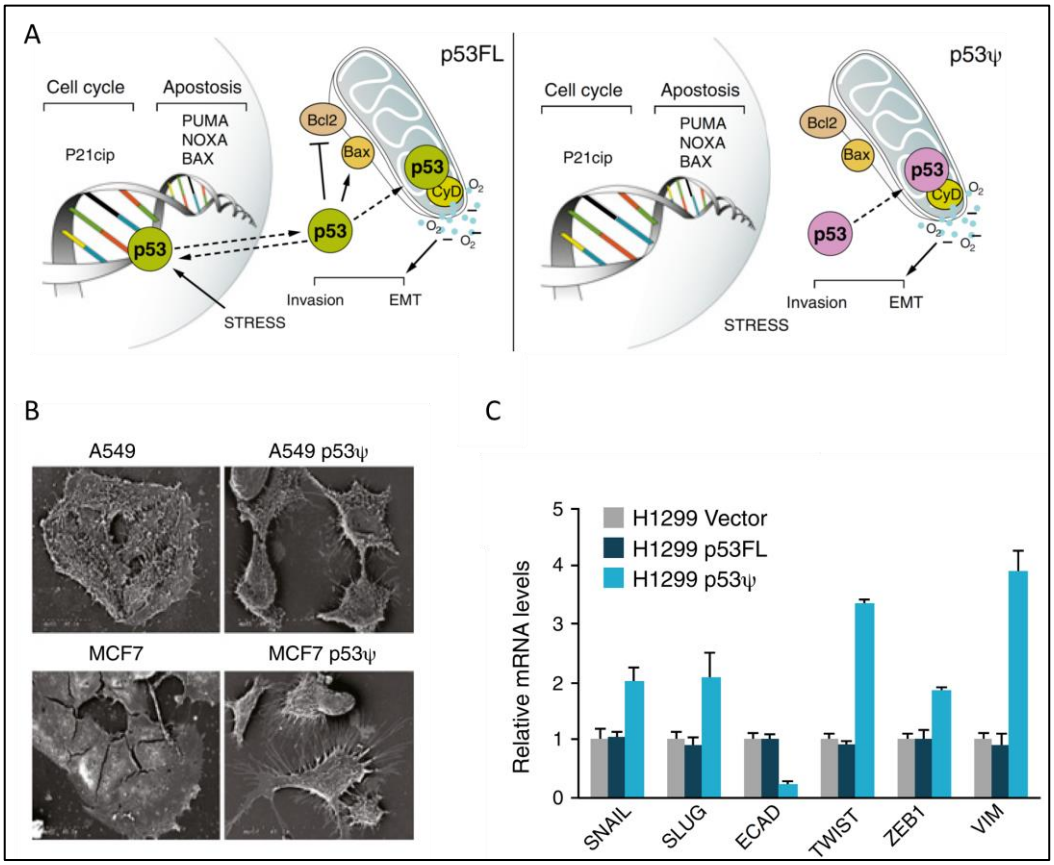

Appendix figure 4. Functional characteristics of P53ψ. A. p53ψ regulates mitochondrial permeability in cyclophilin D dependent manner to increase reactive oxygen species and induce EMT. **B.** Expression of p53ψ promotes EMT in A549 and MCF7 cells. **C.** p53ψ increase EMT related genes. Reprint with permission from [373].

codon 224 (GAG). We used an exon 5 to exon 8 minigene in vitro assay to monitor effect of mutation on pre-mRNA splicing. From our screen, we identified two novels alternatively spliced p53 isoforms due to usage of intronic 3' cryptic splice site. One isoform retains 18 intron 6 nucleotides and maintain ORF to generate 6 amino acid insertion in DNA binding domain. Other isoform, p53ψ-like protein (p53ψ-LP), retained 5 nucleotides from intron 6 which shifted the ORF to generate stop codon in exon 7; hence, p53ψ-LP can possible behave a metastatic promoter.

3. Material and Methods

3.1. Sources for Cell lines

A549 lung cancer cells (#CLL-185), H1792 lung cancer cells (#CRL-5895), HeLa cancer cells (#CCL-2), H716 colorectal cancer cells (#CCL-251), and PC3 lung cancer cells (#CRL-1435) were obtained from American Type Culture Collection (ATCC, Manassas, VA, USA).

3.2 Cell culture conditions

All cell culture reagents were purchased from Thermo Fisher Scientific (Waltham, MA, USA). A549, EBC-1, H1792, and PC3 cells were cultured in 2mM L-Glutamine containing RPMI-1640 (#11875093) supplemented with 10% heat inactivated fetal bovine serum (FBS), and 1% Penicillin/Streptomycin (P/S). HeLa, were cultured in 4.5 g/L D-Glucose, 2 mM L-Glutamine, and 110 mg/L Sodium Pyruvate containing DMEM (#11995065) supplemented with 10% FBS, and 1% P/S. Cells were maintained in humidified incubator with 5% CO_2 and 37^{o}C.

3.3 Sources for antibodies, growth factors, and inhibitor

Mouse anti-p53 DO-1 (#SC-126) was purchased from Santa Cruz Biotechnology (Dallas, Texas, USA). Rabbit anti-p21 (#2947) and rabbit anti-Vimentin (#5741) were purchased from Cell Signaling Technologies (Danvers, MA, USA). These three antibodies were used at 1:1,000 dilution in 5% BSA in TBS-tween (TBS-T). Mouse anti-alpha tubulin was (#T9026, Sigma Aldrich, St. Louis, MO, USA) used at 1:10,000 in 5% non-fat milk in TSB-T. Horseradish peroxidase (HRP) conjugated goat anti-rabbit secondary (#31460) and HRP conjugated goat anti-mouse secondary (#32430) were from Thermo Fisher Scientific and used at 1:10,000 dilution in TSB-T.

3.4 Western blotting

Cell lysates were collected with radioimmunoprecipitation assay (RIPA) buffer containing 1x protease inhibitors (#11697498001, Roche, Madison, WI, USA). Cell lysates were cleared of debris and membranous material by centrifugation at 13,000 x g for 5 minutes and supernatant transferred to a sterile tube. 10 uL of sample was used to measure protein concentration with BCA protein assay (#23224, Thermo Fisher Scientific). 20ug of cell lysates were resolved in 6% or 10% SDS-PAGE gel. Samples from SDS-PAGE gel were transferred to polyvinylidene difluoride (PVDF) membrane (#IPVH00010, Millipore, Burlington, MA, USA). Following transfer, PVDF membranes were blocked with 5% non-fat milk in TBS-tween for 1 hour at room temperature (RT) then incubated with primary antibodies at 4^{o}C overnight. The following day, PVDF membranes were incubated in HRP conjugated secondary antibody in 5% non-fat milk in TBS-tween at room

temperature for 1 hour. Proteins were detected with SuperSignal™ west femto maximum sensitivity substrate (#34095, Thermo Fisher Scientific) and visualized with GeneGnome XRQ Chemiluminescence imaging system (Syngene International Limited, Frederick, MD, USA).

3.5. Cloning of p53 minigene with mutations

Exon 5 to exon 8 p53 minigene was generated by PCR on genomic DNA from HeLa cells. PCR was done with Phusion® high-fidelity DNA polymerase (#M0530S, New England

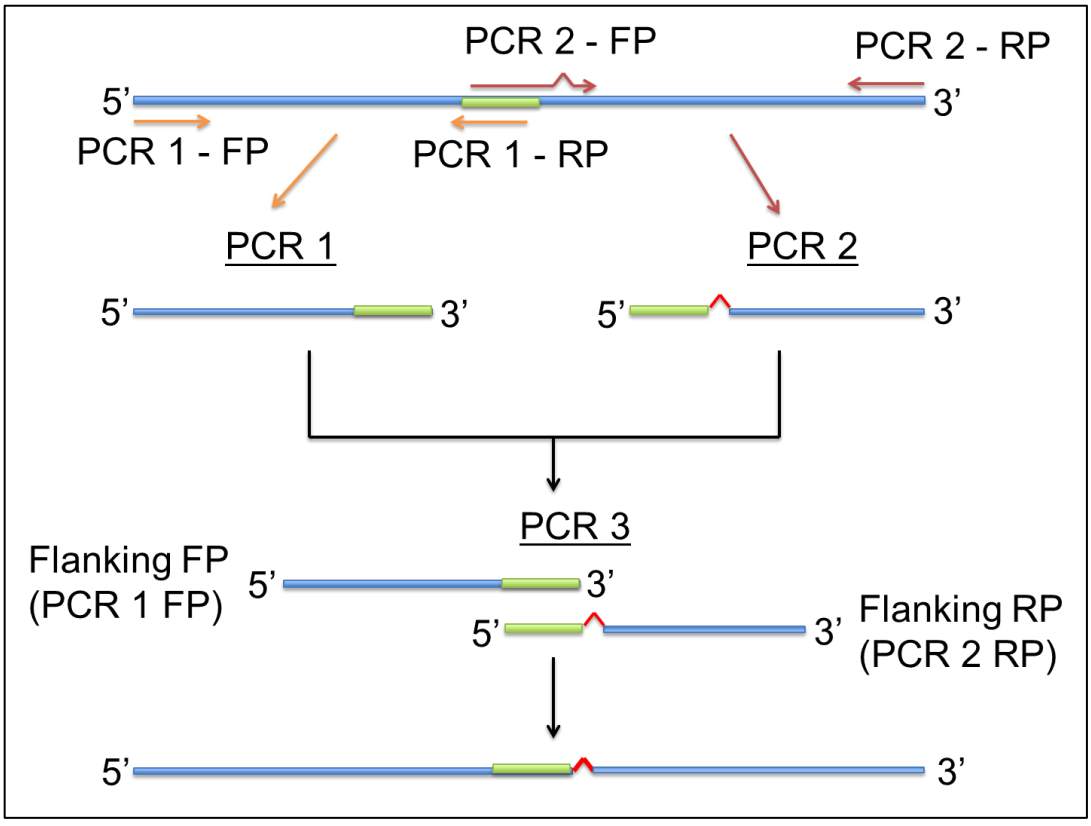

Appendix figure 5. 3 step PCR strategy to generate point mutation in p53 minigene. FP: forward primer and RP: reverse primer.

Biolabs) according to manufacturer's instructions with two specific primers: forward-p53 Exon 5 primer to reverse primer on exon 8. PCR was cloned in as EcoRV and NotI fragment into PcDNA3.1(+) (#V79020, Invitrogen, Carlsbad, CA). All plasmids were verified by sequence analysis with MacVector alignment software to confirm absence of mutations.

To generate point mutation in our minigene, we used a 3 step PCR strategy (appendix figure 5) with a forward primer in the first PCR carrying mutation of choice.

3.6 Minigene splicing assay

To detect pre-mRNA splicing of p53 minigene, we transfected $3.5x10^6$ HeLa cells with 2 ug mutant minigene constructs using lipofectamine® LTX according to manufacturer's protocol (#15338100, Thermo Fisher Scientific). After 24 hours of transfection, total RNA was extracted with TRIzol™ reagent according to manufacturer's protocol (#15596026, Thermo Fisher Scientific). Extracted RNA samples were treated with Turbo™ DNase (#AM1907, Thermo Fisher Scientific) to remove any residual DNA carry over. 1ug of extracted RNA was reverse transcribe with SuperScript™ first-strand synthesis kit. 2 uL of cDNA samples were used in a 2-primer PCR assay. To avoid detection of endogenous p53, reverse primer was placed on plasmid: 3' to minigene insert (appendix figure 6).

With these two primers, 2 uL of cDNA was used for PCR assay using GoTaq® Flexi DNA polymerase (#M8291, Promega, Madison, WI, USA) with the following conditions:

1. Initial denaturation at 95°C for 2 minutes
2. 35 cycles of denaturation for 30 seconds at 95°C, annealing for 30 seconds at 60°C, extension for 45 seconds at 72°C
3. Final extension for 5 minutes at 72°C

PCR reactions was resolved on 3% agarose gel, post-stained with ethidium bromide and imaged with Gel Doc™ EZ Gel Documentation System (Bio-Rad Laboratories, Hercules, CA, USA). Expected PCR products were gel purified with QIAquick gel extraction kit (#28115, Qiagen, Germantown, MD, USA) according to manufacturer's instructions, cloned into TA cloning vector (#K202020, Thermo Fisher Scientific) which was then used to transform DH5α competent bacterial cells (#18258012, Thermo Fisher Scientific). Plasmid was extracted from transformed colonies with QIAprep® spin miniprep kit (Qiagen) according to manufacturer's instructions and sequence analyzed with MacVector alignment software (MacVector, Inc, Apex, NC, USA).

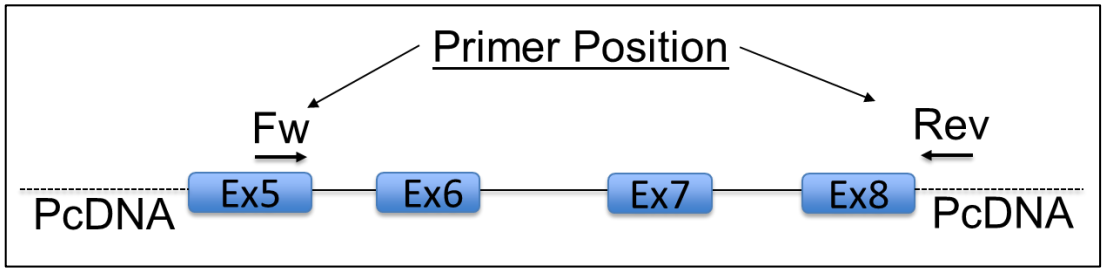

Appendix figure 6. Primer position to detect minigene spliced product and avoid endogenous p53.

4. results

4.1. Mutation in 5'ss of exon 6 alter splice to generate ψ like protein

To study the effect of pre-mRNA splicing with splice site mutation, we constructed Ex5 to Ex8 p53 minigene (appendix figure 6). As expected, after mutating 5'ss of exon 6, we observed altered splicing pattern. Post PCR assay, reaction was cloned into TA cloning

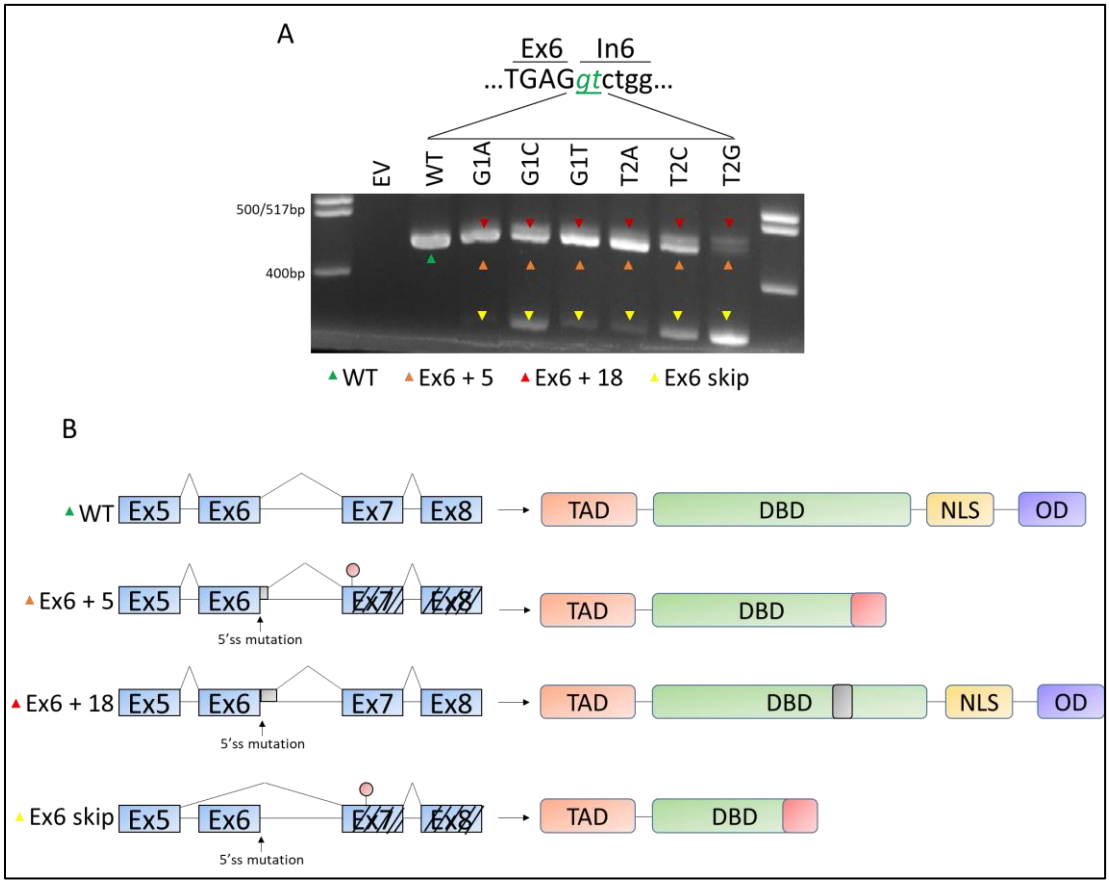

Appendix figure 7. Mutating 5'ss of exon 6 generates mRNA variant with possible metastatic potential. A. pre-mRNA splicing analysis after 24 hours transfection in HeLa cells. Primers to distinguish between endogenous or minigene mRNA are in appendix figure 6. **B.** Schematic of mRNA variant detected in PCRs in panel A and their possible translated protein isoforms.

vector to characterize types of mRNA species generated in context of Ex6 splice site mutation. Most 5'ss mutations induced usage of 2 alternative cryptic splice site within intron 6 except 5'ss T>G that most promoted exon skipping; the first cryptic 5'ss included 5 nucleotides to mature mRNA while other included 18 nucleotide. Interestingly, sequence analysis of 5 nucleotides inclusion in ORF induces a frameshift, generate a stop codon in exon 7 and possibly translate to isoform similar to p53ψ.

4.2. Mutation in codon juxtapose to 5'ss induces alternative splicing

Next, we wanted to examine mutation in coding sequences of exon 6 and their effect on splicing. The most obvious target to mutation is glutamate codon which is the last trinucleotide in exon 6; within mutation spectrum for glutamate codon for this trinucleotide, many were missense mutation in addition to one nonsense and another silent (appendix figure 8).

Nucleotide Position	Original	Mutant	Codon	Amino Acid	Characterization
111	G	A	_AG	Lysine	missense
		C		Glutamine	missense
		T		STOP	nonsense
112	A	C	G_G	Alanine	missense
		G		Glycine	missense
		T		Valine	missense
113	G	A	GA_	Glutamate	silent
		C		Aspartate	missense
		T		Aspartate	missense
GAG → Glutamate					

Appendix figure 8. Mutation spectrum for last codon for exon 6.

Our PCR analysis on RNA generated from p53 minigene shown splicing pattern similar to the one observed for 5'ss mutation (appendix figure 9). Surprisingly, both nonsense and silent mutation yielded RNA with +5 nucleotide inclusion. This is very informative since silent mutation are disregarded in genomic analysis.

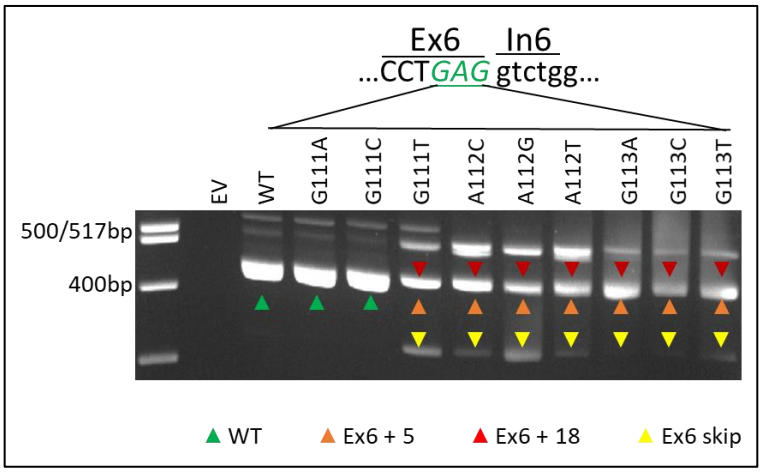

Appendix figure 9. PCR analysis of minigenes with mutation in last codon in exon 6.

4.3. Cells with splice site mutations alters splicing

Based on our results, next we wanted to ask if cancer cells with the same mutation generate splice variants which we observed in our artificial minigene assay. H716 colorectal cancer cells which harbors mutation in codon 224 and H1792 which harbors splice site mutation both showed aberrant splicing of p53 pre-mRNA. As expected, both cells expressed +5 and +18 nucleotide inclusion demonstrated that fact that spice site mutation or mutation juxtapose to splice site can generate mRNA which can express metastatic proteins (appendix figure 10).

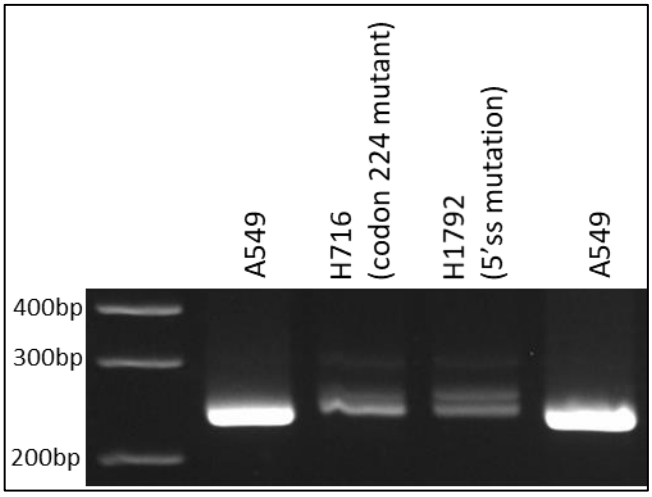

Appendix figure 10. PCR analysis of cancer cell with mutation in last codon of exon 6 or exon 6 splice site.

5. Conclusion and future perspectives

In conclusion, the work presented here sheds light on how mutation, missense, nonsense, or silent, can alter p53 splicing and generate alternative spliced variants that may be modulate EMT pathways and serves as a counteract to p53 FL. p53ψ promotes tissue remodeling, proliferation and survival of cancer stem cells. The proof establishing physiological role of p53ψ will surface from generation of knock-in and knock-out mouse models. It can be predicted that increase in p53ψ will promote tumorigenesis and display aggressive invasive phenotype by regulating potential cancer stem cells. Whatever their outcome, such in vivo studies will be of great value in peeling back yet another layer of complexity in p53 regulation.

Furthermore, with our results from our minigene assay, criteria to evaluate genomic data needs to be revisited. Silent mutation and possible intronic mutation can alter mRNA splicing and generate mutation that have metastatic potential. For this reason, these mutations should be considered before prescribing treatment regimen.

References

1. Cooper, C.S., et al., *Molecular cloning of a new transforming gene from a chemically transformed human cell line.* Nature, 1984. **311**(5981): p. 29-33.
2. Nakamura, T., K. Nawa, and A. Ichihara, *Partial purification and characterization of hepatocyte growth factor from serum of hepatectomized rats.* Biochem Biophys Res Commun, 1984. **122**(3): p. 1450-9.
3. Stoker, M., et al., *Scatter factor is a fibroblast-derived modulator of epithelial cell mobility.* Nature, 1987. **327**(6119): p. 239-42.
4. Di Renzo, M.F., et al., *Expression of the Met/HGF receptor in normal and neoplastic human tissues.* Oncogene, 1991. **6**(11): p. 1997-2003.
5. Trusolino, L., A. Bertotti, and P.M. Comoglio, *MET signalling: principles and functions in development, organ regeneration and cancer.* Nat Rev Mol Cell Biol, 2010. **11**(12): p. 834-48.
6. Organ, S.L. and M.-S. Tsao, *An overview of the c-MET signaling pathway.* Therapeutic advances in medical oncology, 2011. **3**(1 Suppl): p. S7-S19.
7. Park, M., et al., *Mechanism of met oncogene activation.* Cell, 1986. **45**(6): p. 895-904.
8. Borowiak, M., et al., *Met provides essential signals for liver regeneration.* Proceedings of the National Academy of Sciences of the United States of America, 2004. **101**(29): p. 10608-10613.
9. Kwak, Y., et al., *C-MET overexpression and amplification in gliomas.* International journal of clinical and experimental pathology, 2015. **8**(11): p. 14932-14938.
10. Bladt, F., et al., *Essential role for the c-met receptor in the migration of myogenic precursor cells into the limb bud.* Nature, 1995. **376**(6543): p. 768-71.
11. Birchmeier, C., et al., *Met, metastasis, motility and more.* Nat Rev Mol Cell Biol, 2003. **4**(12): p. 915-25.
12. Peters, S. and A.A. Adjei, *MET: a promising anticancer therapeutic target.* Nat Rev Clin Oncol, 2012. **9**(6): p. 314-26.
13. Trusolino, L., A. Bertotti, and P.M. Comoglio, *MET signalling: principles and functions in development, organ regeneration and cancer.* Nature Reviews Molecular Cell Biology, 2010. **11**: p. 834.
14. Kolatsi-Joannou, M., et al., *Expression of hepatocyte growth factor/scatter factor and its receptor, MET, suggests roles in human embryonic organogenesis.* Pediatr Res, 1997. **41**(5): p. 657-65.
15. Gherardi, E., et al., *Targeting MET in cancer: rationale and progress.* Nat Rev Cancer, 2012. **12**(2): p. 89-103.
16. Schmidt, L., et al., *Germline and somatic mutations in the tyrosine kinase domain of the MET proto-oncogene in papillary renal carcinomas.* Nat Genet, 1997. **16**(1): p. 68-73.
17. Rong, S., et al., *Tumorigenicity of the met proto-oncogene and the gene for hepatocyte growth factor.* Mol Cell Biol, 1992. **12**(11): p. 5152-8.
18. Lutterbach, B., et al., *Lung cancer cell lines harboring MET gene amplification are dependent on Met for growth and survival.* Cancer Res, 2007. **67**(5): p. 2081-8.
19. Piotrowska, Z., et al., *MET amplification (amp) as a resistance mechanism to osimertinib.* Journal of Clinical Oncology, 2017. **35**(15_suppl): p. 9020-9020.
20. Karamouzis, M.V., P.A. Konstantinopoulos, and A.G. Papavassiliou, *Targeting MET as a strategy to overcome crosstalk-related resistance to EGFR inhibitors.* Lancet Oncol, 2009. **10**(7): p. 709-17.

21. Xu, J., J. Wang, and S. Zhang, *Mechanisms of resistance to irreversible epidermal growth factor receptor tyrosine kinase inhibitors and therapeutic strategies in non-small cell lung cancer.* Oncotarget, 2017. **8**(52): p. 90557-90578.
22. Smolen, G.A., et al., *Amplification of MET may identify a subset of cancers with extreme sensitivity to the selective tyrosine kinase inhibitor PHA-665752.* Proc Natl Acad Sci U S A, 2006. **103**(7): p. 2316-21.
23. Engelman, J.A., et al., *MET amplification leads to gefitinib resistance in lung cancer by activating ERBB3 signaling.* Science, 2007. **316**(5827): p. 1039-43.
24. Gherardi, E., et al., *Functional map and domain structure of MET, the product of the c-met protooncogene and receptor for hepatocyte growth factor/scatter factor.* Proceedings of the National Academy of Sciences of the United States of America, 2003. **100**(21): p. 12039-12044.
25. Xiao, G.H., et al., *Anti-apoptotic signaling by hepatocyte growth factor/Met via the phosphatidylinositol 3-kinase/Akt and mitogen-activated protein kinase pathways.* Proc Natl Acad Sci U S A, 2001. **98**(1): p. 247-52.
26. Zhu, L., et al., *Acid sphingomyelinase is required for cell surface presentation of Met receptor tyrosine kinase in cancer cells.* J Cell Sci, 2016. **129**(22): p. 4238-4251.
27. Niemann, H.H., *Structural insights into Met receptor activation.* Eur J Cell Biol, 2011. **90**(11): p. 972-81.
28. Junqueira Alves, C., et al., *Origin and evolution of plexins, semaphorins, and Met receptor tyrosine kinases.* Scientific Reports, 2019. **9**(1): p. 1970.
29. Winberg, M.L., et al., *Plexin A is a neuronal semaphorin receptor that controls axon guidance.* Cell, 1998. **95**(7): p. 903-16.
30. Giordano, S., et al., *The semaphorin 4D receptor controls invasive growth by coupling with Met.* Nat Cell Biol, 2002. **4**(9): p. 720-4.
31. Basilico, C., et al., *A high affinity hepatocyte growth factor-binding site in the immunoglobulin-like region of Met.* J Biol Chem, 2008. **283**(30): p. 21267-77.
32. Stamos, J., et al., *Crystal structure of the HGF beta-chain in complex with the Sema domain of the Met receptor.* Embo j, 2004. **23**(12): p. 2325-35.
33. Abella, J.V., et al., *Met/Hepatocyte growth factor receptor ubiquitination suppresses transformation and is required for Hrs phosphorylation.* Mol Cell Biol, 2005. **25**(21): p. 9632-45.
34. Zhao, Y., et al., *Lipopolysaccharide-induced phosphorylation of c-Met tyrosine residue 1003 regulates c-Met intracellular trafficking and lung epithelial barrier function.* American journal of physiology. Lung cellular and molecular physiology, 2013. **305**(1): p. L56-L63.
35. Peschard, P., et al., *Mutation of the c-Cbl TKB domain binding site on the Met receptor tyrosine kinase converts it into a transforming protein.* Mol Cell, 2001. **8**(5): p. 995-1004.
36. Carter, S., S. Urbe, and M.J. Clague, *The met receptor degradation pathway: requirement for Lys48-linked polyubiquitin independent of proteasome activity.* J Biol Chem, 2004. **279**(51): p. 52835-9.
37. Hammond, D.E., et al., *Down-regulation of MET, the receptor for hepatocyte growth factor.* Oncogene, 2001. **20**(22): p. 2761-70.
38. Li, N., et al., *The Listeria protein internalin B mimics hepatocyte growth factor-induced receptor trafficking.* Traffic, 2005. **6**(6): p. 459-73.
39. Mohapatra, B., et al., *Protein tyrosine kinase regulation by ubiquitination: Critical roles of Cbl-family ubiquitin ligases.* Biochimica et Biophysica Acta (BBA) - Molecular Cell Research, 2013. **1833**(1): p. 122-139.

40. Oved, S. and Y. Yarden, *Signal transduction: molecular ticket to enter cells.* Nature, 2002. **416**(6877): p. 133-6.
41. Polo, S. and P.P. Di Fiore, *Endocytosis conducts the cell signaling orchestra.* Cell, 2006. **124**(5): p. 897-900.
42. Foveau, B., et al., *Down-regulation of the met receptor tyrosine kinase by presenilin-dependent regulated intramembrane proteolysis.* Mol Biol Cell, 2009. **20**(9): p. 2495-507.
43. Weber, S. and P. Saftig, *Ectodomain shedding and ADAMs in development.* Development, 2012. **139**(20): p. 3693.
44. Prat, M., et al., *C-terminal truncated forms of Met, the hepatocyte growth factor receptor.* Mol Cell Biol, 1991. **11**(12): p. 5954-62.
45. Ancot, F., et al., *Shedding-generated Met receptor fragments can be routed to either the proteasomal or the lysosomal degradation pathway.* Traffic, 2012. **13**(9): p. 1261-72.
46. Merilahti, J.A.M. and K. Elenius, *Gamma-secretase-dependent signaling of receptor tyrosine kinases.* Oncogene, 2019. **38**(2): p. 151-163.
47. Zhao, Y., et al., *Lysophosphatidic acid modulates c-Met redistribution and hepatocyte growth factor/c-Met signaling in human bronchial epithelial cells through PKC delta and E-cadherin.* Cell Signal, 2007. **19**(11): p. 2329-38.
48. Shida, D., et al., *Lysophosphatidic acid transactivates both c-Met and epidermal growth factor receptor, and induces cyclooxygenase-2 expression in human colon cancer LoVo cells.* World J Gastroenterol, 2005. **11**(36): p. 5638-43.
49. Galvani, A.P., et al., *Suramin modulates cellular levels of hepatocyte growth factor receptor by inducing shedding of a soluble form.* Biochem Pharmacol, 1995. **50**(7): p. 959-66.
50. Jücker, M., et al., *The Met/Hepatocyte growth factor receptor (HGFR) gene is overexpressed in some cases of human leukemia and lymphoma.* Leukemia Research, 1994. **18**(1): p. 7-16.
51. Petrelli, A., et al., *Ab-induced ectodomain shedding mediates hepatocyte growth factor receptor down-regulation and hampers biological activity.* Proceedings of the National Academy of Sciences of the United States of America, 2006. **103**(13): p. 5090.
52. Schelter, F., et al., *A disintegrin and metalloproteinase-10 (ADAM-10) mediates DN30 antibody-induced shedding of the met surface receptor.* J Biol Chem, 2010. **285**(34): p. 26335-40.
53. Coxon, A., et al., *Soluble c-Met receptors inhibit phosphorylation of c-Met and growth of hepatocyte growth factor: c-Met-dependent tumors in animal models.* Mol Cancer Ther, 2009. **8**(5): p. 1119-25.
54. Miyazawa, K., et al., *Molecular cloning and sequence analysis of cDNA for human hepatocyte growth factor.* Biochem Biophys Res Commun, 1989. **163**(2): p. 967-73.
55. Nakamura, T., et al., *Purification and subunit structure of hepatocyte growth factor from rat platelets.* FEBS Lett, 1987. **224**(2): p. 311-6.
56. Tatsumi, R. and R.E. Allen, *Active hepatocyte growth factor is present in skeletal muscle extracellular matrix.* Muscle Nerve, 2004. **30**(5): p. 654-8.
57. Naldini, L., et al., *Extracellular proteolytic cleavage by urokinase is required for activation of hepatocyte growth factor/scatter factor.* Embo j, 1992. **11**(13): p. 4825-33.
58. Jakubczak, J.L., W.J. LaRochelle, and G. Merlino, *NK1, a natural splice variant of hepatocyte growth factor/scatter factor, is a partial agonist in vivo.* Molecular and cellular biology, 1998. **18**(3): p. 1275-1283.

59. Frisch, R.N., et al., *Hepatocyte growth factor and alternative splice variants - expression, regulation and implications in osteogenesis and bone health and repair.* Expert Opin Ther Targets, 2016. **20**(9): p. 1087-98.
60. Vigna, E. and P.M. Comoglio, *Targeting the oncogenic Met receptor by antibodies and gene therapy.* Oncogene, 2015. **34**(15): p. 1883-9.
61. Zhang, S.Q., et al., *Receptor-specific regulation of phosphatidylinositol 3'-kinase activation by the protein tyrosine phosphatase Shp2.* Mol Cell Biol, 2002. **22**(12): p. 4062-72.
62. Wang, W., et al., *Essential roles of Gab1 tyrosine phosphorylation in growth factor-mediated signaling and angiogenesis.* International journal of cardiology, 2015. **181**: p. 180-184.
63. Aasrum, M., et al., *The involvement of the docking protein Gab1 in mitogenic signalling induced by EGF and HGF in rat hepatocytes.* Biochimica et Biophysica Acta (BBA) - Molecular Cell Research, 2013. **1833**(12): p. 3286-3294.
64. Belov, A.A. and M. Mohammadi, *Grb2, a double-edged sword of receptor tyrosine kinase signaling.* Science signaling, 2012. **5**(249): p. pe49-pe49.
65. Giubellino, A., T.R. Burke, Jr., and D.P. Bottaro, *Grb2 signaling in cell motility and cancer.* Expert opinion on therapeutic targets, 2008. **12**(8): p. 1021-1033.
66. Ponzetto, C., et al., *Specific uncoupling of GRB2 from the Met receptor. Differential effects on transformation and motility.* J Biol Chem, 1996. **271**(24): p. 14119-23.
67. Xie, Q., et al., *SF/HGF-c-Met autocrine and paracrine promote metastasis of hepatocellular carcinoma.* World journal of gastroenterology, 2001. **7**(6): p. 816-820.
68. Mildner, M., et al., *Hepatocyte Growth Factor Establishes Autocrine and Paracrine Feedback Loops for the Protection of Skin Cells after UV Irradiation.* Journal of Investigative Dermatology, 2007. **127**(11): p. 2637-2644.
69. Tjin, E.P.M., et al., *Functional analysis of HGF/MET signaling and aberrant HGF-activator expression in diffuse large B-cell lymphoma.* Blood, 2006. **107**(2): p. 760.
70. Grugan, K.D., et al., *Fibroblast-secreted hepatocyte growth factor plays a functional role in esophageal squamous cell carcinoma invasion.* Proceedings of the National Academy of Sciences of the United States of America, 2010. **107**(24): p. 11026-11031.
71. Plotnikov, A., et al., *The MAPK cascades: Signaling components, nuclear roles and mechanisms of nuclear translocation.* Biochimica et Biophysica Acta (BBA) - Molecular Cell Research, 2011. **1813**(9): p. 1619-1633.
72. Thatcher, J.D., *The Ras-MAPK Signal Transduction Pathway.* Science Signaling, 2010. **3**(119): p. tr1.
73. Stang, S., D. Bottorff, and J.C. Stone, *ras effector loop mutations that dissociate p120GAP and neurofibromin interactions.* Mol Carcinog, 1996. **15**(1): p. 64-9.
74. Nakhaeizadeh, H., et al., *The RAS-Effector Interface: Isoform-Specific Differences in the Effector Binding Regions.* PLOS ONE, 2016. **11**(12): p. e0167145.
75. Catling, A.D., et al., *A proline-rich sequence unique to MEK1 and MEK2 is required for raf binding and regulates MEK function.* Mol Cell Biol, 1995. **15**(10): p. 5214-25.
76. Xu, S., et al., *Differential regulation of mitogen-activated protein/ERK kinase (MEK)1 and MEK2 and activation by a Ras-independent mechanism.* Mol Endocrinol, 1997. **11**(11): p. 1618-25.
77. Shama, J., et al., *Major contribution of MEK1 to the activation of ERK1/ERK2 and to the growth of LS174T colon carcinoma cells.* Biochem Biophys Res Commun, 2008. **372**(4): p. 845-9.
78. Costa, M., et al., *Dynamic regulation of ERK2 nuclear translocation and mobility in living cells.* J Cell Sci, 2006. **119**(Pt 23): p. 4952-63.

79. Berti, D.A. and R. Seger, *The Nuclear Translocation of ERK.* Methods Mol Biol, 2017. **1487**: p. 175-194.
80. Rodrigues, G.A., M. Park, and J. Schlessinger, *Activation of the JNK pathway is essential for transformation by the Met oncogene.* The EMBO Journal, 1997. **16**(10): p. 2634.
81. Dai, R., et al., *The tyrosine kinase c-Met contributes to the pro-tumorigenic function of the p38 kinase in human bile duct cholangiocarcinoma cells.* The Journal of biological chemistry, 2012. **287**(47): p. 39812-39823.
82. Xiang, C., J. Chen, and P. Fu, *HGF/Met Signaling in Cancer Invasion: The Impact on Cytoskeleton Remodeling.* Cancers, 2017. **9**(5): p. 44.
83. Usatyuk, P.V., et al., *Role of c-Met/phosphatidylinositol 3-kinase (PI3k)/Akt signaling in hepatocyte growth factor (HGF)-mediated lamellipodia formation, reactive oxygen species (ROS) generation, and motility of lung endothelial cells.* The Journal of biological chemistry, 2014. **289**(19): p. 13476-13491.
84. Hervieu, A. and S. Kermorgant, *The Role of PI3K in Met Driven Cancer: A Recap.* Frontiers in molecular biosciences, 2018. **5**: p. 86-86.
85. Hemmings, B.A. and D.F. Restuccia, *PI3K-PKB/Akt pathway.* Cold Spring Harbor perspectives in biology. **4**(9): p. a011189-a011189.
86. Hammond, D.E., et al., *Endosomal dynamics of Met determine signaling output.* Molecular biology of the cell, 2003. **14**(4): p. 1346-1354.
87. Barrow-McGee, R. and S. Kermorgant, *Met endosomal signalling: in the right place, at the right time.* Int J Biochem Cell Biol, 2014. **49**: p. 69-74.
88. Kermorgant, S. and P.J. Parker, *Receptor trafficking controls weak signal delivery: a strategy used by c-Met for STAT3 nuclear accumulation.* The Journal of cell biology, 2008. **182**(5): p. 855-863.
89. Johnston, P.A. and J.R. Grandis, *STAT3 signaling: anticancer strategies and challenges.* Molecular interventions, 2011. **11**(1): p. 18-26.
90. Prochazka, L., R. Tesarik, and J. Turanek, *Regulation of alternative splicing of CD44 in cancer.* Cell Signal, 2014. **26**(10): p. 2234-9.
91. Orian-Rousseau, V., et al., *CD44 is required for two consecutive steps in HGF/c-Met signaling.* Genes & development, 2002. **16**(23): p. 3074-3086.
92. Bourrguignon, L.Y., et al., *Involvement of CD44 and its variant isoforms in membrane-cytoskeleton interaction, cell adhesion and tumor metastasis.* J Neurooncol, 1995. **26**(3): p. 201-8.
93. Wang, Y., et al., *Cytoskeletal regulation of CD44 membrane organization and interactions with E-selectin.* The Journal of biological chemistry, 2014. **289**(51): p. 35159-35171.
94. Ghatak, S., et al., *Overexpression of c-Met and CD44v6 receptors contributes to autocrine TGF-beta1 signaling in interstitial lung disease.* J Biol Chem, 2014. **289**(11): p. 7856-72.
95. Hasenauer, S., et al., *Internalization of Met requires the co-receptor CD44v6 and its link to ERM proteins.* PloS one, 2013. **8**(4): p. e62357-e62357.
96. Orian-Rousseau, V., et al., *Hepatocyte growth factor-induced Ras activation requires ERM proteins linked to both CD44v6 and F-actin.* Molecular biology of the cell, 2007. **18**(1): p. 76-83.
97. Singleton, P.A., et al., *CD44 regulates hepatocyte growth factor-mediated vascular integrity. Role of c-Met, Tiam1/Rac1, dynamin 2, and cortactin.* J Biol Chem, 2007. **282**(42): p. 30643-57.
98. Bertotti, A., P.M. Comoglio, and L. Trusolino, *Beta4 integrin activates a Shp2-Src signaling pathway that sustains HGF-induced anchorage-independent growth.* J Cell Biol, 2006. **175**(6): p. 993-1003.

99. Liu, Y., et al., *Coordinate integrin and c-Met signaling regulate Wnt gene expression during epithelial morphogenesis.* Development (Cambridge, England), 2009. **136**(5): p. 843-853.
100. Schaeper, U., et al., *Coupling of Gab1 to C-Met, Grb2, and Shp2 Mediates Biological Responses.* The Journal of Cell Biology, 2000. **149**(7): p. 1419.
101. Lai, A.Z., J.V. Abella, and M. Park, *Crosstalk in Met receptor oncogenesis.* Trends Cell Biol, 2009. **19**(10): p. 542-51.
102. Jo, M., et al., *Cross-talk between epidermal growth factor receptor and c-Met signal pathways in transformed cells.* J Biol Chem, 2000. **275**(12): p. 8806-11.
103. Mueller, K.L., et al., *EGFR/Met association regulates EGFR TKI resistance in breast cancer.* J Mol Signal, 2010. **5**: p. 8.
104. Ishibe, S., et al., *Met and the epidermal growth factor receptor act cooperatively to regulate final nephron number and maintain collecting duct morphology.* Development, 2009. **136**(2): p. 337-45.
105. Xu, K.P. and F.S. Yu, *Cross talk between c-Met and epidermal growth factor receptor during retinal pigment epithelial wound healing.* Invest Ophthalmol Vis Sci, 2007. **48**(5): p. 2242-8.
106. Puri, N. and R. Salgia, *Synergism of EGFR and c-Met pathways, cross-talk and inhibition, in non-small cell lung cancer.* J Carcinog, 2008. **7**: p. 9.
107. Chausovsky, A., et al., *Morphogenetic effects of neuregulin (neu differentiation factor) in cultured epithelial cells.* Molecular biology of the cell, 1998. **9**(11): p. 3195-3209.
108. Follenzi, A., et al., *Cross-talk between the proto-oncogenes Met and Ron.* Oncogene, 2000. **19**(27): p. 3041-9.
109. Chang, K., et al., *Roles of c-Met and RON kinases in tumor progression and their potential as therapeutic targets.* Oncotarget, 2015. **6**(6): p. 3507-3518.
110. Yeh, C.-Y., et al., *Transcriptional activation of the Axl and PDGFR-α by c-Met through a ras- and Src-independent mechanism in human bladder cancer.* BMC Cancer, 2011. **11**(1): p. 139.
111. Ueno, M., et al., *c-Met-dependent multipotent labyrinth trophoblast progenitors establish placental exchange interface.* Developmental cell, 2013. **27**(4): p. 373-386.
112. Huh, C.-G., et al., *Hepatocyte growth factor/c-met signaling pathway is required for efficient liver regeneration and repair.* Proceedings of the National Academy of Sciences of the United States of America, 2004. **101**(13): p. 4477.
113. Webster, M.T. and C.-M. Fan, *c-MET Regulates Myoblast Motility and Myocyte Fusion during Adult Skeletal Muscle Regeneration.* PLOS ONE, 2013. **8**(11): p. e81757.
114. Bandow, K., et al., *Hepatocyte growth factor/scatter factor stimulates migration of muscle precursors in developing mouse tongue.* J Cell Physiol, 2004. **201**(2): p. 236-43.
115. Adachi, N., et al., *Stepwise participation of HGF/MET signaling in the development of migratory muscle precursors during vertebrate evolution.* Zoological letters, 2018. **4**: p. 18-18.
116. González, M.N., et al., *HGF potentiates extracellular matrix-driven migration of human myoblasts: involvement of matrix metalloproteinases and MAPK/ERK pathway.* Skeletal Muscle, 2017. **7**(1): p. 20.
117. Myokai, F., et al., *Expression of the hepatocyte growth factor gene during chick limb development.* Dev Dyn, 1995. **202**(1): p. 80-90.
118. Heymann, S., et al., *Regulation and function of SF/HGF during migration of limb muscle precursor cells in chicken.* Dev Biol, 1996. **180**(2): p. 566-78.
119. Maina, F., et al., *Coupling Met to specific pathways results in distinct developmental outcomes.* Mol Cell, 2001. **7**(6): p. 1293-306.

120. Bard-Chapeau, E.A., et al., *Concerted functions of Gab1 and Shp2 in liver regeneration and hepatoprotection.* Mol Cell Biol, 2006. **26**(12): p. 4664-74.
121. Itoh, M., et al., *Role of Gab1 in heart, placenta, and skin development and growth factor- and cytokine-induced extracellular signal-regulated kinase mitogen-activated protein kinase activation.* Molecular and cellular biology, 2000. **20**(10): p. 3695-3704.
122. Debnath, J. and J.S. Brugge, *Modelling glandular epithelial cancers in three-dimensional cultures.* Nat Rev Cancer, 2005. **5**(9): p. 675-88.
123. Muller, M., A. Morotti, and C. Ponzetto, *Activation of NF-kappaB is essential for hepatocyte growth factor-mediated proliferation and tubulogenesis.* Mol Cell Biol, 2002. **22**(4): p. 1060-72.
124. Rosario, M. and W. Birchmeier, *How to make tubes: signaling by the Met receptor tyrosine kinase.* Trends Cell Biol, 2003. **13**(6): p. 328-35.
125. Leroy, P. and K.E. Mostov, *Slug is required for cell survival during partial epithelial-mesenchymal transition of HGF-induced tubulogenesis.* Molecular biology of the cell, 2007. **18**(5): p. 1943-1952.
126. O'Brien, L.E., et al., *ERK and MMPs sequentially regulate distinct stages of epithelial tubule development.* Dev Cell, 2004. **7**(1): p. 21-32.
127. Rosenthal, E.L., et al., *Role of the plasminogen activator and matrix metalloproteinase systems in epidermal growth factor- and scatter factor-stimulated invasion of carcinoma cells.* Cancer Res, 1998. **58**(22): p. 5221-30.
128. Monvoisin, A., et al., *Involvement of matrix metalloproteinase type-3 in hepatocyte growth factor-induced invasion of human hepatocellular carcinoma cells.* Int J Cancer, 2002. **97**(2): p. 157-62.
129. Huh, C.G., et al., *Hepatocyte growth factor/c-met signaling pathway is required for efficient liver regeneration and repair.* Proc Natl Acad Sci U S A, 2004. **101**(13): p. 4477-82.
130. Borowiak, M., et al., *Met provides essential signals for liver regeneration.* Proc Natl Acad Sci U S A, 2004. **101**(29): p. 10608-13.
131. Ueki, T., et al., *Hepatocyte growth factor gene therapy of liver cirrhosis in rats.* Nat Med, 1999. **5**(2): p. 226-30.
132. Kaido, T., et al., *Continuous HGF supply from HGF-expressing fibroblasts transplanted into spleen prevents CCl4-induced acute liver injury in rats.* Biochem Biophys Res Commun, 1996. **218**(1): p. 1-5.
133. Maroun, C.R., et al., *The tyrosine phosphatase SHP-2 is required for sustained activation of extracellular signal-regulated kinase and epithelial morphogenesis downstream from the met receptor tyrosine kinase.* Mol Cell Biol, 2000. **20**(22): p. 8513-25.
134. Liu, Y., *Hepatocyte growth factor in kidney fibrosis: therapeutic potential and mechanisms of action.* Am J Physiol Renal Physiol, 2004. **287**(1): p. F7-16.
135. Kim, W.H., et al., *Growth inhibition and apoptosis in liver myofibroblasts promoted by hepatocyte growth factor leads to resolution from liver cirrhosis.* Am J Pathol, 2005. **166**(4): p. 1017-28.
136. Dai, C. and Y. Liu, *Hepatocyte growth factor antagonizes the profibrotic action of TGF-beta1 in mesangial cells by stabilizing Smad transcriptional corepressor TGIF.* J Am Soc Nephrol, 2004. **15**(6): p. 1402-12.
137. Chmielowiec, J., et al., *c-Met is essential for wound healing in the skin.* J Cell Biol, 2007. **177**(1): p. 151-62.
138. Blanpain, C. and E. Fuchs, *Epidermal homeostasis: a balancing act of stem cells in the skin.* Nat Rev Mol Cell Biol, 2009. **10**(3): p. 207-17.

139. Kato, T., *Biological roles of hepatocyte growth factor-Met signaling from genetically modified animals.* Biomedical reports, 2017. **7**(6): p. 495-503.
140. Dunsmore, S.E., et al., *Mechanisms of hepatocyte growth factor stimulation of keratinocyte metalloproteinase production.* J Biol Chem, 1996. **271**(40): p. 24576-82.
141. Cataisson, C., et al., *MET signaling in keratinocytes activates EGFR and initiates squamous carcinogenesis.* Science Signaling, 2016. **9**(433): p. ra62.
142. Matsumoto, K., et al., *Hepatocyte growth factor/MET in cancer progression and biomarker discovery.* Cancer Sci, 2017. **108**(3): p. 296-307.
143. Awad, M.M., *Impaired c-Met Receptor Degradation Mediated by MET Exon 14 Mutations in Non-Small-Cell Lung Cancer.* J Clin Oncol, 2016. **34**(8): p. 879-81.
144. Lee, G.D., et al., *MET Exon 14 Skipping Mutations in Lung Adenocarcinoma: Clinicopathologic Implications and Prognostic Values.* Journal of Thoracic Oncology, 2017. **12**(8): p. 1233-1246.
145. Lu, X., et al., *MET Exon 14 Mutation Encodes an Actionable Therapeutic Target in Lung Adenocarcinoma.* Cancer Research, 2017. **77**(16): p. 4498.
146. Tovar, E.A. and C.R. Graveel, *MET in human cancer: germline and somatic mutations.* Annals of translational medicine, 2017. **5**(10): p. 205-205.
147. Minuti, G. and L. Landi, *MET deregulation in breast cancer.* Annals of translational medicine, 2015. **3**(13): p. 181-181.
148. Ho-Yen, C.M., J.L. Jones, and S. Kermorgant, *The clinical and functional significance of c-Met in breast cancer: a review.* Breast cancer research : BCR, 2015. **17**(1): p. 52-52.
149. de Melo Gagliato, D., et al., *Analysis of MET genetic aberrations in patients with breast cancer at MD Anderson Phase I unit.* Clinical breast cancer, 2014. **14**(6): p. 468-474.
150. Arnold, L., J. Enders, and S.M. Thomas, *Activated HGF-c-Met Axis in Head and Neck Cancer.* Cancers, 2017. **9**(12): p. 169.
151. Rothenberger, N.J. and L.P. Stabile, *Hepatocyte Growth Factor/c-Met Signaling in Head and Neck Cancer and Implications for Treatment.* Cancers (Basel), 2017. **9**(4).
152. Seiwert, T.Y., et al., *The MET receptor tyrosine kinase is a potential novel therapeutic target for head and neck squamous cell carcinoma.* Cancer research, 2009. **69**(7): p. 3021-3031.
153. Hartmann, S., N.E. Bhola, and J.R. Grandis, *HGF/Met Signaling in Head and Neck Cancer: Impact on the Tumor Microenvironment.* Clinical Cancer Research, 2016. **22**(16): p. 4005.
154. Vsiansky, V., et al., *Prognostic role of c-Met in head and neck squamous cell cancer tissues: a meta-analysis.* Scientific Reports, 2018. **8**(1): p. 10370.
155. Herbst, R.S., D. Morgensztern, and C. Boshoff, *The biology and management of non-small cell lung cancer.* Nature, 2018. **553**: p. 446.
156. Gelsomino, F., et al., *Targeting the MET gene for the treatment of non-small-cell lung cancer.* Crit Rev Oncol Hematol, 2014. **89**(2): p. 284-99.
157. Salgia, R., *MET in Lung Cancer: Biomarker Selection Based on Scientific Rationale.* Molecular Cancer Therapeutics, 2017. **16**(4): p. 555.
158. Fang, L., et al., *MET amplification assessed using optimized FISH reporting criteria predicts early distant metastasis in patients with non-small cell lung cancer.* Oncotarget, 2018. **9**(16): p. 12959-12970.
159. Dziadziuszko, R., et al., *Correlation between MET gene copy number by silver in situ hybridization and protein expression by immunohistochemistry in non-small cell lung cancer.* J Thorac Oncol, 2012. **7**(2): p. 340-7.
160. de Aguirre, I., et al., *c-Met Mutational Analysis in the Sema and Juxtamembrane Domains in Small-Cell-Lung-Cancer.* Translational oncogenomics, 2006. **1**: p. 11-18.

161. Okuda, K., et al., *Met gene copy number predicts the prognosis for completely resected non-small cell lung cancer.* Cancer Sci, 2008. **99**(11): p. 2280-5.
162. Jeon, H.-M. and J. Lee, *MET: roles in epithelial-mesenchymal transition and cancer stemness.* Annals of translational medicine, 2017. **5**(1): p. 5-5.
163. Kanaji, N., et al., *Hepatocyte growth factor produced in lung fibroblasts enhances non-small cell lung cancer cell survival and tumor progression.* Respir Res, 2017. **18**(1): p. 118.
164. Ma, P.C., et al., *Downstream signalling and specific inhibition of c-MET/HGF pathway in small cell lung cancer: implications for tumour invasion.* British Journal Of Cancer, 2007. **97**: p. 368.
165. Maulik, G., et al., *Modulation of the c-Met/Hepatocyte Growth Factor Pathway in Small Cell Lung Cancer.* Clinical Cancer Research, 2002. **8**(2): p. 620.
166. Ajani, J.A., et al., *Gastric adenocarcinoma.* Nat Rev Dis Primers, 2017. **3**: p. 17036.
167. Carcas, L., *Gastric cancer review.* Journal of Carcinogenesis, 2014. **13**(1): p. 14-14.
168. Wroblewski, L.E., R.M. Peek, Jr., and K.T. Wilson, *Helicobacter pylori and gastric cancer: factors that modulate disease risk.* Clinical microbiology reviews, 2010. **23**(4): p. 713-739.
169. Anestis, A., I. Zoi, and M.V. Karamouzis, *Current advances of targeting HGF/c-Met pathway in gastric cancer.* Ann Transl Med, 2018. **6**(12): p. 247.
170. Zhang, J., et al., *MET overexpression, gene amplification and relevant clinicopathological features in gastric adenocarcinoma.* Oncotarget, 2016. **8**(6): p. 10264-10273.
171. Lorenzato, A., et al., *Novel Somatic Mutations of the MET Oncogene in Human Carcinoma Metastases Activating Cell Motility and Invasion.* Cancer Research, 2002. **62**(23): p. 7025.
172. Xie, C., et al., *Expression of c-Met and hepatocyte growth factor in various gastric pathologies and its association with Helicobacter pylori infection.* Oncology letters, 2017. **14**(5): p. 6151-6155.
173. Lee, D., et al., *MET-Amplified Intramucosal Gastric Cancer Widely Metastatic after Complete Endoscopic Submucosal Dissection.* Cancer research and treatment : official journal of Korean Cancer Association, 2015. **47**(1): p. 120-125.
174. Riihimäki, M., et al., *Metastatic spread in patients with gastric cancer.* Oncotarget, 2016. **7**(32): p. 52307-52316.
175. Janjigian, Y.Y., et al., *MET expression and amplification in patients with localized gastric cancer.* Cancer epidemiology, biomarkers & prevention : a publication of the American Association for Cancer Research, cosponsored by the American Society of Preventive Oncology, 2011. **20**(5): p. 1021-1027.
176. Inoue, T., et al., *Activation of c-Met (hepatocyte growth factor receptor) in human gastric cancer tissue.* Cancer Sci, 2004. **95**(10): p. 803-8.
177. Lee, J.H., et al., *A novel germ line juxtamembrane Met mutation in human gastric cancer.* Oncogene, 2000. **19**(43): p. 4947-53.
178. Kleeff, J., et al., *Pancreatic cancer.* Nat Rev Dis Primers, 2016. **2**: p. 16022.
179. Modica, C., et al., *MET/HGF Co-Targeting in Pancreatic Cancer: A Tool to Provide Insight into the Tumor/Stroma Crosstalk.* International journal of molecular sciences, 2018. **19**(12): p. 3920.
180. Wei, L., et al., *Cancer-associated fibroblasts promote progression and gemcitabine resistance via the SDF-1/SATB-1 pathway in pancreatic cancer.* Cell Death & Disease, 2018. **9**(11): p. 1065.
181. Pan, B., et al., *Cancer-associated fibroblasts in pancreatic adenocarcinoma.* Future Oncol, 2015. **11**(18): p. 2603-10.

182. Qu, C., et al., *Cancer-Associated Fibroblasts in Pancreatic Cancer: Should They Be Deleted or Reeducated?* Integr Cancer Ther, 2018. **17**(4): p. 1016-1019.
183. Ferdek, P.E. and M.A. Jakubowska, *Biology of pancreatic stellate cells-more than just pancreatic cancer.* Pflugers Archiv : European journal of physiology, 2017. **469**(9): p. 1039-1050.
184. Xu, Z., et al., *Role of pancreatic stellate cells in pancreatic cancer metastasis.* The American journal of pathology, 2010. **177**(5): p. 2585-2596.
185. Apte, M.V., et al., *A starring role for stellate cells in the pancreatic cancer microenvironment.* Gastroenterology, 2013. **144**(6): p. 1210-1219.
186. Puls, T.J., et al., *3D collagen fibrillar microstructure guides pancreatic cancer cell phenotype and serves as a critical design parameter for phenotypic models of EMT.* PLOS ONE, 2017. **12**(11): p. e0188870.
187. Thomas, D. and P. Radhakrishnan, *Tumor-stromal crosstalk in pancreatic cancer and tissue fibrosis.* Molecular Cancer, 2019. **18**(1): p. 14.
188. Longo, V., et al., *Angiogenesis in pancreatic ductal adenocarcinoma: A controversial issue.* Oncotarget, 2016. **7**(36): p. 58649-58658.
189. Whipple, C. and M. Korc, *Targeting angiogenesis in pancreatic cancer: rationale and pitfalls.* Langenbecks Arch Surg, 2008. **393**(6): p. 901-10.
190. Garcea, G., et al., *Hypoxia and angiogenesis in pancreatic cancer.* ANZ J Surg, 2006. **76**(9): p. 830-42.
191. Duffy, J.P., et al., *Influence of hypoxia and neoangiogenesis on the growth of pancreatic cancer.* Mol Cancer, 2003. **2**: p. 12.
192. Di Renzo, M.F., et al., *Expression of the Met/hepatocyte growth factor receptor in human pancreatic cancer.* Cancer Res, 1995. **55**(5): p. 1129-38.
193. Delitto, D., et al., *c-Met signaling in the development of tumorigenesis and chemoresistance: potential applications in pancreatic cancer.* World journal of gastroenterology, 2014. **20**(26): p. 8458-8470.
194. Hill, K.S., et al., *Met receptor tyrosine kinase signaling induces secretion of the angiogenic chemokine interleukin-8/CXCL8 in pancreatic cancer.* PloS one, 2012. **7**(7): p. e40420-e40420.
195. Pothula, S.P., et al., *Targeting the HGF/c-MET pathway: stromal remodelling in pancreatic cancer.* Oncotarget, 2017. **8**(44): p. 76722-76739.
196. Ebert, M., et al., *Coexpression of the c-met proto-oncogene and hepatocyte growth factor in human pancreatic cancer.* Cancer Res, 1994. **54**(22): p. 5775-8.
197. Yu, J., et al., *Overexpression of c-met in the early stage of pancreatic carcinogenesis; altered expression is not sufficient for progression from chronic pancreatitis to pancreatic cancer.* World journal of gastroenterology, 2006. **12**(24): p. 3878-3882.
198. Luna, J., et al., *DYRK1A modulates c-MET in pancreatic ductal adenocarcinoma to drive tumour growth.* Gut, 2018.
199. Saito, K., et al., *Stromal mesenchymal stem cells facilitate pancreatic cancer progression by regulating specific secretory molecules through mutual cellular interaction.* Journal of Cancer, 2018. **9**(16): p. 2916-2929.
200. Herreros-Villanueva, M., A. Zubia-Olascoaga, and L. Bujanda, *c-Met in pancreatic cancer stem cells: therapeutic implications.* World journal of gastroenterology, 2012. **18**(38): p. 5321-5323.
201. Yan, B., et al., *Paracrine HGF/c-MET enhances the stem cell-like potential and glycolysis of pancreatic cancer cells via activation of YAP/HIF-1alpha.* Exp Cell Res, 2018. **371**(1): p. 63-71.

202. Zhou, P., et al., *The epithelial to mesenchymal transition (EMT) and cancer stem cells: implication for treatment resistance in pancreatic cancer.* Molecular cancer, 2017. **16**(1): p. 52-52.
203. Nishida, N., et al., *Angiogenesis in cancer.* Vascular health and risk management, 2006. **2**(3): p. 213-219.
204. Carmeliet, P., *VEGF as a key mediator of angiogenesis in cancer.* Oncology, 2005. **69 Suppl 3**: p. 4-10.
205. Huang, J., et al., *Regression of established tumors and metastases by potent vascular endothelial growth factor blockade.* Proc Natl Acad Sci U S A, 2003. **100**(13): p. 7785-90.
206. Gotink, K.J. and H.M.W. Verheul, *Anti-angiogenic tyrosine kinase inhibitors: what is their mechanism of action?* Angiogenesis, 2010. **13**(1): p. 1-14.
207. Cohen, M.H., et al., *FDA drug approval summary: bevacizumab (Avastin) plus Carboplatin and Paclitaxel as first-line treatment of advanced/metastatic recurrent nonsquamous non-small cell lung cancer.* Oncologist, 2007. **12**(6): p. 713-8.
208. Al-Husein, B., et al., *Antiangiogenic therapy for cancer: an update.* Pharmacotherapy, 2012. **32**(12): p. 1095-1111.
209. Loges, S., T. Schmidt, and P. Carmeliet, *Mechanisms of resistance to anti-angiogenic therapy and development of third-generation anti-angiogenic drug candidates.* Genes & cancer, 2010. **1**(1): p. 12-25.
210. Piguet, A.-C., et al., *Impact of MET targeting on tumor-associated angiogenesis and growth of MET mutations-driven models of liver cancer.* Genes & cancer, 2015. **6**(7-8): p. 317-327.
211. Bussolino, F., et al., *Hepatocyte growth factor is a potent angiogenic factor which stimulates endothelial cell motility and growth.* J Cell Biol, 1992. **119**(3): p. 629-41.
212. Ding, S., et al., *HGF receptor up-regulation contributes to the angiogenic phenotype of human endothelial cells and promotes angiogenesis in vitro.* Blood, 2003. **101**(12): p. 4816-22.
213. Matsumura, A., et al., *HGF regulates VEGF expression via the c-Met receptor downstream pathways, PI3K/Akt, MAPK and STAT3, in CT26 murine cells.* Int J Oncol, 2013. **42**(2): p. 535-42.
214. Chen, X., et al., *Synergistic antitumor effects of cMet inhibitor in combination with anti-VEGF in colorectal cancer patient-derived xenograft models.* Journal of Cancer, 2018. **9**(7): p. 1207-1217.
215. Nakagawa, T., et al., *E7050: A dual c-Met and VEGFR-2 tyrosine kinase inhibitor promotes tumor regression and prolongs survival in mouse xenograft models.* Cancer Science, 2010. **101**(1): p. 210-215.
216. Ren, Y., et al., *Abstract B189: Synergistic effect of c-Met inhibitor savolitinib in combination with a VEGFR inhibitor fruquintinib in clear cell renal cell carcinoma xenograft models.* Molecular Cancer Therapeutics, 2015. **14**(12 Supplement 2): p. B189.
217. Hara, S., et al., *Hypoxia enhances c-Met/HGF receptor expression and signaling by activating HIF-1alpha in human salivary gland cancer cells.* Oral Oncol, 2006. **42**(6): p. 593-8.
218. Eckerich, C., et al., *Hypoxia can induce c-Met expression in glioma cells and enhance SF/HGF-induced cell migration.* Int J Cancer, 2007. **121**(2): p. 276-83.
219. Tacchini, L., et al., *Hepatocyte growth factor signalling stimulates hypoxia inducible factor-1 (HIF-1) activity in HepG2 hepatoma cells.* Carcinogenesis, 2001. **22**(9): p. 1363-71.

220. Scarpino, S., et al., *Increased expression of Met protein is associated with up-regulation of hypoxia inducible factor-1 (HIF-1) in tumour cells in papillary carcinoma of the thyroid.* J Pathol, 2004. **202**(3): p. 352-8.
221. Geiger, T.R. and D.S. Peeper, *Metastasis mechanisms.* Biochim Biophys Acta, 2009. **1796**(2): p. 293-308.
222. Kucerova, L., et al., *Tyrosine kinase inhibitor SU11274 increased tumorigenicity and enriched for melanoma-initiating cells by bioenergetic modulation.* BMC cancer, 2016. **16**: p. 308-308.
223. Basilico, C., et al., *Targeting the MET oncogene by concomitant inhibition of receptor and ligand via an antibody-"decoy" strategy.* Int J Cancer, 2018.
224. Liu, X. and D. Fan, *The epithelial-mesenchymal transition and cancer stem cells: functional and mechanistic links.* Curr Pharm Des, 2015. **21**(10): p. 1279-91.
225. Yashiro, M., et al., *A c-Met inhibitor increases the chemosensitivity of cancer stem cells to the irinotecan in gastric carcinoma.* Br J Cancer, 2013. **109**(10): p. 2619-28.
226. Neuss, S., et al., *Functional expression of HGF and HGF receptor/c-met in adult human mesenchymal stem cells suggests a role in cell mobilization, tissue repair, and wound healing.* Stem Cells, 2004. **22**(3): p. 405-14.
227. Mizuno, K., et al., *Hepatocyte growth factor stimulates growth of hematopoietic progenitor cells.* Biochem Biophys Res Commun, 1993. **194**(1): p. 178-86.
228. Urbanek, K., et al., *Cardiac stem cells possess growth factor-receptor systems that after activation regenerate the infarcted myocardium, improving ventricular function and long-term survival.* Circ Res, 2005. **97**(7): p. 663-73.
229. Yamada, M., et al., *High concentrations of HGF inhibit skeletal muscle satellite cell proliferation in vitro by inducing expression of myostatin: a possible mechanism for reestablishing satellite cell quiescence in vivo.* Am J Physiol Cell Physiol, 2010. **298**(3): p. C465-76.
230. Ishikawa, T., et al., *Hepatocyte growth factor/c-met signaling is required for stem-cell-mediated liver regeneration in mice.* Hepatology, 2012. **55**(4): p. 1215-26.
231. Safaie Qamsari, E., et al., *The c-Met receptor: Implication for targeted therapies in colorectal cancer.* Tumour Biol, 2017. **39**(5): p. 1010428317699118.
232. Sun, S., et al., *Targeting the c-Met/FZD8 Signaling Axis Eliminates Patient-Derived Cancer Stem–like Cells in Head and Neck Squamous Carcinomas.* Cancer Research, 2014. **74**(24): p. 7546.
233. de Sousa, E.M.F., et al., *Targeting Wnt Signaling in Colon Cancer Stem Cells.* Clinical Cancer Research, 2011. **17**(4): p. 647.
234. Vermeulen, L., et al., *Wnt activity defines colon cancer stem cells and is regulated by the microenvironment.* Nat Cell Biol, 2010. **12**(5): p. 468-76.
235. Kim, K.H., et al., *Wnt/β-catenin signaling is a key downstream mediator of MET signaling in glioblastoma stem cells.* Neuro-oncology, 2013. **15**(2): p. 161-171.
236. Holland, Jane D., et al., *Combined Wnt/β-Catenin, Met, and CXCL12/CXCR4 Signals Characterize Basal Breast Cancer and Predict Disease Outcome.* Cell Reports, 2013. **5**(5): p. 1214-1227.
237. Mahtouk, K., et al., *The HGF/MET pathway as target for the treatment of multiple myeloma and B cell lymphomas*. Vol. 1806. 2010. 208-19.
238. Tesio, M., et al., *Enhanced c-Met activity promotes G-CSF-induced mobilization of hematopoietic progenitor cells via ROS signaling.* Blood, 2011. **117**(2): p. 419-28.
239. Liu, S., *HGF-MET as a breast cancer biomarker.* Aging, 2015. **7**(3): p. 150-151.

240. Ono, K., et al., *Involvement of hepatocyte growth factor in the development of bone metastasis of a mouse mammary cancer cell line, BALB/c-MC.* Bone, 2006. **39**(1): p. 27-34.
241. Kuang, W., et al., *Hepatocyte growth factor induces breast cancer cell invasion via the PI3K/Akt and p38 MAPK signaling pathways to up-regulate the expression of COX2.* American journal of translational research, 2017. **9**(8): p. 3816-3826.
242. Masuya, D., et al., *The tumour-stromal interaction between intratumoral c-Met and stromal hepatocyte growth factor associated with tumour growth and prognosis in non-small-cell lung cancer patients.* British journal of cancer, 2004. **90**(8): p. 1555-1562.
243. Kanaji, N., et al., *Hepatocyte growth factor produced in lung fibroblasts enhances non-small cell lung cancer cell survival and tumor progression.* Respiratory Research, 2017. **18**(1): p. 118.
244. Raghav, K.P.S., A.M. Gonzalez-Angulo, and G.R. Blumenschein Jr, *Role of HGF/MET axis in resistance of lung cancer to contemporary management.* Translational Lung Cancer Research, 2012. **1**(3): p. 179-193.
245. Nakajima, M., et al., *The prognostic significance of amplification and overexpression of c-met and c-erb B-2 in human gastric carcinomas.* Cancer, 1999. **85**(9): p. 1894-902.
246. Ortiz-Zapater, E., et al., *MET-EGFR dimerization in lung adenocarcinoma is dependent on EGFR mtations and altered by MET kinase inhibition.* PloS one, 2017. **12**(1): p. e0170798-e0170798.
247. Dulak, A.M., et al., *HGF-independent potentiation of EGFR action by c-Met.* Oncogene, 2011. **30**(33): p. 3625-3635.
248. Furcht, C.M., J.M. Buonato, and M.J. Lazzara, *EGFR-activated Src family kinases maintain GAB1-SHP2 complexes distal from EGFR.* Sci Signal, 2015. **8**(376): p. ra46.
249. Yamamoto, N., et al., *Tyrosine phosphorylation of p145^{met} mediated by EGFR and Src is required for serum-independent survival of human bladder carcinoma cells.* Journal of Cell Science, 2006. **119**(22): p. 4623.
250. Mueller, K.L., et al., *Met and c-Src cooperate to compensate for loss of epidermal growth factor receptor kinase activity in breast cancer cells.* Cancer research, 2008. **68**(9): p. 3314-3322.
251. Reznik, T.E., et al., *Transcription-dependent epidermal growth factor receptor activation by hepatocyte growth factor.* Mol Cancer Res, 2008. **6**(1): p. 139-50.
252. Nath, D., et al., *Shedding of c-Met is regulated by crosstalk between a G-protein coupled receptor and the EGF receptor and is mediated by a TIMP-3 sensitive metalloproteinase.* J Cell Sci, 2001. **114**(Pt 6): p. 1213-20.
253. Merlin, S., et al., *Deletion of the ectodomain unleashes the transforming, invasive, and tumorigenic potential of the MET oncogene.* Cancer Sci, 2009. **100**(4): p. 633-8.
254. Yano, S., et al., *Hepatocyte Growth Factor Induces Gefitinib Resistance of Lung Adenocarcinoma with Epidermal Growth Factor Receptor–Activating Mutations.* Cancer Research, 2008. **68**(22): p. 9479.
255. Ju, L. and C. Zhou, *Association of integrin beta1 and c-MET in mediating EGFR TKI gefitinib resistance in non-small cell lung cancer.* Cancer cell international, 2013. **13**(1): p. 15-15.
256. Huang, P.H., et al., *Quantitative analysis of EGFRvIII cellular signaling networks reveals a combinatorial therapeutic strategy for glioblastoma.* Proc Natl Acad Sci U S A, 2007. **104**(31): p. 12867-72.
257. Greenall, S.A., et al., *EGFRvIII-mediated transactivation of receptor tyrosine kinases in glioma: mechanism and therapeutic implications.* Oncogene, 2015. **34**(41): p. 5277-87.

258. An, Z., et al., *Epidermal growth factor receptor and EGFRvIII in glioblastoma: signaling pathways and targeted therapies.* Oncogene, 2018. **37**(12): p. 1561-1575.
259. Saunders, V.C., et al., *Identification of an EGFRvIII-JNK2-HGF/c-Met-Signaling Axis Required for Intercellular Crosstalk and Glioblastoma Multiforme Cell Invasion.* Mol Pharmacol, 2015. **88**(6): p. 962-9.
260. Santini, F.C., S. Kunte, and A. Drilon, *Combination MET- and EGFR-directed therapy in MET-overexpressing non-small cell lung cancers: time to move on to better biomarkers?* Translational lung cancer research, 2017. **6**(3): p. 393-395.
261. Solomon, B., *Trials and Tribulations of EGFR and MET Inhibitor Combination Therapy in NSCLC.* Journal of Thoracic Oncology, 2017. **12**(1): p. 9-11.
262. Hsu, J.L. and M.-C. Hung, *The role of HER2, EGFR, and other receptor tyrosine kinases in breast cancer.* Cancer metastasis reviews, 2016. **35**(4): p. 575-588.
263. Paulson, A.K., et al., *MET and ERBB2 are coexpressed in ERBB2+ breast cancer and contribute to innate resistance.* Mol Cancer Res, 2013. **11**(9): p. 1112-21.
264. Shattuck, D.L., et al., *Met receptor contributes to trastuzumab resistance of Her2-overexpressing breast cancer cells.* Cancer Res, 2008. **68**(5): p. 1471-7.
265. Fuse, N., et al., *Prognostic impact of HER2, EGFR, and c-MET status on overall survival of advanced gastric cancer patients.* Gastric Cancer, 2016. **19**(1): p. 183-91.
266. Ha, S.Y., et al., *HER2-positive gastric cancer with concomitant MET and/or EGFR overexpression: a distinct subset of patients for dual inhibition therapy.* Int J Cancer, 2015. **136**(7): p. 1629-35.
267. Khoury, H., et al., *HGF converts ErbB2/Neu epithelial morphogenesis to cell invasion.* Molecular biology of the cell, 2005. **16**(2): p. 550-561.
268. Shattuck, D.L., et al., *Met Receptor Contributes to Trastuzumab Resistance of Her2-Overexpressing Breast Cancer Cells.* Cancer Research, 2008. **68**(5): p. 1471.
269. Ko, B., et al., *MET/HGF pathway activation as a paradigm of resistance to targeted therapies.* Annals of translational medicine, 2017. **5**(1): p. 4-4.
270. Gkolfinopoulos, S. and G. Mountzios, *Beyond EGFR and ALK: targeting rare mutations in advanced non-small cell lung cancer.* Annals of translational medicine, 2018. **6**(8): p. 142-142.
271. Yamaoka, T., M. Ohba, and T. Ohmori, *Molecular-Targeted Therapies for Epidermal Growth Factor Receptor and Its Resistance Mechanisms.* International journal of molecular sciences, 2017. **18**(11): p. 2420.
272. Mishra, R., A.B. Hanker, and J.T. Garrett, *Genomic alterations of ERBB receptors in cancer: clinical implications.* Oncotarget, 2017. **8**(69): p. 114371-114392.
273. Breindel, J.L., et al., *EGF Receptor Activates MET through MAPK to Enhance Non–Small Cell Lung Carcinoma Invasion and Brain Metastasis.* Cancer Research, 2013. **73**(16): p. 5053.
274. Nakagawa, T., et al., *Combined therapy with mutant-selective EGFR inhibitor and Met kinase inhibitor for overcoming erlotinib resistance in EGFR-mutant lung cancer.* Mol Cancer Ther, 2012. **11**(10): p. 2149-57.
275. Bean, J., et al., *MET amplification occurs with or without T790M mutations in EGFR mutant lung tumors with acquired resistance to gefitinib or erlotinib.* Proc Natl Acad Sci U S A, 2007. **104**(52): p. 20932-7.
276. Mueller, K.L., et al., *Met and c-Src cooperate to compensate for loss of epidermal growth factor receptor kinase activity in breast cancer cells.* Cancer Res, 2008. **68**(9): p. 3314-22.
277. Acunzo, M., et al., *Cross-talk between MET and EGFR in non-small cell lung cancer involves miR-27a and Sprouty2.* Proc Natl Acad Sci U S A, 2013. **110**(21): p. 8573-8.

278. Namiki, Y., et al., *Preclinical study of a "tailor-made" combination of NK4-expressing gene therapy and gefitinib (ZD1839, Iressa) for disseminated peritoneal scirrhous gastric cancer.* Int J Cancer, 2006. **118**(6): p. 1545-55.
279. Mo, H.-N. and P. Liu, *Targeting MET in cancer therapy.* Chronic diseases and translational medicine, 2017. **3**(3): p. 148-153.
280. Cao, B., et al., *Neutralizing monoclonal antibodies to hepatocyte growth factor/scatter factor (HGF/SF) display antitumor activity in animal models.* Proc Natl Acad Sci U S A, 2001. **98**(13): p. 7443-8.
281. Song, S.W., et al., *Inhibition of tumor growth in a mouse xenograft model by the humanized anti-HGF monoclonal antibody YYB-101 produced in a large-scale CHO cell culture.* J Microbiol Biotechnol, 2013. **23**(9): p. 1327-38.
282. Catenacci, D.V.T., et al., *Rilotumumab plus epirubicin, cisplatin, and capecitabine as first-line therapy in advanced MET-positive gastric or gastro-oesophageal junction cancer (RILOMET-1): a randomised, double-blind, placebo-controlled, phase 3 trial.* Lancet Oncol, 2017. **18**(11): p. 1467-1482.
283. Tan, E.-H., et al., *Phase 1b Trial of Ficlatuzumab, a Humanized Hepatocyte Growth Factor Inhibitory Monoclonal Antibody, in Combination With Gefitinib in Asian Patients With NSCLC.* Clinical pharmacology in drug development, 2018. **7**(5): p. 532-542.
284. Merchant, M., et al., *Monovalent antibody design and mechanism of action of onartuzumab, a MET antagonist with anti-tumor activity as a therapeutic agent.* Proc Natl Acad Sci U S A, 2013. **110**(32): p. E2987-96.
285. Jin, H., et al., *MetMAb, the One-Armed 5D5 Anti-c-Met Antibody, Inhibits Orthotopic Pancreatic Tumor Growth and Improves Survival.* Cancer Research, 2008. **68**(11): p. 4360.
286. Kelly, K., *MS 17.04 MET-Lung: A Phase III Trial of Onartuzumab (METMab) Plus Erlotinib vs Erlotinib in Previously Treated Stage IIIB or IV NSCLC.* Journal of Thoracic Oncology, 2017. **12**(11): p. S1709-S1710.
287. Yan, S.B., et al., *MET-targeting antibody (emibetuzumab) and kinase inhibitor (merestinib) as single agent or in combination in a cancer model bearing MET exon 14 skipping.* Invest New Drugs, 2018. **36**(4): p. 536-544.
288. Roskoski, R., Jr., *Classification of small molecule protein kinase inhibitors based upon the structures of their drug-enzyme complexes.* Pharmacol Res, 2016. **103**: p. 26-48.
289. Hughes, P.E., et al., *In Vitro and In Vivo Activity of AMG 337, a Potent and Selective MET Kinase Inhibitor, in MET-Dependent Cancer Models.* Mol Cancer Ther, 2016. **15**(7): p. 1568-79.
290. Du, Z., et al., *Preclinical Evaluation of AMG 337, a Highly Selective Small Molecule MET Inhibitor, in Hepatocellular Carcinoma.* Mol Cancer Ther, 2016. **15**(6): p. 1227-37.
291. Zhang, B., et al., *Characteristics and Response to Crizotinib in ALK-Rearranged, Advanced Non-Adenocarcinoma, Non-Small Cell Lung Cancer (NA-NSCLC) Patients: a Retrospective Study and Literature Review.* Target Oncol, 2018. **13**(5): p. 631-639.
292. Schrock, A.B., et al., *Mutation of MET Y1230 as an Acquired Mechanism of Crizotinib Resistance in NSCLC with MET Exon 14 Skipping.* J Thorac Oncol, 2017. **12**(7): p. e89-e90.
293. Heist, R.S., et al., *Acquired Resistance to Crizotinib in NSCLC with MET Exon 14 Skipping.* J Thorac Oncol, 2016. **11**(8): p. 1242-1245.
294. Awad, M.M., et al., *Mechanisms of acquired resistance to MET tyrosine kinase inhibitors (TKIs) in MET exon 14 (METex14) mutant non-small cell lung cancer (NSCLC).* Journal of Clinical Oncology, 2018. **36**(15_suppl): p. 9069-9069.
295. Grullich, C., *Cabozantinib: Multi-kinase Inhibitor of MET, AXL, RET, and VEGFR2.* Recent Results Cancer Res, 2018. **211**: p. 67-75.

296. Yakes, F.M., et al., *Cabozantinib (XL184), a novel MET and VEGFR2 inhibitor, simultaneously suppresses metastasis, angiogenesis, and tumor growth.* Mol Cancer Ther, 2011. **10**(12): p. 2298-308.
297. Fuse, M.J., et al., *Mechanisms of Resistance to NTRK Inhibitors and Therapeutic Strategies in NTRK1-Rearranged Cancers.* Mol Cancer Ther, 2017. **16**(10): p. 2130-2143.
298. Liu, X., et al., *Drug resistance profiles of mutations in the RET kinase domain.* Br J Pharmacol, 2018. **175**(17): p. 3504-3515.
299. Tiran, Z., et al., *A novel recombinant soluble splice variant of Met is a potent antagonist of the hepatocyte growth factor/scatter factor-Met pathway.* Clin Cancer Res, 2008. **14**(14): p. 4612-21.
300. Vorlova, S., et al., *Induction of antagonistic soluble decoy receptor tyrosine kinases by intronic polyA activation.* Mol Cell, 2011. **43**(6): p. 927-39.
301. Tian, B. and J.L. Manley, *Alternative polyadenylation of mRNA precursors.* Nat Rev Mol Cell Biol, 2017. **18**(1): p. 18-30.
302. Cartegni, L., S.L. Chew, and A.R. Krainer, *Listening to silence and understanding nonsense: exonic mutations that affect splicing.* Nat Rev Genet, 2002. **3**(4): p. 285-98.
303. Faustino, N.A. and T.A. Cooper, *Pre-mRNA splicing and human disease.* Genes Dev, 2003. **17**(4): p. 419-37.
304. Coltri, P.P., M.G.P. Dos Santos, and G.H.G. da Silva, *Splicing and cancer: Challenges and opportunities.* Wiley Interdiscip Rev RNA, 2019: p. e1527.
305. Kornblihtt, A.R., et al., *Alternative splicing: a pivotal step between eukaryotic transcription and translation.* Nature Reviews Molecular Cell Biology, 2013. **14**: p. 153.
306. Kalsotra, A. and T.A. Cooper, *Functional consequences of developmentally regulated alternative splicing.* Nat Rev Genet, 2011. **12**(10): p. 715-29.
307. Kurosaki, T. and L.E. Maquat, *Nonsense-mediated mRNA decay in humans at a glance.* J Cell Sci, 2016. **129**(3): p. 461-7.
308. Fredericks, A.M., et al., *RNA-Binding Proteins: Splicing Factors and Disease.* Biomolecules, 2015. **5**(2): p. 893-909.
309. Havens, M.A., D.M. Duelli, and M.L. Hastings, *Targeting RNA splicing for disease therapy.* Wiley Interdiscip Rev RNA, 2013. **4**(3): p. 247-66.
310. Havens, M.A. and M.L. Hastings, *Splice-switching antisense oligonucleotides as therapeutic drugs.* Nucleic Acids Res, 2016. **44**(14): p. 6549-63.
311. Kumar, M. and G.G. Carmichael, *Antisense RNA: Function and Fate of Duplex RNA in Cells of Higher Eukaryotes.* Microbiology and Molecular Biology Reviews, 1998. **62**(4): p. 1415.
312. Iannitti, T., et al., *Phosphorothioate and Phosphorodiamidate Morpholino Oligomers: Effectiveness and Toxicity*. 2014.
313. Dias, N. and C.A. Stein, *Antisense Oligonucleotides: Basic Concepts and Mechanisms.* Molecular Cancer Therapeutics, 2002. **1**(5): p. 347.
314. Havens, M.A. and M.L. Hastings, *Splice-switching antisense oligonucleotides as therapeutic drugs.* Nucleic acids research, 2016. **44**(14): p. 6549-6563.
315. Chi, X., P. Gatti, and T. Papoian, *Safety of antisense oligonucleotide and siRNA-based therapeutics.* Drug Discov Today, 2017. **22**(5): p. 823-833.
316. Mah, J.K., *An Overview of Recent Therapeutics Advances for Duchenne Muscular Dystrophy.* Methods Mol Biol, 2018. **1687**: p. 3-17.
317. Falzarano, M.S., et al., *Duchenne Muscular Dystrophy: From Diagnosis to Therapy.* Molecules, 2015. **20**(10): p. 18168-84.
318. Bello, L. and E. Pegoraro, *Genetic diagnosis as a tool for personalized treatment of Duchenne muscular dystrophy.* Acta Myol, 2016. **35**(3): p. 122-127.

319. Aartsma-Rus, A., I.B. Ginjaar, and K. Bushby, *The importance of genetic diagnosis for Duchenne muscular dystrophy.* J Med Genet, 2016. **53**(3): p. 145-51.
320. Habara, Y., et al., *In vitro splicing analysis showed that availability of a cryptic splice site is not a determinant for alternative splicing patterns caused by +1G-->A mutations in introns of the dystrophin gene.* J Med Genet, 2009. **46**(8): p. 542-7.
321. Cao, L., et al., *Wild-type mouse models to screen antisense oligonucleotides for exon-skipping efficacy in Duchenne muscular dystrophy.* PLoS One, 2014. **9**(11): p. e111079.
322. Nakamura, A. and S. Takeda, *Mammalian models of Duchenne Muscular Dystrophy: pathological characteristics and therapeutic applications.* J Biomed Biotechnol, 2011. **2011**: p. 184393.
323. Takeshima, Y., et al., *Intravenous Infusion of an Antisense Oligonucleotide Results in Exon Skipping in Muscle Dystrophin mRNA of Duchenne Muscular Dystrophy*. Vol. 59. 2006. 690-4.
324. Lim, K.R.Q., R. Maruyama, and T. Yokota, *Eteplirsen in the treatment of Duchenne muscular dystrophy.* Drug design, development and therapy, 2017. **11**: p. 533-545.
325. Aartsma-Rus, A. and A.M. Krieg, *FDA Approves Eteplirsen for Duchenne Muscular Dystrophy: The Next Chapter in the Eteplirsen Saga.* Nucleic acid therapeutics, 2017. **27**(1): p. 1-3.
326. D'Amico, A., et al., *Spinal muscular atrophy.* Orphanet journal of rare diseases, 2011. **6**: p. 71-71.
327. Cartegni, L., et al., *Determinants of exon 7 splicing in the spinal muscular atrophy genes, SMN1 and SMN2.* Am J Hum Genet, 2006. **78**(1): p. 63-77.
328. Cartegni, L. and A.R. Krainer, *Disruption of an SF2/ASF-dependent exonic splicing enhancer in SMN2 causes spinal muscular atrophy in the absence of SMN1.* Nat Genet, 2002. **30**(4): p. 377-84.
329. Cartegni, L. and A.R. Krainer, *Correction of disease-associated exon skipping by synthetic exon-specific activators.* Nat Struct Biol, 2003. **10**(2): p. 120-5.
330. Hua, Y., et al., *Antisense correction of SMN2 splicing in the CNS rescues necrosis in a type III SMA mouse model.* Genes & development, 2010. **24**(15): p. 1634-1644.
331. Haché, M., et al., *Intrathecal Injections in Children With Spinal Muscular Atrophy: Nusinersen Clinical Trial Experience.* Journal of child neurology, 2016. **31**(7): p. 899-906.
332. Aartsma-Rus, A., *FDA Approval of Nusinersen for Spinal Muscular Atrophy Makes 2016 the Year of Splice Modulating Oligonucleotides.* Nucleic Acid Ther, 2017. **27**(2): p. 67-69.
333. Zammarchi, F., et al., *Antitumorigenic potential of STAT3 alternative splicing modulation.* Proc Natl Acad Sci U S A, 2011. **108**(43): p. 17779-84.
334. Spraggon, L. and L. Cartegni, *Antisense Modulation of RNA Processing as a Therapeutic Approach in Cancer Therapy.* Drug Discov Today Ther Strateg, 2013. **10**(3): p. e139-e148.
335. Spraggon, L. and L. Cartegni, *U1 snRNP-Dependent Suppression of Polyadenylation: Physiological Role and Therapeutic Opportunities in Cancer.* Int J Cell Biol, 2013. **2013**: p. 846510.
336. Ma, L., C. Guo, and Q.Q. Li, *Role of alternative polyadenylation in epigenetic silencing and antisilencing.* Proceedings of the National Academy of Sciences of the United States of America, 2014. **111**(1): p. 9-10.
337. Wood, A.J., et al., *Epigenetic control of alternative mRNA processing at the imprinted Herc3/Nap1l5 locus.* Nucleic Acids Research, 2012. **40**(18): p. 8917-8926.
338. Mayr, C. and D.P. Bartel, *Widespread shortening of 3'UTRs by alternative cleavage and polyadenylation activates oncogenes in cancer cells.* Cell, 2009. **138**(4): p. 673-684.

339. Li, L., et al., *3'UTR shortening identifies high-risk cancers with targeted dysregulation of the ceRNA network.* Scientific Reports, 2014. **4**: p. 5406.
340. Masamha, C.P., *The drive to generate multiple forms of oncogenic cyclin D1 transcripts in mantle cell lymphoma.* Biomarker research, 2017. **5**: p. 16-16.
341. Gunderson, S.I., M. Polycarpou-Schwarz, and I.W. Mattaj, *U1 snRNP inhibits pre-mRNA polyadenylation through a direct interaction between U1 70K and poly(A) polymerase.* Mol Cell, 1998. **1**(2): p. 255-64.
342. Furth, P.A., et al., *Sequences homologous to 5' splice sites are required for the inhibitory activity of papillomavirus late 3' untranslated regions.* Mol Cell Biol, 1994. **14**(8): p. 5278-89.
343. Kaida, D., et al., *U1 snRNP protects pre-mRNAs from premature cleavage and polyadenylation.* Nature, 2010. **468**(7324): p. 664-8.
344. Mueller, A.A., et al., *Intronic polyadenylation of PDGFRalpha in resident stem cells attenuates muscle fibrosis.* Nature, 2016. **540**(7632): p. 276-279.
345. Uehara, Y., et al., *Placental defect and embryonic lethality in mice lacking hepatocyte growth factor/scatter factor.* Nature, 1995. **373**(6516): p. 702-5.
346. Houldsworth, J., et al., *Gene amplification in gastric and esophageal adenocarcinomas.* Cancer Res, 1990. **50**(19): p. 6417-22.
347. Pennacchietti, S., et al., *Hypoxia promotes invasive growth by transcriptional activation of the met protooncogene.* Cancer Cell, 2003. **3**(4): p. 347-61.
348. Malchers, F., et al., *Mechanisms of Primary Drug Resistance in FGFR1-Amplified Lung Cancer.* Clin Cancer Res, 2017. **23**(18): p. 5527-5536.
349. Borowicz, S., et al., *The soft agar colony formation assay.* J Vis Exp, 2014(92): p. e51998.
350. Park, J.E. and L. Cartegni, *In Vitro Modulation of Endogenous Alternative Splicing Using Splice-Switching Antisense Oligonucleotides.* Methods Mol Biol, 2017. **1648**: p. 39-52.
351. Khoury, M.P. and J.-C. Bourdon, *The isoforms of the p53 protein.* Cold Spring Harbor perspectives in biology, 2010. **2**(3): p. a000927-a000927.
352. Vousden, K.H. and X. Lu, *Live or let die: the cell's response to p53.* Nat Rev Cancer, 2002. **2**(8): p. 594-604.
353. Millau, J.F., N. Bastien, and R. Drouin, *P53 transcriptional activities: a general overview and some thoughts.* Mutat Res, 2009. **681**(2-3): p. 118-33.
354. Khoury, M.P. and J.C. Bourdon, *p53 Isoforms: An Intracellular Microprocessor?* Genes Cancer, 2011. **2**(4): p. 453-65.
355. Bourdon, J.C., et al., *p53 isoforms can regulate p53 transcriptional activity.* Genes Dev, 2005. **19**(18): p. 2122-37.
356. Joruiz, S.M. and J.C. Bourdon, *p53 Isoforms: Key Regulators of the Cell Fate Decision.* Cold Spring Harb Perspect Med, 2016. **6**(8).
357. Rufini, A., et al., *Senescence and aging: the critical roles of p53.* Oncogene, 2013. **32**(43): p. 5129-43.
358. Mondal, A.M., et al., *Delta133p53alpha, a natural p53 isoform, contributes to conditional reprogramming and long-term proliferation of primary epithelial cells.* Cell Death Dis, 2018. **9**(7): p. 750.
359. Robu, M.E., et al., *p53 activation by knockdown technologies.* PLoS Genet, 2007. **3**(5): p. e78.
360. Aoubala, M., et al., *p53 directly transactivates Delta133p53alpha, regulating cell fate outcome in response to DNA damage.* Cell Death Differ, 2011. **18**(2): p. 248-58.

361. Sawhney, S., et al., *Alpha-enolase is upregulated on the cell surface and responds to plasminogen activation in mice expressing a 133p53alpha mimic.* PLoS One, 2015. **10**(2): p. e0116270.
362. Marcel, V., et al., *Diverse p63 and p73 isoforms regulate Delta133p53 expression through modulation of the internal TP53 promoter activity.* Cell Death Differ, 2012. **19**(5): p. 816-26.
363. Horikawa, I., et al., *Autophagic degradation of the inhibitory p53 isoform Delta133p53alpha as a regulatory mechanism for p53-mediated senescence.* Nat Commun, 2014. **5**: p. 4706.
364. Bernard, H., et al., *The p53 isoform, Delta133p53alpha, stimulates angiogenesis and tumour progression.* Oncogene, 2013. **32**(17): p. 2150-60.
365. Bernard, H., et al., *The p53 isoform, Δ133p53, stimulates angiogenesis and tumour progression*. Vol. 32. 2012.
366. Gadea, G., et al., *TP53 drives invasion through expression of its Δ133p53β variant.* eLife, 2016. **5**: p. e14734.
367. Mills, A.A., *p53: link to the past, bridge to the future.* Genes Dev, 2005. **19**(18): p. 2091-9.
368. Marcel, V., et al., *Modulation of p53beta and p53gamma expression by regulating the alternative splicing of TP53 gene modifies cellular response.* Cell Death Differ, 2014. **21**(9): p. 1377-87.
369. Graupner, V., et al., *Functional characterization of p53β and p53γ, two isoforms of the tumor suppressor p53.* Cell Cycle, 2009. **8**(8): p. 1238-1248.
370. Silden, E., et al., *Expression of TP53 Isoforms p53β or p53γ Enhances Chemosensitivity in TP53null Cell Lines.* PLOS ONE, 2013. **8**(2): p. e56276.
371. Zoric, A., A. Horvat, and N. Slade, *Differential effects of diverse p53 isoforms on TAp73 transcriptional activity and apoptosis.* Carcinogenesis, 2013. **34**(3): p. 522-9.
372. Hayman, L., et al., *What is the potential of p53 isoforms as a predictive biomarker in the treatment of cancer?* Expert Review of Molecular Diagnostics, 2019. **19**(2): p. 149-159.
373. Senturk, S., et al., *p53Psi is a transcriptionally inactive p53 isoform able to reprogram cells toward a metastatic-like state.* Proc Natl Acad Sci U S A, 2014. **111**(32): p. E3287-96.